

THE RADIO AND ELECTRONIC ENGINEER

The Journal of the Institution of Electronic and Radio Engineers

FOUNDED 1925 INCORPORATED BY ROYAL CHARTER 1961

"To promote the advancement of radio, electronics and kindred subjects by the exchange of information in these branches of engineering."

VOLUME 29

JUNE 1965

NUMBER 6

AN INTERNATIONAL OUTLOOK FOR ENGINEERS

ONE of the problems in scientific and technological progress is that of finding the best way to promote exchange of views between scientists and engineers, not only of the same nationality but on a much broader, indeed world-wide, basis. In no discipline is this more necessary than that of radio and electronics, which must be a truly international field of endeavour if it is to flourish for the greater good of mankind.

The professional radio and electronic engineer has been and is being served to a growing extent by the activities of this Institution within the British Commonwealth. Sections have been operating in India and New Zealand for nearly fifteen years; in India an Indian Divisional Council has been set up which, through its own *Proceedings* and administrative office, fosters links with the Institution in Great Britain which have benefits in the short and long term for both sides. The Institution's Council has recently authorized the opening of an office in Canada to serve the growing number of members in that country, while local Section activities take place in Pakistan, New Zealand, Malaysia, Central and East Africa, as well as in South Africa. All these facilities for members have the aim of bringing radio and electronic engineers into closer contact.

So much for the Institution in the Commonwealth. Recent announcements by the British Prime Minister of closer links in technological matters with France, for instance in the manufacture of aircraft and in electronics, will be supported by I.E.R.E. activity in that country. For many years there has been a nucleus of Institution members, mainly in the Paris region, but the only local exchanges have been extremely informal. In April, however, the opportunity offered by the International Components Exhibition was used to convene a meeting at which a Committee was set up to plan a programme of activities, some of which would be in collaboration with similar French societies. Among the proposals being considered by the French Committee is one which could contribute significantly to alleviating the problem we have been considering, namely of promoting the international exchange of views between engineers by means of visits to research establishments, factories and other installations in each other's country.

This proposal for overseas technical visits is but one of the ways in which an international outlook among engineers might be encouraged. The views of members in Great Britain and France (and in other countries), as well as of other readers of this *Journal*, would be welcomed, and in particular offers of assistance in arranging such tours. Is there anything else that the Institution can do? Suggestions are invited on this international problem.

F. W. S.

INSTITUTION NOTICES

Institution Premiums and Awards

The Council of the Institution announces that the following awards are to be made for outstanding papers published in *The Radio and Electronic Engineer* during 1964:

THE CLERK MAXWELL PREMIUM

"The Digital Analysis of Electron-optical Systems" by B. A. Carré and W. M. Wreathall (June).

THE HEINRICH HERTZ PREMIUM

"Planar Arrays with Unequally Spaced Elements" by M. I. Skolnik and J. W. Sherman (September).

THE LORD RUTHERFORD AWARD

"Investigation of Relaxation Oscillations in the Output from a Ruby Laser" by D. D. Bhawalkar, W. A. Gambling and R. C. Smith (April).

THE A. F. BULGIN PREMIUM

"An Analogue Polarization Follower for Measuring the Faraday Rotation of Satellite Signals" by Gottfried Vogt (October).

THE J. C. BOSE PREMIUM

"Transistor Current-switching Circuits" by Y. N. Bapat (May).

THE MARCONI AWARD

"A Side-lobe Suppression System for Primary Radar" by J. Croney and P. R. Wallis (October).

THE LESLIE MCMICHAEL PREMIUM

"Some Bandwidth Compression Systems for Speech Transmission" by J. S. Williams (June).

THE J. LANGHAM THOMPSON PREMIUM

"A Low Cost Magnetic Tape Control System for Machine Tools" by P. H. G. Burgess and R. L. Duthie (April).

THE LORD BRABAZON AWARD

"The Combination of Pulse Compression with Frequency Scanning for Three-dimensional Radars" by K. Milne (August).

THE CHARLES BABBAGE AWARD

"The Design of Second-harmonic Detector Heads and their Application to the Reading of Digital Information and the Measurement of Low Speeds of Rotation" by D. B. G. Edwards, E. M. Dunstan and C. J. Tunis (February).

THE DR. NORMAN PARTRIDGE MEMORIAL PREMIUM

"Correlation Techniques in Studio Testing" by A. N. Burd (May).

The following Premiums and Awards are withheld as papers of suitable standard have not been pub-

lished during the year: the Rediffusion Television Premium, the P. Perring Thoms Premium, the V. K. Zworykin Award, the Arthur Gay Premium, and the Hugh Brennan Premium.

The Premiums and Awards will be presented at the Annual General Meeting in London in January 1966.

Conference on U.H.F. Television

The International Conference on "U.H.F. Television" will now be held in London on Monday and Tuesday, 22nd and 23rd November. This Conference is being organized jointly by the Institution, the Electronics Division of the Institution of Electrical Engineers, the U.K. and Eire Sections of the Institute of Electrical and Electronic Engineers and the Television Society. Although the Conference was originally planned for the late Autumn, the date was brought forward to 1st and 2nd September to coincide with the 1965 Radio and Television Show. (See notice on page 134, *The Radio and Electronic Engineer*, March 1965.) Since the Radio Show has now been cancelled the original date has been re-adopted.

The programme will include:

Planning and Propagation; Transmitters and Translators; Aerials, Feeders and Parametric Amplifiers; Integrated Tuners and Receiver Techniques.

A programme of technical visits will also be arranged.

Further information, including registration forms, may be obtained on application to the Joint U.H.F. Television Conference Secretariat, I.E.R.E., 8-9 Bedford Square, London, W.C.1.

Engineering Inspection in the Future

The 1965 National Inspection Conference will be devoted to examining and discussing the likely changes in the management and technique of engineering inspection in the future. It will be held at New College, Oxford, from 20th to 23rd September.

A feature of the Conference will be the syndicate discussions during the second day of the specific changes probable in a series of industries.

Further information may be obtained from the Institution of Engineering Inspection (Oxford Conference), 616 Grand Buildings, Trafalgar Square, London, W.C.2.

Back Copies of The Journal

Members are asked to note that a sufficient number of copies of *The Radio and Electronic Engineer*, Volume 25, has now been received. No more copies of these issues should, therefore, be sent to the Institution.

The Rhometer: A Continuous Impurity Monitor for Liquid Metal Circuits

By

R. DEHN, M.Sc.
(Member)†

AND

A. R. EAMES, B.Sc.‡

Read at a meeting of the Northern Sub-Section of the Scottish Section in Thurso on 1st April 1965.

Summary: The rhometer uses the change in resistivity with impurity content of liquid metals, mainly sodium and sodium-potassium alloy, to measure the amount of impurities, such as oxide and hydride, etc., down to a few parts per million.

It is a 'non-contact' or electrodeless instrument, in that the liquid metal flows through a toroidal pipe which forms one turn of a 50-c/s transformer. The output from this transformer is fed to a phase-sensitive rectifier, and changes in resistivity are then indicated on a standard chart recorder. A special circuit compensates for changes in resistivity caused by changes in temperature of the liquid metal.

Operating experience with the rhometer in the primary coolant circuits of the Dounreay Fast Reactor is described in detail, and some possible future trends in the further development of the instrument are briefly discussed.

1. Introduction

The solubility of most impurities, particularly oxide, in liquid metals, such as sodium, decreases rapidly with decreasing temperature. This fact may be used both for measuring, and for reducing, the impurity content. The rhometer, originally proposed by Blake¹ and developed by Eames² is an instrument for measuring changes in the impurity content of liquid metals, such as sodium, or sodium-potassium alloy. In these metals even a small increase in impurity content, e.g. oxides, hydrides, etc., substantially increases the electrical resistivity. The instrument effectively measures the electrical resistance of a toroidal stainless steel pipe through which the liquid metal flows, and therefore serves as an 'on-line' impurity monitor. A special compensating circuit ensures that indications are corrected for resistivity changes caused by temperature variations. Harrison and Roach³ have employed a similar principle to measure the electrical conductivity of highly radioactive solutions for process control.

The *absolute* accuracy of the measurements is limited by the tolerance in the dimensions of the toroidal pipe, and is about 2%. The stability and sensitivity, however, are of the order of 0.01% and make it possible to detect changes in oxygen content down to one part per million.

† U.K. Atomic Energy Authority, Dounreay Experimental Reactor Establishment, Thurso, Caithness, Scotland.

‡ U.K. Atomic Energy Authority, Engineering Group, Risley, near Warrington, Lancashire.

1.1. Technical Terms used in Liquid Metal Circuit Technology

A *Plugging Meter* is a mechanical instrument for measuring impurity content. It consists essentially of an orifice plate in the liquid metal pipe which can be cooled, usually by an external air-stream, and flow and temperature recorders. The temperature of the flowing liquid metal is reduced until dissolved oxide begins to precipitate. This blocks the orifice and is indicated by a sudden reduction in flow. The temperature at which this occurs is known as the *Plugging Temperature* and is a measure of the impurity content, mainly oxide. The lower the plugging temperature, the lower the impurity content of the liquid metal.

A *Cold Trap* is a simple device for decreasing the impurity content of liquid metal circuits and keeping it at a consistently low level during operation. The cold trap consists essentially of a vessel through which the liquid metal flows. The vessel is cooled by an external air stream and contains a stainless steel mesh basket. As the temperature is reduced, dissolved oxide and certain other impurities precipitate and are retained by the mesh. The operation is known as *Cold Trapping*. The primary coolant circuit of the Dounreay Fast Reactor contains a 70% sodium and 30% potassium mixture. The circuit is equipped with a number of cold traps as well as a special *Cold Trap Loop* containing a larger trap and a full range of instruments, such as temperature and flow recorders, a plugging meter and a rhometer.

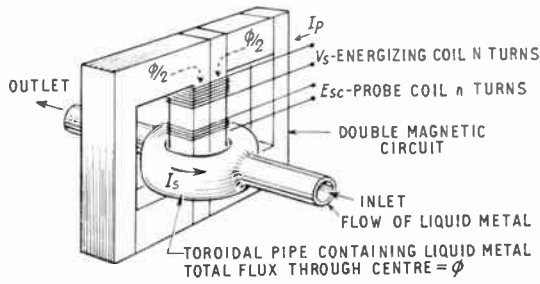


Fig. 1. Basic arrangement of resistivity meter.

2. Principle of Operation

The basic arrangement is shown in Fig. 1. An energizing coil of N turns connected across a supply voltage V_s sets up a magnetic flux ϕ through the centre leg of the iron circuit. A secondary current I_s circulates in the toroidal pipe containing the liquid metal, and the e.m.f., E_s , responsible for this current is magnified n times by the probe coil of n turns. The vector diagram is shown in Fig. 2. The transformer is designed so that the magnetizing and iron loss components of current are very small compared with the primary current I_p . Hence, very nearly:

$$I_s = NI_p$$

If E_{sc} is the voltage developed across the probe coil,

$$\frac{E_{sc}}{nNI_p} = Z_s, \text{ the total impedance of the toroid}$$

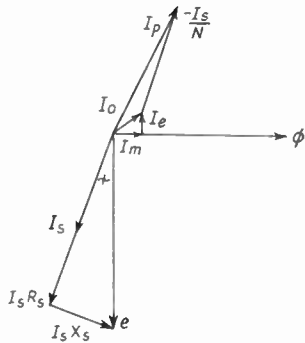


Fig. 2. Vector diagram for meter.

Hence by measuring E_{sc} and I_p , the resistivity of the liquid metal can be found

$$\text{resistivity } \rho = \frac{R_T R_s}{R_T - R_s} \frac{A_F}{g} \dots\dots(1)$$

where R_T = resistance of empty pipe around toroid.

A_F = cross-sectional area of liquid metal in toroid.

g = average circumference of toroid.

R_s = secondary load resistance.

$$R_s = \left[\left(\frac{E_{sc}}{nNI_p} \right)^2 - X_s^2 \right]^{\frac{1}{2}} \dots\dots(2)$$

A measuring circuit in the form of an a.c. bridge is shown in Fig. 3. A variable resistor R is used to balance the in-phase component of the secondary load, while variable inductor M is used to balance the quadrature component. At balance:

$$R_s = \frac{R}{nN} \dots\dots(3)$$

Balance conditions for this bridge circuit are frequency independent (transformer iron losses being neglected). In practice, the detector is made phase sensitive so that the variable inductor need not be balanced accurately, and so that changes in quadrature balance conditions will not affect the meter output signal.

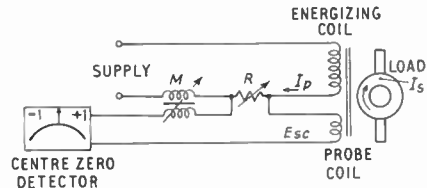
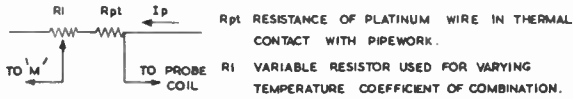


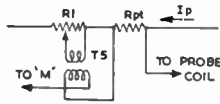
Fig. 3. Measuring and balancing circuit.

The phase-sensitive detector is also inherently polarity conscious, enabling the circuit to be so connected that a reduction in liquid-metal resistivity will cause the detector to give a negative reading, and a resistivity increase to give a positive reading. The sensitivity of the detector can also be adjusted so that full-scale deflection is equivalent to a specific resistivity increase, e.g. 1%. The phase-sensitive detector measures voltage components in phase with I_p , and therefore measures the full value of the out-of-balance voltage. The variable resistance R is arranged in a series of switched decades, calibrated to read resistivity changes in per cent.

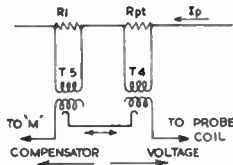
When looking for small changes in resistivity owing to impurities within the liquid metal, care must be taken to eliminate errors owing to the liquid-metal temperature coefficient: when using sodium, a change of a few degrees Celsius can mask any small impurity effects. This difficulty is overcome by making the balancing resistor R have the same temperature coefficient as the sodium-toroidal pipe combination, and keeping R in intimate thermal contact with the pipework. A platinum resistance wire is used in thermal contact with the pipe, and the temperature coefficient is made variable using the circuit shown in



(a) Using resistor R_1 to reduce temperature coefficient of combination.



(b) Using transformer T_5 enabling R_1 to increase temperature coefficient.



(c) Using two transformers to give variable temperature coefficient while keeping compensator voltage constant at the working temperature.

Fig. 4. Methods of varying temperature coefficient.

Fig. 4(c). The circuit is arranged so that when the transformer tapplings are changed the voltage output from the combination remains unchanged at the normal working temperature. If K_1 = proportion of secondary winding selected on T4, then

$$\alpha_c = K_1 \alpha_{Pt}$$

where α_c = temperature coefficient of combination
 α_{Pt} = temperature coefficient of platinum
 (When $K_1 = 1$, the number of turns selected from T5 is zero.)

The temperature coefficient can be adjusted as different liquid metals are used. The resistance temperature coefficient of a liquid-metal toroidal-pipe combination may not be accurately known, in which case the controls can be adjusted until temperature balance is obtained.

In practice, perfect temperature compensation can only be obtained at one temperature, owing to the second-order terms in the temperature coefficients. Errors introduced owing to deviation from this one temperature can be observed, and due allowance made. This is discussed in detail in Section 5.

The circuit shown in Fig. 4(c) does not allow for varying the output voltage (or compensator voltage) so as to balance the circuit as in Fig. 3. It is important that the resistors R_{Pt} and R_1 should not be paralleled with another resistor connected across T4 and T5 secondaries, unless this additional resistor is of high value. The circuit is to be stable to $\pm 0.01\%$. The leads from the platinum resistor, which is mounted adjacent to the toroidal pipe, to the transformer T4, which is mounted in the control unit, may be up to several hundred feet long, and the resistances of these leads will vary with ambient temperature. Hence the current through these leads must be kept to a minimum. A method for varying the output from T4 and T5 (Fig. 5) utilizes a transformer T6: this has the effect of presenting a low source impedance to the phase rectifier, without loading the compensator circuit.

2.1. Errors

The principal sources of error are: iron losses in the transformer, by-pass current in external pipe-work, flow-dependent error due to a temperature difference between toroid and compensator winding, and changes in R_{Pt} due to variations in I_p , caused by mains voltage fluctuations.

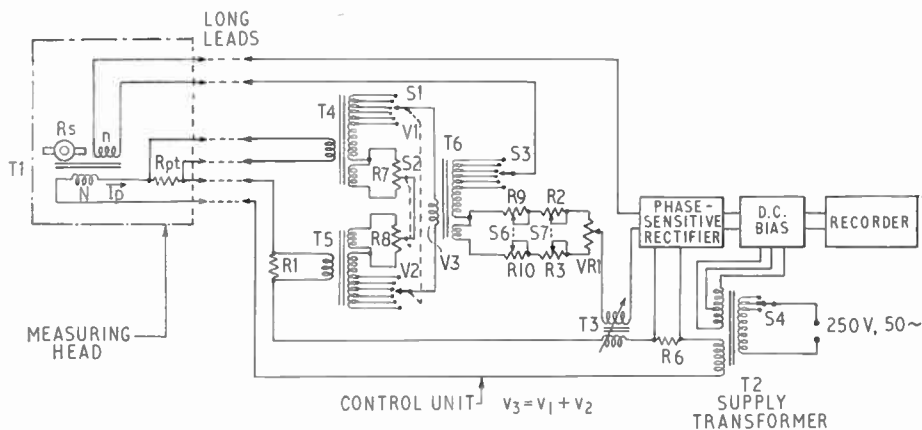


Fig. 5. Explanatory circuit diagram of resistivity meter.

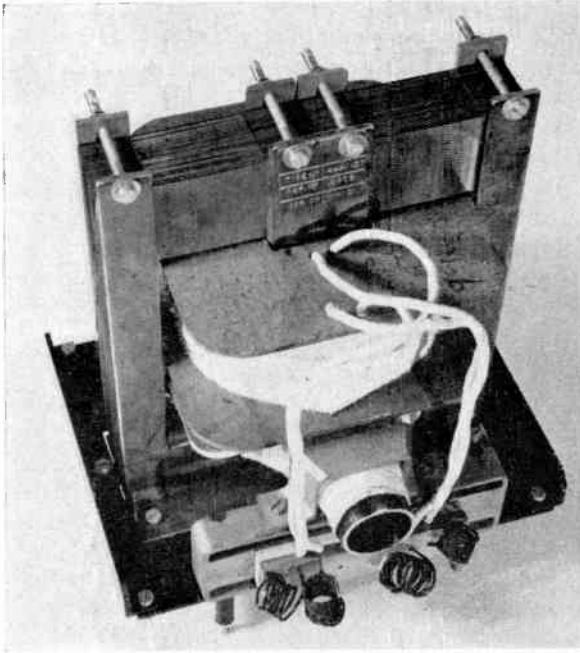


Fig. 6. Rhometer measuring head.

Eames has analysed these various errors in detail and has shown that, for a well-designed instrument, they are negligible except for the flow dependent error. Even this is generally small, and a simple correction can be applied in accurate work.

3. General Description of Instrument

Figure 6 shows the measuring head, and Fig. 7 the control unit of the instrument. The first three controls

from left to right are the decade switches to adjust the resistivity balance in steps of 10%, 1% and 0.1% respectively. The fourth is a continuous fine control with a total range of 0.1%, and the smallest scale division equal to 0.001%. The remaining two controls are used for setting the effective temperature coefficient, α_c , to the value appropriate to the temperature and type of liquid metal in use. Figure 8 shows the complete circuit diagram of the control unit. The main function of the supply transformer T2 is to energize the main winding of N turns on the resistivity meter. The current I_p passes through the platinum compensator R_{Pt} , the temperature coefficient adjusting resistor R1, and the phase reference resistor R6. The functions of T4 and T5 have been described (Fig. 4(c)). S1 and S2 are coarse and fine temperature compensation controls, and are calibrated directly in temperature coefficient. For stability reasons, resistors cannot be used on S2, so that a decade of tappings on the transformers T4 and T5 is necessary: decade resistances would need to have a high value compared with the resistance of the transformer windings; this would present too much source impedance to the output circuits.

Transformer T6, together with S3, S6, S7 and VR1, gives provision for balancing the circuit where the controls are calibrated directly in percentage resistivity. The magnetizing current for T6 would cause an error in the final reading if T6 were connected across T4 and T5 as in Fig. 5, since the winding resistances of T4 and T5 would vary with the ambient temperature. Hence this transformer is connected into the circuit as in Fig. 8 so that it obtains its magnetizing current from the probe coil. For S6 a tapped winding is used since an arrangement using resistors would load T6 too

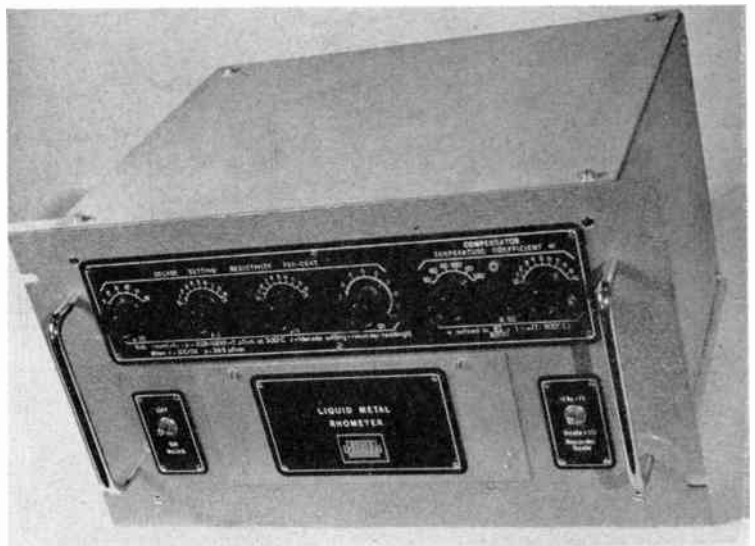


Fig. 7. Rhometer control unit.

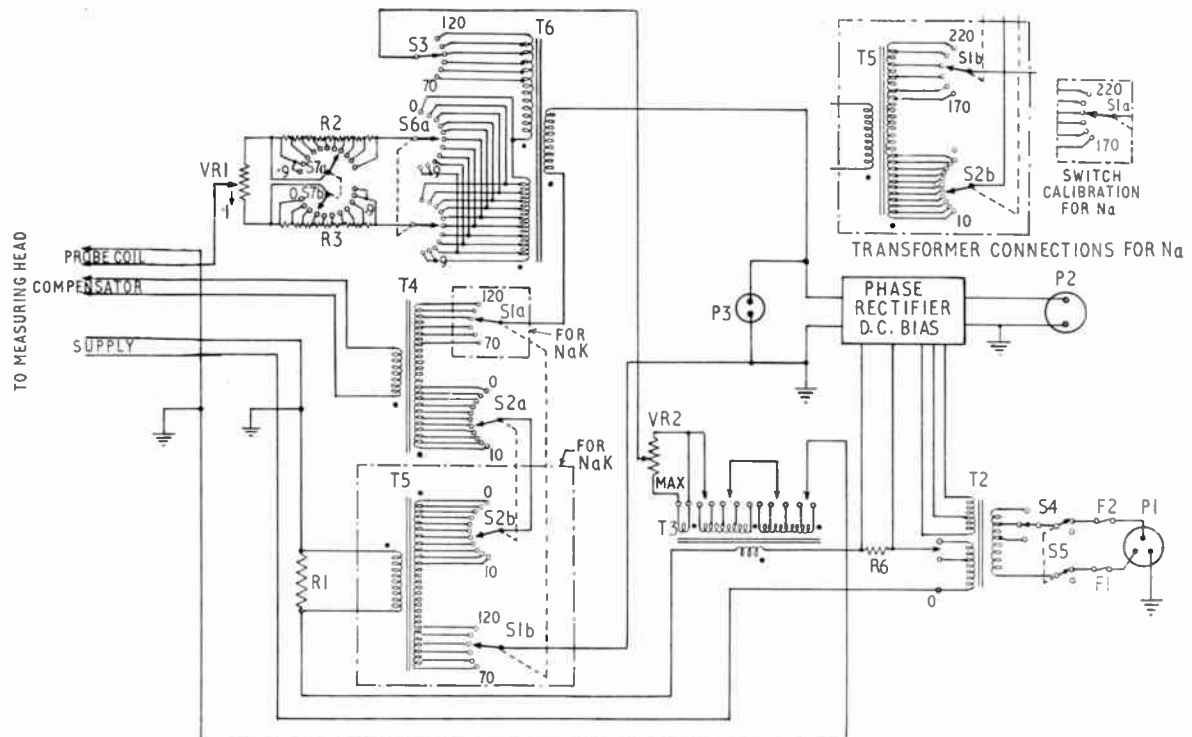


Fig. 8. Control unit. Circuit diagram.

much, and again an error would be introduced when the primary winding resistance varied. The loading presented by R2, R3 and VR1 is negligible. The out-of-balance signal is fed to the phase-sensitive rectifier.

For liquid metals whose temperature coefficient is greater than the platinum wire the polarity of T5 is reversed as shown in the insert in Fig. 8: this causes the voltage from R1 to subtract from the voltage across R_p.

The original phase-sensitive rectifier which used full-wave diode gates has now been superseded by a transistor circuit which results in better stability and a five-fold increase in sensitivity. Its circuit diagram is shown in Fig. 9. It has been designed to drive a strip chart or similar recorder having a sensitivity of -5, 0, +5 mV, and the most sensitive range provided by the output switch S represents -0.2, 0, +0.2% resistivity change. Two transistors of type SAC40 are connected to each side of the centre-tapped secondary winding on transformer T7. Their collectors are connected together as shown so that the collector to emitter off-set voltages, which appear across each transistor when driven into the saturated conducting condition, are in opposition to one another and do not therefore produce an output voltage. The reference transformer T8 drives each pair of transistors in alternate half-cycles of mains frequency, so as to achieve full-wave

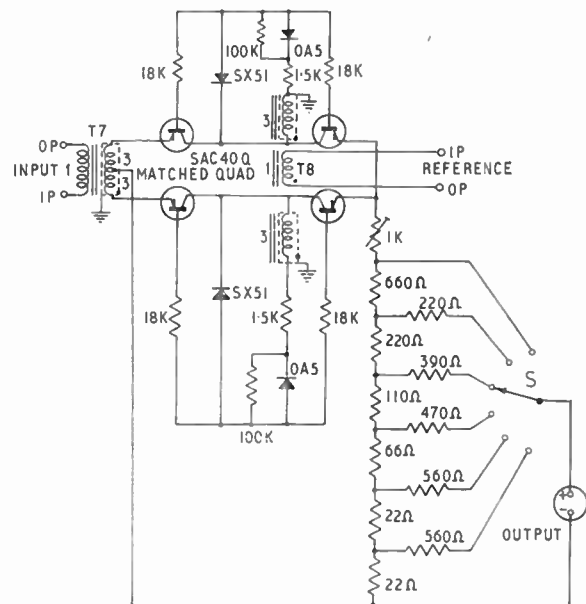


Fig. 9. Phase sensitive rectifier.

rectification. The 1.5 kΩ resistors and the Zener diodes SX51 stabilize the driving currents to the transistor bases. The optimum base driving current for the transistors is that current which results in an off-set voltage which is independent of the normal

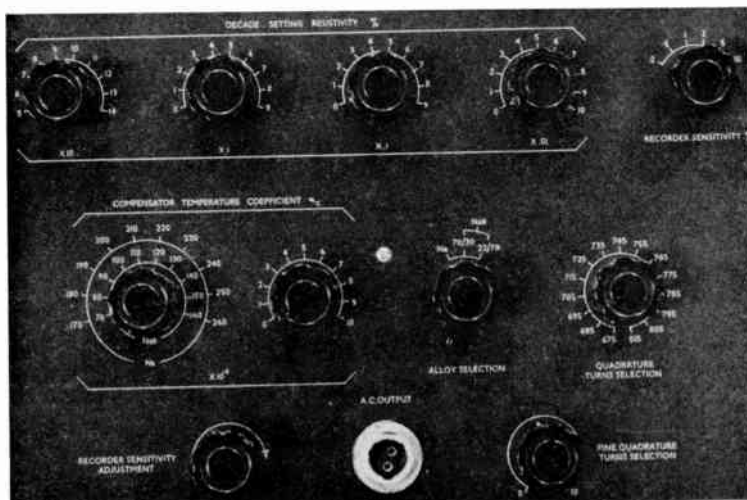


Fig. 10. Mark II control unit.

range of ambient temperatures encountered: this current is about $250 \mu\text{A}$ for an SAC40 transistor and this fixes the value of the base drive resistors to about $18 \text{ k}\Omega$.

Each diode (OA5) prevents unnecessary loading of the transformer T8 during the reverse half-cycles, while each $100 \text{ k}\Omega$ resistor provides a small positive base current for switching the transistors into the non-conducting state. The transistors are matched so that the standing direct output voltage (with the input short-circuited) is not greater than $50 \mu\text{V}$, representing an error of 0.002% resistivity change.

The attenuator is designed to give ranges of ± 0.2 , 0.5 , 1.0 , 2.0 , 5.0 and 10.0% resistivity change for full scale deflection of the recorder, and is designed with an output impedance of about 600Ω . The potentiometer ($1 \text{ k}\Omega$) is used for calibrating the sensitivity of the instrument. The recorder should preferably be of the null balancing type using an electronic amplifier with a relatively high input impedance.

The first commercially produced instrument was known as the Mk. I rhometer. As a result of operating experience with this instrument an improved version has been designed, known as the rhometer Mk. II. One of its main distinguishing features is the transistor phase-sensitive rectifier just described. This can be wired into the existing Mk. I control unit to improve its performance; the instrument so modified is known as the Mk. IA rhometer. The Mk. II control unit is shown in Fig. 10.

The other main differences between the Mk. I and Mk. II versions of the instrument are:—

- (a) In the Mk. I rhometer three transformers, T4, T5 and T6 (Fig. 8), are used in the control unit

for balancing temperature coefficient and resistivity. In the Mk. II rhometer only one transformer is used for this function, known as the comparator transformer. The main advantage of this arrangement is a reduction in iron and copper losses which are temperature dependent, so that ambient temperature variations have negligible effect upon stability.

- (b) The annulus and the temperature compensator winding are brought closer together in the head unit, thus reducing the flow error and simplifying installation.
- (c) The range of the temperature coefficient has been extended to enable the instrument to be used at higher liquid-metal temperatures, up to about 600°C . The upper limit of the Mk. I version was 300°C , because of the smaller range covered by its temperature coefficient controls. When operating near the upper limit of the liquid-metal temperature range, 500° to 600°C , it may be necessary to cool the transformer laminations to prevent their temperature exceeding 300°C .
- (d) The transformer T5 and the value of the platinum compensator R_p , in the Mk. I rhometer were suitable for only one particular liquid metal, e.g. 70/30 NaK, so that the circuit had to be modified, and the compensator changed, before the instrument could be used with another liquid metal, e.g. pure Na. The comparator transformer in the Mk. II version is so designed that the instrument may be used over a much wider range of liquid metals and alloys, the appropriate one being selected by a simple front panel switch.

4. Interpretation of Readings

In clean circuit conditions the resistivity of the liquid metal will remain steady, to within $\pm 0.01\%$ in a typical reactor circuit, and to within about 0.001% on a controlled loop.

A dirty circuit usually gives a fluctuating recording as shown in Fig. 11, even if particulate oxides are not actually flowing through the main circuits. Under such conditions, oxides, etc., usually find cool sections in the circuit where they can precipitate: such spots include valve bellows, static lines, etc. Temperature variations, flow variations and turbulence will agitate these precipitates causing changes in impurity level which will give rise to resistivity fluctuations. Adjustments made to the circuit conditions, such as opening and shutting valves, often cause contaminants to be released into the system causing temporary resistivity fluctuations.

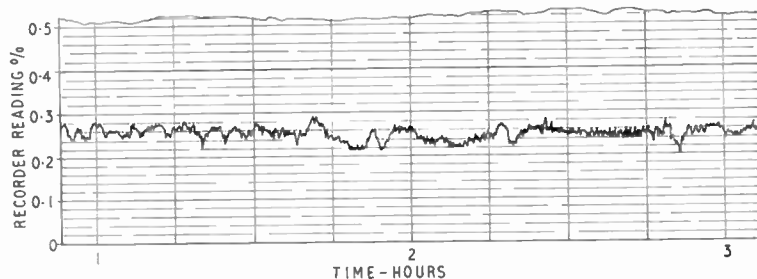
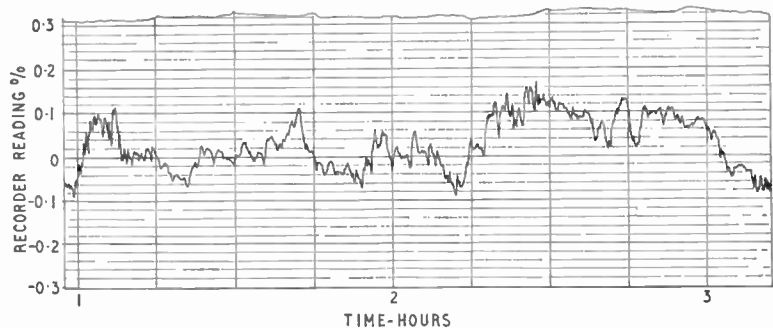


Fig. 11. Fluctuating trace obtained under dirty conditions.

Fig. 12. Large fluctuations owing to a high level of contamination.



These fluctuations in dirty conditions usually contain comparatively long period variations of the order of several seconds or greater. A very dirty circuit can give large fluctuations as indicated in Fig. 12.

When 'cold trapping' a circuit (see Section 1.1), the fluctuations in resistivity seen on the recorder trace will slowly decrease in amplitude until a steady trace is obtained indicating cleaner conditions.

Insoluble materials will cause positive spikes on the rhometer recorder trace as they pass through the rhometer head, giving an output signal proportional

to particle volume. If the internal volume of the stainless steel annular pipe is V , and the volume of a particle of high electrical resistivity passing through the annulus is v , then the magnitude of the recorder spike will be:

$$S = \frac{v}{V} \times 100\% = \frac{\pi d^3}{6V} \times 100\%$$

where d is the particle diameter in inches (cm). The volume of the annulus V is 15 in^3 (246 cm^3), whence

$$s = 3.5 d^3\% \quad (0.21 d^3\%)$$

The minimum spike detectable without using special techniques is 0.001% . This gives the smallest particle diameter which can be seen on the recorder as 0.065 in (0.165 cm). It is important to note that the rhometer output increases as the cube of the particle diameter. This analysis is, of course, approximate and applies in any case to small particles only.

The time taken for the particle to go through the annulus depends on the flow rate and this will determine the time duration of each spike. At 3 gal/min (13.6 l./min) (the best operating flow for a rhometer) this time is approximately 1 second. The type of trace to be expected when particulate matter is present is shown in Fig. 13, which is a recording obtained from a NaK loop just after filling and before cold trapping had commenced. The size of the spikes in this recording indicates particle sizes of the order of 0.07 in up to 0.2 in (1.65 mm to 5.1 mm) diameter. The passage of large numbers of very small particles could give a

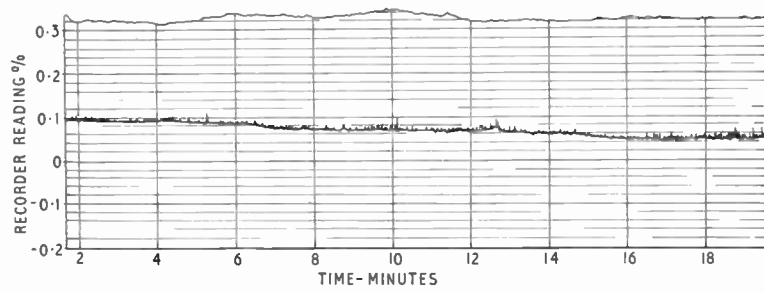


Fig. 13. Spiky trace owing to the presence of particulate matter.

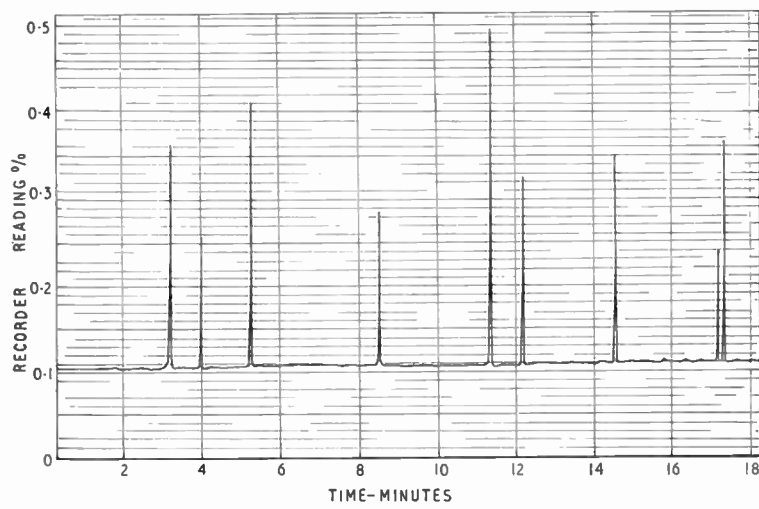


Fig. 14. Large pulses caused by gas bubbles passing through meter.

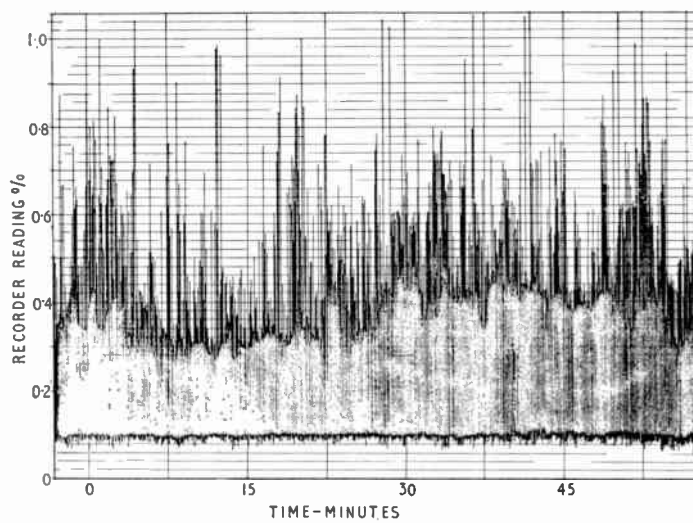


Fig. 15. Oscillating trace caused by gas entrainment.

rapidly fluctuating trace like that shown in Figs. 11 or 12 where the individual spikes are not easily discernible.

Gas entrainment in a rig or reactor circuit can occur in a number of ways, but experience in rhometer operation indicates that gas inclusion usually occurs in the form of fairly large bubbles.

Figure 14 is a reproduction of a recording which indicated a bubble of gas going through the annulus every minute or so. The smallest gas bubble gave a spike of 0.13% and the largest a spike of 0.38% resistivity. These signals are equivalent to bubble diameters of the order of 0.25 in (0.62 cm).

Figure 15 shows the type of trace to be expected with severe gas entrainment. Such gas entrainment makes accurate determination of the resistivity of the liquid metal impossible, but gas must be considered as a particulate impurity which must not be allowed in the circuit and steps must be taken to eliminate it. After its elimination the accurate resistivity of the liquid metal will be recorded.

Experience shows that gas entrainment gives large spikes of 0.2% to 2.0% resistivity change, while solid oxide particles give small spikes of 0.2% down to the smallest detectable size and, therefore, these different contaminants are usually distinguishable.

Under otherwise steady conditions, the rhometer may occasionally indicate a long term drift, i.e. a slow increase or decrease in apparent mean resistivity. This could be caused by:

- (a) Increase in metallic impurity content, if metallic impurities enter the liquid metal circuit as a result of slow corrosion of rig or reactor materials. The drift in this case will be positive.
- (b) Corrosion of the stainless steel annulus. If the metal remains in solution then, as under (a) above, the drift will be positive. If there is a mass transfer as well, i.e. the corrosion products are removed from the system, then the drift will be negative because of the increase in area of the toroid.
- (c) Alloy drift in NaK systems. If the sodium/potassium ratio in a NaK system should change for any reason, the resistivity will also change. For example, in a 70/30 NaK system, a change to 69/31 NaK, i.e. decrease in sodium, will cause an increase in resistivity of 1.93% at 300°C.

5. Temperature Effects

Compensation for the change in resistivity with temperature is an essential part of the rhometer design. This has already been referred to (Sect. 2) and will now be discussed in detail. The temperature coefficients for typical liquid metals, referred to

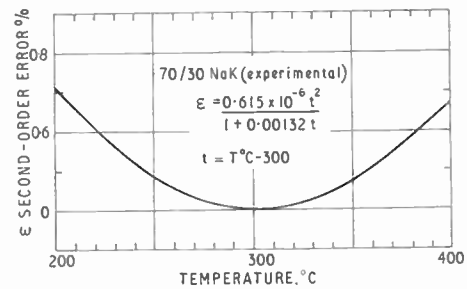


Fig. 16. Rhometer reading against temperature: 70/30 NaK against platinum.

300°C, are: 0.2%/degC for Na and 0.13%/degC for 70/30 NaK, so that in the absence of any temperature compensation the temperature would have to be held constant to $\pm 0.05\%/degC$ if low-level impurity changes are to be observed.

As has been explained in Section 2, the rhometer circuit enables the effective temperature coefficient of resistance of the platinum compensator to be adjusted to any desired value over a wide range. Thus the temperature coefficient of the liquid metal used can be matched exactly. However, this is strictly valid only at one particular temperature, because of the effect of the second-order temperature coefficient exhibited by most conductors on the standard Celsius scale. In particular, NaK has a positive second-order coefficient, Na has either a zero, or a positive one, and platinum a negative coefficient. Hence it is impossible to achieve perfect compensation over a wide temperature range, and Fig. 16 shows a typical error curve of 70/30 NaK against platinum. The first order coefficients have been adjusted to match at 300°C.

If the rhometer is to be operated over wide temperature excursions then temperature correction can be applied by using curves similar to that shown in Fig. 16.

For approximate work temperature correction can be applied over a range of 200 degC using one such correction curve. For more accurate work in which changes of 0.01% are important, it is advisable to use the temperature compensation controls to shift the minimum point of the correction curve to the required temperature. Hence a family of correction curves is used, and the rhometer becomes accurate over a wide temperature range. Such curves have been obtained experimentally for Mk. IA rhometers on the Dounreay Fast Reactor primary circuit (70/30 NaK) (see Sect. 6). In theory these should be universally applicable to all Mk. IA instruments operating on 70/30 NaK. In view of component tolerances, however, it has been found advisable for accurate work to obtain individual curves for each instrument if possible.

6. Operating Experience

Mark IA rhometers have been in almost continuous operational use for nearly two years in the primary liquid metal coolant circuit in the Dounreay Fast Reactor. In one particular position the liquid metal temperature and flow have been so steady that, in general, no corrections have had to be applied to the readings. It became quickly apparent, however, that in order to enable the instruments to be used in varying conditions and, in particular, to increase the operators' confidence in their readings, some fairly extensive calibration, as explained in Section 5 above, would be necessary. For this purpose the rhometer installed in the permanent cold trap loop was used. It was intended to obtain a comprehensive set of data from which to evaluate the three basic graphs necessary for accurate work over an extended temperature range, that is:

- (a) The optimum setting of the temperature coefficient, α_c , at any temperature.
- (b) The 'off-set factors', δ , necessary for direct comparison of resistivity readings taken at different settings of the temperature coefficient.
- (c) A universal temperature correction curve to be applied to resistivity readings obtained at temperatures other than $\pm 10^\circ\text{C}$ of the optimum temperature as in (a) above.

It was also hoped, by using different plugging temperatures, to obtain an absolute calibration for the rhometer on the basis of solubility data.

Several series of readings were taken at plugging temperatures of 70°C , 110°C , 140°C , 170°C and 200°C . In each case conditions were allowed to become steady, and resistivity readings were then taken at 5 deg intervals from 120°C , or the plugging temperature whichever was the lower, up to 305°C . At each temperature the temperature coefficient setting was varied from 100 to $130 \times 10^{-5}/\text{degC}$ in 16 equal steps. Thus it became possible to plot indicated resistivity against temperature for the whole range of temperature coefficient settings and for different levels of contamination (plugging temperatures).

A family of curves for the lowest plugging temperature, 70°C , is shown in Fig. 17. These curves, as predicted by theory, are chiefly characterized by:

One common point, all curves show the same resistivity reading at 295°C , very near the theoretical design figure of 300°C .

The temperatures and resistivities at the minima of the curves increase with increasing α_c .

The curves approximate to second degree parabolas, particularly near their minima.

In order to assess the function represented by these

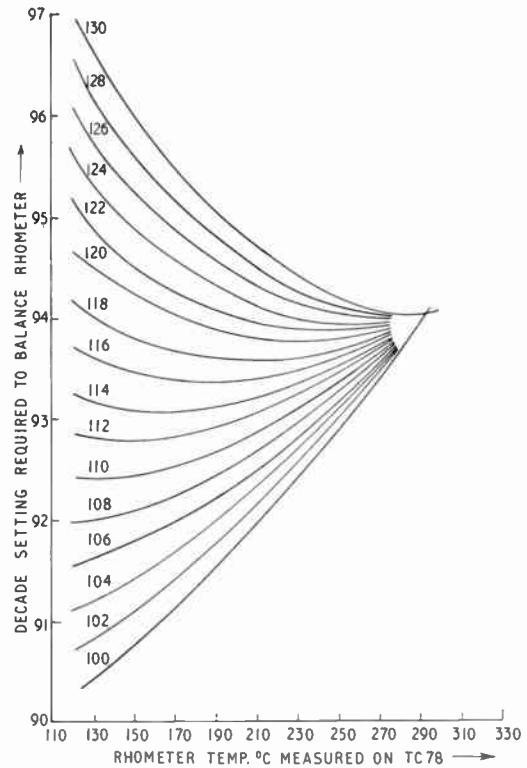


Fig. 17. Variation in indicated resistivity with rhometer temperature for various temperature coefficient settings. (Plugging temperature constant at approximately 70°C .)

curves as accurately as possible and to obtain the best possible numerical data as outlined above, a digital computer was employed. The least-squares fit to each curve of both a second- and a third-order polynomial was obtained. These were expressed in the form:

$$r - r_0 = a_1 \cdot (t - t_0)^2 \quad \dots\dots(4)$$

and

$$r - r_0 = a_1 \cdot (t - t_0)^3 + a_2(t - t_0)^2 \quad \dots\dots(5)$$

where t_0 represents the temperature at which the indicated resistivity is a minimum (r_0), and is the 'optimum' temperature for the particular setting of the temperature coefficient; r is the actual resistivity indicated by the rhometer at a temperature t .

Although the second-order polynomial represents a fairly good fit, the third order was examined in addition, because both theory and past experience have suggested some asymmetry in these curves which might possibly be taken into account by assigning a rather small, and probably negative, value to the coefficient a_1 in equation (5) above. However, the computer results for the third-order fits were, for the most part, disappointing, but the second-order fits yielded some very useful results for most of the sets.

The values obtained for the higher plugging temperatures were rather inconsistent indicating that conditions at the time of the experiment were possibly not quite steady.

The values of r_0 and t_0 obtained for all curves were used to plot the optimum temperature coefficient setting as a function of temperature for the different plugging temperatures. This is shown in Fig. 18. It is fairly clear from this that variations with plugging temperature are *random* in nature, rather than systematic. It was therefore concluded that the optimum setting of α_c is substantially independent of the contamination level of the liquid metal.

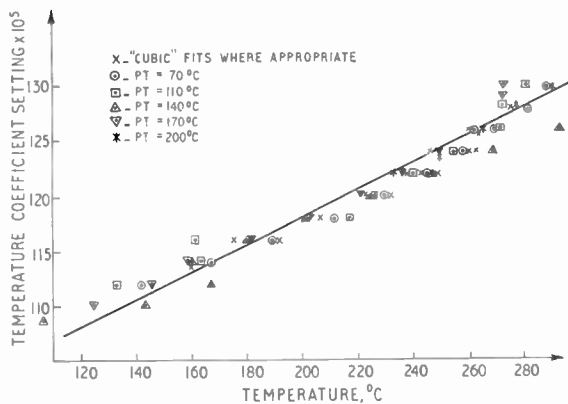


Fig. 18. Optimum setting of temperature coefficient against temperature for different plugging temperatures.

The least-squares fit to all the points yielded the relation:

$$\alpha_c = 0.124t + 93.41 \quad \dots\dots(6)$$

which is very close to the relation generally used in the past, i.e.

$$\alpha_c = 0.125t + 93.0$$

The values obtained for plugging temperatures of 70°C and 110°C were also used to plot the 'off-set factors'. This is the correction which has to be applied to any resistivity reading to relate this to some standard reading or 'base line' at a different setting of the temperature coefficient. Originally a standard setting of $\alpha_c = 130$ had been chosen, corresponding to a liquid metal temperature of nearly 300°C. Subsequently a lower value was adopted because the liquid metal temperature was usually between 230°C and 240°C. Fig. 19 shows these two off-set factors.

The average difference in indicated resistivity between the two plugging temperatures suggests a change in equivalent impurity content of some 20 to 25 parts in 10^6 .

The off-set factor as defined is a *correction* to be applied to a given reading, and it may be either positive or negative. As can be seen from the graphs, the off-set factor increases with decreasing temperature (or temperature coefficient). The correction is therefore positive if it is desired to refer a particular reading to a higher temperature, and vice versa.

Although it had been previously assumed that the variation of indicated resistivity with temperature could be represented by one universal function under all conditions, e.g. Fig. 16, it was found that the coefficient a in equation (4) actually increases slightly with increasing temperature. Its average value was about 6×10^{-7} , which agrees reasonably well with Eames' previous figure of 6.15×10^{-7} in Fig. 16. If a small third-order correction is applied in addition—equation (5)—the final expression for the temperature correction becomes,

$$\delta r = 7.4 \times 10^{-7} \cdot \delta t^2 - 10^{-9} \cdot \delta t^3 \quad \dots\dots(7)$$

A plot of this is shown in Fig. 20.

Once these calibration experiments had been completed the final graphs were issued to the operators to enable them to use the rhometer as an operational instrument for continuous monitoring of the impurity content of the primary coolant.

The main experience of continuous operation since January 1963 has been obtained so far from the

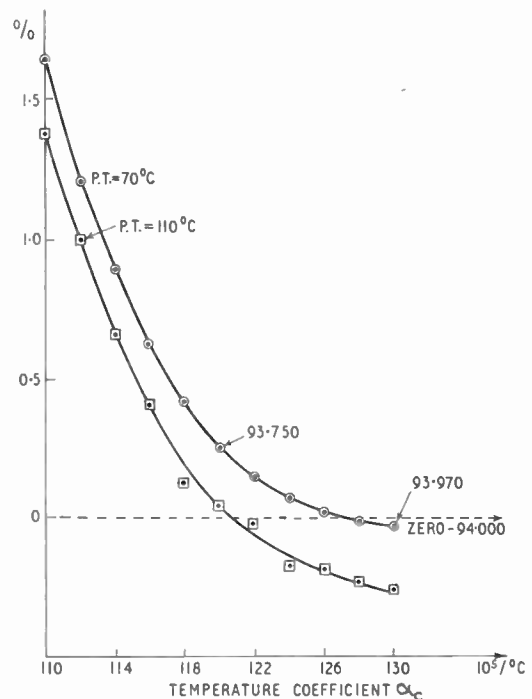


Fig. 19. Off-set factors.

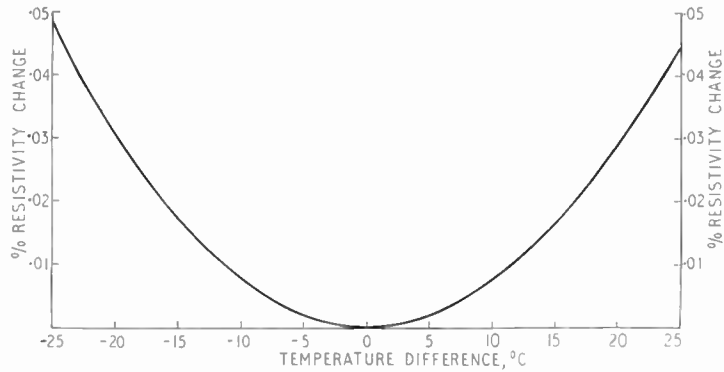


Fig. 20. Plot of the temperature correction expression.

rhometer installed in the main circuit, whereas the one in the permanent cold trap loop has been used largely for calibration and for occasional checks.

The instrument has been stable and has given reliable indications of long-term trends and of changes in the impurity content of the liquid metal. The rate of flow through the trap in this position has been of the order of 5–6 gal/min (22–27 l./min), and the liquid metal temperature has been in the range 215° to 240°C, both for normal operation at or near full reactor power. Conditions have generally been steady enough to allow the instrument to be used on its most sensitive range, $\pm 0.2\%$ f.s.d. Small ‘step’ negative excursions of the recorded rhometer trace which have been observed at irregular intervals on one of the instruments are believed to be caused by some kind of mechanical movement of the Mk. I head and/or compensator pipe.

During reactor runs the rhometer readings have been recorded about once every hour. After being reduced to standard conditions by means of the graphs

provided, the readings have been plotted against the corresponding plugging meter readings, expressed in parts per million of equivalent impurity content (see Fig. 21). The plugging meter is situated in the permanent cold trap loop.

The long-term agreement between the two instruments has been very good, i.e. the indication of general trends. There have been occasional short variations, such as the rhometer excursions mentioned above, which were observed on only one of the two instruments. The general agreement is regarded on the whole as satisfactory, and it is felt that the Mk. IA version used in 70/30 NaK has been reasonably reliable and has shown good long-term stability. Furthermore, at very low impurity levels, say less than 12 parts in 10^6 , the plugging meter becomes unreliable, and only the rhometer has, in fact, been used under these conditions.

The fact that its readings can easily be corrected and interpreted by using a set of standard graphs has been a major contributing factor towards increasing operators’ confidence in the instrument.

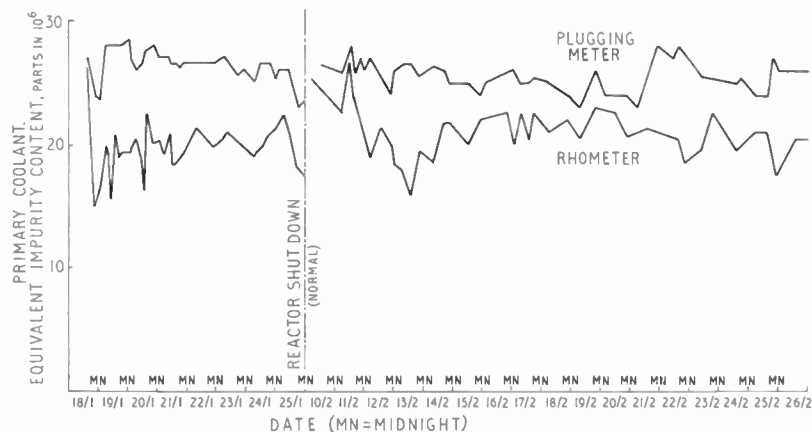


Fig. 21. Typical record of variation in impurity content of primary coolant with time.

7. Future Trends

The Mk. IA rhometer will probably become obsolete in the fairly near future as it is being replaced by the Mk. II version (cf. Sect. 3). Some of the results obtained with the Mk. IA will be useful for Mk. II operation, but detailed calibration work will have to be carried out again for the Mk. II. In addition, as future work will be concentrated more and more on Na rather than NaK a different set of calibration data will, in any case, be required.

Eames has shown that, in theory, a better approximation to the resistance/temperature characteristics of NaK and Na should be possible by using gold instead of platinum for the compensator. This should permit the use of the instrument over a much wider temperature range without the need for corrections. This is a promising line of further rhometer development. Experimental verification of the calculated behaviour of a gold compensator is required mainly because the second-order temperature coefficients of resistivity of the liquid metals are probably not known with sufficient accuracy.

8. Conclusions

Mark IA rhometers have shown good long-term stability on 70/30 NaK circuits. The readings can easily be corrected and interpreted by using a set of standard graphs. These can be obtained by operating a rhometer under carefully controlled conditions of temperature and high purity in an isolated loop.

Future work is required mainly on acquiring more data on rhometer sensitivity to various specific impurities, both in NaK and Na.

Temperature calibration data in Na should be obtained against the present platinum compensator. Finally it appears desirable to extend the temperature range over which operation is possible without any corrections, probably by replacing the platinum by a gold compensator.

9. Acknowledgment

The authors wish to thank Messrs. Bruce Peebles & Co. Ltd., Edinburgh, who manufactured the instruments referred to in this paper. The present U.K.A.E.A. licensees for the manufacture of rhometers are Messrs. James Scott (Electronic Engineering) Ltd., Glasgow.

10. References

1. L. R. Blake, "Resistivity monitor to indicate oxide content of sodium", *Proc. Instn. Elect. Engrs*, 107, Part A, No. 34, pp. 383-94, August 1960. (I.E.E. Paper No. 3278M, August 1960.)
2. L. R. Blake and A. R. Eames, "Electrical resistivity meter monitors oxygen content of liquid metals", *Nucleonics*, May 1961, p. 66.
3. E. Harrison and P. F. Roach, "An electrodeless conductivity meter for process control", *J. Brit.I.R.E.*, 26, pp. 25-33, July 1963.

Manuscript first received by the Institution on 11th January 1965 and in final form on 22nd March 1965. (Paper No. 983.)

© The Institution of Electronic and Radio Engineers, 1965

of current interest . . .

Seastations for Air Traffic Control

A new company called Seastation Telecommunications Limited has been formed to develop and supply trans-oceanic telecommunication systems to provide urgently needed navigation and communication facilities for the rapidly increasing high-speed air-traffic, especially on the North Atlantic routes. These facilities will consist of permanent floating seastations for carrying radio, radar and other aeronautical navigational equipment, interconnected with each other and with shore stations by a submarine cable communication system. The new company is undertaking a design study for such a system in collaboration with the Ministry of Aviation.

A floating seastation has been designed which can be moored in mid-ocean in deep sea and which is suitable both for the termination of a submarine cable and also for the installation of radio equipment. Communications from aircraft in the vicinity of the seastation can be passed to the distant shore by means of the submarine cable, and reliable circuits of the very highest quality can be obtained from aircraft to land and *vice versa*. The installation of seastations at intervals along the routes overflown by aircraft crossing the oceans can provide entirely dependable communication with these aircraft at all times.

The seastation consists of a tubular structure typically about 400 ft in length and 16 ft in diameter, floating vertically in the sea with the greater part of its length immersed. The top end of the cylinder supports a superstructure well above the reach of waves and providing accommodation for equipment, for crew, for a helicopter landing deck and for aerial systems. The bottom end of the cylinder is moored by three cables to anchorage on the sea bottom. The submarine telephone cables leave the bottom of the seastation and fall in catenaries to the ocean bed. Power is supplied by diesel oil generators.

The motions of the sea decrease rapidly with distance below the sea surface and the configuration of the seastation described makes use of this fact to the maximum advantage, achieving remarkable stability in the roughest weather. Calculations which have been confirmed by scale model tank tests indicate that for 95% of the time in the North Atlantic the half amplitude pitch or roll will not exceed 0.5 deg and the vertical motion 0.5 ft. Even for extreme conditions performance meets operational requirements in full.

The submarine cable with its installations on land and in the seastation follows well-proven practice and differs from previous cables only in respect of the catenary connections which are specially engineered. The cable and the seastations remain at sea for the life of the system which is designed for a minimum of

twenty years with only routine maintenance of equipment in the seastation.

The primary communication services provided from a seastation are intended to be radio in the v.h.f. and u.h.f. wavebands for air traffic control, for airline company traffic and for passenger-to-shore conversations. But this is by no means the only use of seastations. A number of navigational services for aircraft can be accommodated and primary and secondary radar facilities can be added. Weather reporting and weather forecasting are other uses and all the services can be envisaged as applicable to ships as well as to aircraft.

Mullard Donation to Space Science Research

University College London, following a promise by the Mullard Company to contribute £65,000 towards space science research, is to establish an outpost of the Physics Department specifically devoted to space research. They have purchased Holmbury House, near Dorking, Surrey, which will be known as the Mullard Space Science Laboratory and will be headed by Professor R. L. F. Boyd. The other group in the College engaged in space research, led by Dr. G. V. Groves, will remain in London.

The Department of Physics at University College, London, has played a pioneering role in this field. Sir Harrie Massey, F.R.S., Quain Professor of Physics at University College in the University of London, who is head of the Department and also Chairman of the recently formed Government Council on Scientific Policy, was responsible for initiating scientific space research in this country in 1953.

The group in the Physics Department, led by Professor R. L. F. Boyd, made the first experiments in the U.K. using rockets for the study of the upper atmosphere. This group has grown rapidly and was responsible for some two-thirds of the experiments so successfully flown in *Ariel I*, the first Anglo-American satellite.

Over the next three years the Department's extensive research programme is planned to utilize no less than eight satellites and many more high altitude research rockets. The main investigations with which they will be concerned are in the fields of ultra-violet and X-ray astronomy, both of the sun and of other celestial objects and the study of the ionosphere and the interplanetary medium.

Initially there will be a staff of about fifty at Holmbury House, a large Victorian mansion. It is hoped that the laboratory will be fully operative by the beginning of the next academic year (starting October 1965), and it is anticipated that the group will grow to about 100 people in five to seven years' time.

The Determination of the Parameters of a Dynamic Process

By

PETER C. YOUNG,
Dip.Tech.(Eng.), D.L.C. †

Summary: The paper shows how the mathematical methods of steepest descent may be used to minimize certain functions of the 'satisfaction error' of a dynamic process. This minimization procedure forms the basis of certain automatic techniques for determining the coefficients or parameters of the process transfer function. The techniques, which are easily mechanized from normal analogue computer components, appear to be limited to the investigation of low order processes. In addition to their value as a new approach to the experimental analysis of dynamic systems (termed the 'analysis of dynamic experiments'), it is shown that equipment of this type could be utilized in the design of a simple 'self adaptive' control system. Finally, possible future developments are discussed, with particular emphasis on the employment of digital mechanization.

List of Symbols

t	time	E_1	magnitude of 'satisfaction' error ($ E $)
$p_r(t)$	time dependent variables appearing in the general process dynamic equation (these could be such signals as the input disturbance and its derivatives, the dependent variable, and its derivatives or combinations and multiples of these, etc. ($r = 0 \rightarrow r = k$))	E_2	square of 'satisfaction' error (E^2)
$p_r(0)+$	initial condition of time dependent variables $p_r(t)$	$\text{sign } E = E/ E = E/E_1$	
a_r	parameters or coefficients which describe the process within the structure of the process equation ($r = 0 \rightarrow r = k$)	s	Laplace operator
a_{rc}	calculated values of parameters ($r = 0 \rightarrow r = k$)	∇	gradient of a vector
$f(t)$	input forcing function or disturbance	i_r	unit vectors in co-ordinate directions
$p = p(t)$	dependent variable	K_r	constant terms (where r can be various integers)
$\dot{p} = \frac{dp}{dt}$		$D(s)$	general filter transfer function
E	'error in satisfaction of process equation' or 'satisfaction' error	a_n, b_m	process parameters in general process linear differential equation ($n = 0 \rightarrow N; m = 0 \rightarrow M$)
		$\left. \begin{array}{l} \frac{d^m f(t)}{dt^m} \\ \frac{d^n p(t)}{dt^n} \end{array} \right\}$	derivatives of input forcing function and process dependent variable in general process linear differential equation ($m = 0 \rightarrow M; n = 0 \rightarrow N$)
		ε	small interval of time
		$\frac{1}{c_r}$	low-pass filter time-constant ($r = 1 \rightarrow L$)

1. Introduction

The engineer is often confronted with the problem of identifying the dynamic characteristics of a physical process in some usable mathematical terms. Although he may sometimes attempt to solve this problem by a purely theoretical approach, it is usually easier, and more desirable, to make use of both theoretical and experimental information. This paper provides a brief introduction to certain automatic process

identification schemes which might be considered as effectively mechanizing this theoretical-experimental technique.

A 'parameter determination computer' (p.d.c.) is programmed by making an estimate of the *form* of the continuous dynamic equations which provide the best mathematical model of the process dynamic performance characteristics. The computer accepts information on the reaction of the process to its normal 'in operation' input disturbances. It is then able to compute those coefficients or parameters which best describe the process within the structure of the

† Loughborough College of Advanced Technology, Loughborough, Leicestershire.

estimated mathematical model, and 'track' any slow changes which may occur in these parameters.

The 'parameter tracking' methods used in the p.d.c. were developed initially from the technique of 'implicit synthesis' suggested by Clymer.¹ This technique was itself developed from the well-known method of 'implicit computation', which has been used for some considerable time on analogue computers as a means of achieving a division circuit, and for the solution of algebraic linear simultaneous equations, etc.^{2a} The methods are based upon the minimization of certain functions of the 'satisfaction error' of a process. It is shown that this minimization procedure can be treated as the descent of a time variable hypersurface with a characteristic valley-like structure. The treatment appears perfectly general for any process described by an equation of the form:

$$\sum_{r=0}^{r=k} a_r \cdot p_r(t) = 0$$

where $p_r(t)$ are time dependent variables appearing in the general process dynamic equation. These could be such variables as the input disturbance and its derivatives, the dependent variable and its derivatives or combinations and multiples of these, etc., and a_r are parameters or coefficients describing the process within the structure of the above equation.

In this general form the equation could describe either a linear or a non-linear process.

In addition to supplying a new approach to the analysis of dynamic experiments, it is shown that this type of automatic process identification scheme could be used as the basis of a simple 'self adaptive control system'. In this connection, the techniques described here are compared, briefly, with the better known and closely related 'model reference' procedures.

At their present state of development, the various analogue parameter determination computers appear to be limited to the investigation of low order processes. However, more sophisticated hybrid (analogue-digital) equipment has been developed which has greater accuracy and speed of response than the purely analogue equipment, and should be able to track many more unknown parameters.

2. Parameter Estimation by Consideration of the 'Satisfaction' Error

In the context of this paper, the parameter tracking problem is concerned with the determination of the coefficients, a_r , of processes described by equations of the form

$$\sum_{r=0}^{r=k} a_r \cdot p_r(t) = 0 \quad \dots\dots(1)$$

where $p_r(t)$ are time variable functions, whilst a_r are constant or very slowly varying coefficients (i.e. slowly varying when compared with the variables $p_r(t)$).

A simple example of such a process would be an approximately first-order dynamic system which could reasonably be described by an equation of the form:

$$a_0 p + a_1 \dot{p} = f(t)$$

or

$$a_0 p + a_1 \dot{p} - f(t) = 0 \quad \dots\dots(2)$$

where $f(t)$ is an arbitrary forcing disturbance to the process

p is the output dependent variable

$\dot{p} = \frac{dp}{dt}$, is the first derivative of p .

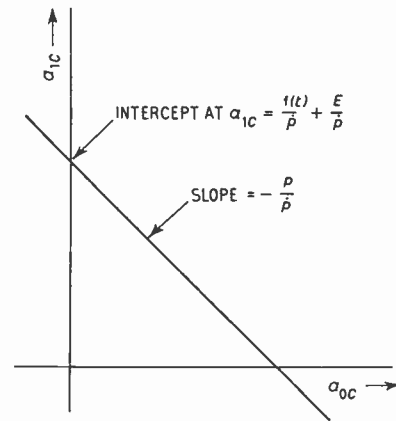


Fig. 1. Straight line in $a_{1c}-a_{0c}$ plane.

Now by allowing $p = p_0(t)$, $\dot{p} = p_1(t)$ and $f(t) = p_2(t)$, the equation (2) may be written:

$$\sum_{r=0}^{r=2} a_r \cdot p_r(t) = 0$$

where $a_2 = -1$, which is a particular case of the general equation (1).

In order to illustrate the fundamental principles involved in the determination of the value of the coefficients a_r for any process, it will be convenient to refer initially to the system described by equation (2).

Suppose we select any arbitrary values for the coefficients a_0 and a_1 , and call these a_{0c} and a_{1c} respectively. Substitution of these values into eqn. (2) will give the equation:

$$a_{0c} p + a_{1c} \dot{p} - f(t) = E \quad \dots\dots(3)$$

where E is some function which will depend upon the degree of error between both a_{0c} and a_0 and also a_{1c} and a_1 ; E , which will have the value zero only when a_{0c} and a_{1c} satisfy eqn. (2), is sometimes called the

'error in satisfaction of the process equation' or, more simply, the 'satisfaction error'.

At any arbitrary instant of time p , \dot{p} and $f(t)$ can be considered constant. Equation (3) can then be written:

$$a_{1c} = -\frac{p}{\dot{p}} a_{0c} + \left(\frac{f(t)}{\dot{p}} + \frac{E}{\dot{p}} \right) \dots\dots(4)$$

Equation (4) is the equation of a straight line in the $a_{1c}-a_{0c}$ plane (see Fig. 1). The slope of the straight line will be given by the value of $-p/\dot{p}$ at the instant of time selected whilst the value of $\left(\frac{f(t)}{\dot{p}} + \frac{E}{\dot{p}} \right)$ at this same instant of time, will supply the value of the intercept of the line with the a_{1c} ordinate.

Variation of the value of E will produce a set of parallel straight lines as shown in Fig. 2. If only the magnitude of E is considered (i.e. $|E|$ which will be called E_1) then the straight lines might be regarded as contours in the $a_{1c}-a_{0c}$ plane. The contours describe a valley-like surface, the valley bottom being indicated by the line $E_1 = 0$ (Fig. 2).

This analysis suggests that at any arbitrary instant of time an infinite number of values of a_{0c} and a_{1c} satisfy the criterion $E_1 = 0$ (i.e. all pairs of values occurring along the line $E_1 = 0$).

Suppose the variations of $f(t)$ and the dependent variables p and \dot{p} for a particular first-order system are considered. A simple illustration would be the response of a one-second time-constant first-order system subjected to a unit-step input. The equation

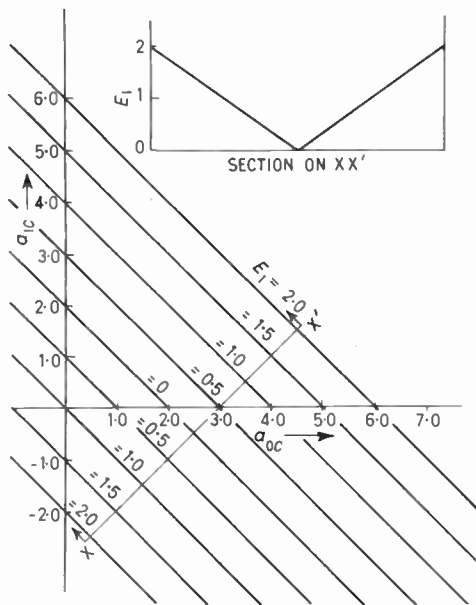


Fig. 2. The instantaneous surface E_1 .

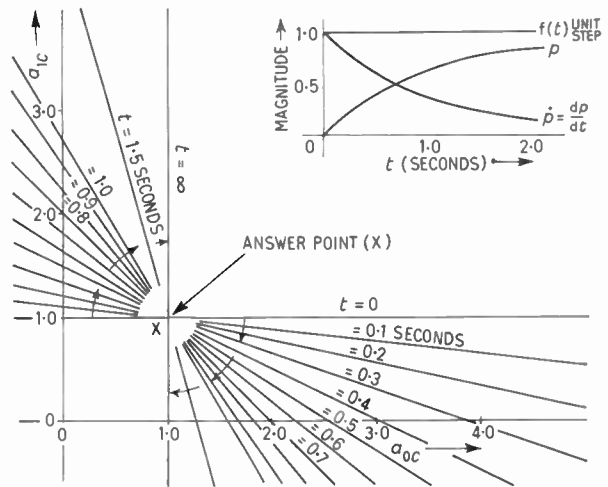


Fig. 3. Variation of line $E = 0$ for unit step input.

describing the error parameter surface would be of the form

$$|a_{0c}p + a_{1c}\dot{p} - 1| = |E| = E_1 \dots\dots(5)$$

The variations of p and \dot{p} caused by a unit step input are shown in the inset to Fig. 3. When E_1 is considered zero, a series of straight lines can be constructed from eqn. (6)

$$a_{1c} = -\frac{p}{\dot{p}} a_{0c} + \left(\frac{1}{\dot{p}} \right) \dots\dots(6)$$

by substitution of values of p and \dot{p} occurring at several instants of time after the application of the unit step. Each straight line represents the position of the line $E_1 = 0$ in the $a_{1c}-a_{0c}$ plane at the particular instant of time considered (Fig. 3).

It is apparent from this figure that during the transient caused by the unit step disturbance, the line $E_1 = 0$ rotates about the point X ($a_{1c} = 1.0$, $a_{0c} = 1.0$). This line has zero slope at the initiation of the step and approaches an infinite slope as the transients die out. It is only the point X which satisfies eqn. (7)

$$a_{0c}p + a_{1c}\dot{p} - 1 = 0 \dots\dots(7)$$

at all instants of time. Reference to Fig. 3(b) indicates that the solution for the problem in question is $a_{1c} = 1.0$ and $a_{0c} = 1.0$, and this agrees with the system chosen (i.e. $\frac{1}{1+S}$, unity gain, one-second constant).

It is interesting to note that on the application of repeated alternate positive and negative unit-step inputs, the line $E_1 = 0$ rotates about the point X in a similar manner to that noted for a single unit-step input. However, provided the frequency of fluctuation of the input is within the bandwidth of the system the

line instantaneously returns to a slope of +0.5 at each reversal of the step forcing function. The process reacts to the change in input and the line rotates in a clockwise direction, through an angle which approaches $(90 + \tan^{-1} 0.5)$ degrees asymptotically as the transients die out.

By similar reasoning, it will be seen that the line $E_1 = 0$ will rotate about the point X for any arbitrary finite input. A change in the input to the system merely modifies the pattern of rotation of the line and does not affect the point of rotation.

Thus, if an arbitrary finite input to the process is denoted by $f(t)$, the coefficients given by the point (X) satisfy the eqn (8);

$$a_{0c}p + a_{1c}\dot{p} - f(t) = 0 \quad \dots\dots(8)$$

at all instants of time.

Up to this stage only the rotational behaviour of the line $E_1 = 0$ has been discussed. However, if we investigate the surface described by eqn. (5) it is apparent that it has the characteristic valley formation (Fig. 2) with the line $E_1 = 0$ indicating the valley bottom. As time varies, therefore, the line $E_1 = 0$ and consequently the associated surface;

$$E_1 = |a_{1c}\dot{p} + a_{0c}p - f(t)| \quad \dots\dots(9)$$

rotate about the answer point, provided $f(t)$ is a finite input.

By consideration of the above remarks, it is possible to make the specific conclusion that the values of the parameters a_0 and a_1 of a first-order process described by the equation:

$$a_0p + a_1\dot{p} - f(t) = 0 \quad \dots\dots(10)$$

may be determined by investigation of the instantaneous surface,

$$E_1 = |a_{0c}p + a_{1c}\dot{p} - f(t)| \quad \dots\dots(11)$$

in the $a_{0c}-a_{1c}-E_1$ space, together with the pattern of rotation of this surface during transients of p and \dot{p} caused by fluctuations in the forcing disturbance $f(t)$.

Now the coefficient a_k of the equation

$$\sum_{r=0}^{r=k} a_r \cdot p_r(t) = 0 \quad \dots\dots(12)$$

may be assumed unity without loss of generality. Thus by analogy with the first-order case considered above, it may be concluded that, in general, the k coefficients (a_0, a_1, \dots, a_{k-1}) of eqn. (12) may be determined by investigation of the nature and movements of the hypersurface of k dimensions, contained in a Euclidean space of $(k+1)$ dimensions,

$$a_{0c} - a_{1c} - a_{2c} \dots a_{(k-1)c} - E_1$$

and described by the equation:

$$\left| \sum_{r=0}^{r=k} a_{rc} \cdot p_r(t) \right| = E_1 \quad \dots\dots(13)$$

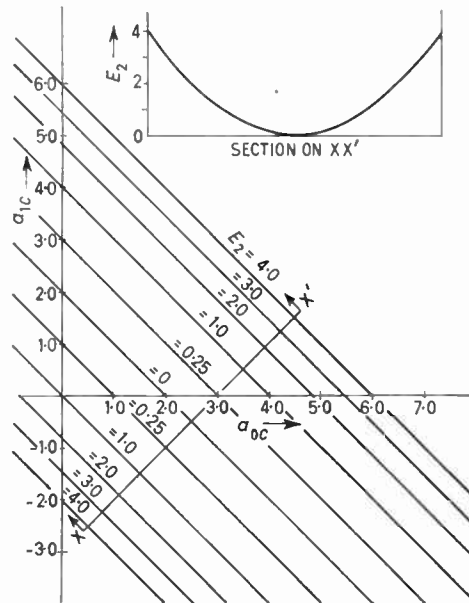


Fig. 4. The instantaneous surface E_2 .

where $a_{kc} = 1.0$.

By similar analysis, it can be shown that the hypersurface,

$$\left[\sum_{r=0}^{r=k} a_{rc} \cdot p_r(t) \right]^2 = E^2 = E_2 \quad \dots\dots(14)$$

where $a_{kc} = 1.0$, has similar properties to the hypersurface represented by eqn. (13), and so the conclusions of the last paragraph will also apply to this function. An illustration of such a surface for a first-order process described by eqn. (8) is shown in Fig. 4. Here, the equation of the surface in the $a_{0c}-a_{1c}-E_2$ space is

$$[a_{0c}p + a_{1c}\dot{p} - f(t)]^2 = E_2 \quad \dots\dots(15)$$

and the instantaneous valley is parabolic in cross-section. The error parameter E_2 has the advantage of being always positive and, consequently, the eqn. (14) naturally represents a valley-type of hypersurface in the $a_{0c}-a_{1c}-\dots-a_{(k-1)c}-E_2$ space. It is no longer required to consider the magnitude of the error quantity, as was found necessary with the straight 'satisfaction' error, E .

3. The Method of Steepest Descent

The parameter tracking technique is concerned with the continuous adjustment of parameters such as a_{rc} in eqn. (13), until they achieve values a_r which satisfy the eqn. (12) at all instants of time. Such a technique can be considered as a traversal of the error parameter hypersurface from any arbitrary co-ordinates a_{rc} to the point satisfying the criterion that the error

parameter (E_1 or E_2 in the context of this paper) is minimum at all instants of time.

It is possible to conclude from the previous section that such a process would require descent of the instantaneous valley in the error parameter hypersurface, and convergence to the co-ordinates of the axis of rotation of this valley.

There are numerous ways of performing such a tracking task, but the one which will be discussed here is that achieved by taking the path of steepest descent. In the context of the problem under consideration, the path of steepest descent (or steepest negative gradient) of the instantaneous valley is defined as that path which is the tangent to the negative gradient of the error function (E_1 or E_2) at each point. It can be shown that, for a stationary function in an n dimensional Euclidean space, this path decreases the value of the error parameter most rapidly with respect to the distance travelled.^{2(c),4}

The gradient vector of a function $E(a_0, a_1, \dots, a_{k-1})$ in the $a_0 \rightarrow a_{k-1}$ space can be defined as,

$$\text{grad } E = \nabla E = \sum_{r=0}^{r=k-1} \frac{\partial E}{\partial a_r} i_r \quad \dots\dots(16)$$

where i_r are unit vectors in the $(k-1)$ co-ordinate directions

$$\left(\text{e.g. } \nabla E_1 = \frac{\partial E_1}{\partial a_{0c}} i_0 + \frac{\partial E_1}{\partial a_{1c}} i_1 + \dots + \frac{\partial E_1}{\partial a_{(k-1)c}} i_{k-1} \right)$$

It is readily shown that the differential equations describing the path of steepest descent are:

$$\frac{da_r}{dt} = -K \frac{\partial E}{\partial a_r} \quad (r = 0 \rightarrow k-1) \quad \dots\dots(17)$$

where K is a positive constant which will determine the rate at which descent occurs.^{2(c),4}

For example equations on E_1 hypersurface of k dimensions:

$$\begin{aligned} \frac{da_{0c}}{dt} &= -K \frac{\partial E_1}{\partial a_{0c}} \\ \frac{da_{1c}}{dt} &= -K \frac{\partial E_1}{\partial a_{1c}}, \text{ etc.} \\ \frac{da_{(k-1)c}}{dt} &= -K \frac{\partial E_1}{\partial a_{(k-1)c}} \end{aligned}$$

It is common practice to describe the method of steepest descent as the 'least magnitude' method when applied to descent on the hypersurface E_1 , and the 'least squares' method when applied to the hypersurface E_2 .

Although the problem under consideration concerns the descent of a time variable hypersurface, a purely qualitative assessment of the situation indicates that, by application of the method of steepest descent, it is

possible to make the running point (i.e. the instantaneous values of a_{rc}) converge on the answer point (the value of $a_{rc} \equiv a_r$ which satisfies eqn. (12)).

In order to achieve this object it appears necessary that:

- (a) The answer point, as defined by the point of rotation of the hypersurface, is stationary or only slowly varying in position.
- (b) The rate of descent, which is governed by the magnitude of the gain K (eqn. (17)), should be reasonably large.
- (c) The input to the process is such that the hypersurface continues to make rotational fluctuations about the answer point. Should the hypersurface be stationary or only rotating slowly in one direction (as would be the case for a constant input), then the path can become indeterminate once the running point achieves the valley bottom (i.e. error parameter = 0). For this reason, it is necessary that sufficient fluctuations are induced so that the running point is forced to converge on the answer point.

A simple theoretical analysis of the problem (Appendix 2) suggests that, although the above conditions are necessary, they are not, in themselves, sufficient to completely ensure the asymptotic behaviour of these particular steepest descent procedures. However, the conditions should be a reasonable guarantee that the necessary convergence will be achieved. In addition to this, Kaya and Yamamura⁷ have correctly regarded the least-squares tracking procedure as the solution of a set of simultaneous algebraic equations with variable coefficients, and have assessed its stability by the well-known stability criterion of Goldberg and Brown.^{2b,12} Their analysis has indicated that the stability of the 'least squares' mechanization (see Section 4.1) is ensured, provided the process input does not remain constant for a long period of time. This conclusion is in general agreement with provision (c) above.

4. Computer Mechanization

The previous sections have described certain theoretical methods of identifying an unknown dynamic process. The success of these methods is dependent upon an ability:

- (a) To make a reasonable estimate of the form of the mathematical model which best describes the process.
- (b) To observe continuously the normal operation input/output signals of the process.

It is now necessary to describe how these theoretical techniques can form the basis of certain automatic 'parameter determination computers' (p.d.c.) which

are constructed entirely from ordinary analogue computer components.

In line with previous analysis, this description will be limited to computers capable of investigating linear first-order processes.

4.1. Parameter Tracking by the 'Least Squares' Method

Consider the first-order process which it is assumed may be described by eqn. (10). The square of the satisfaction error will be given by:

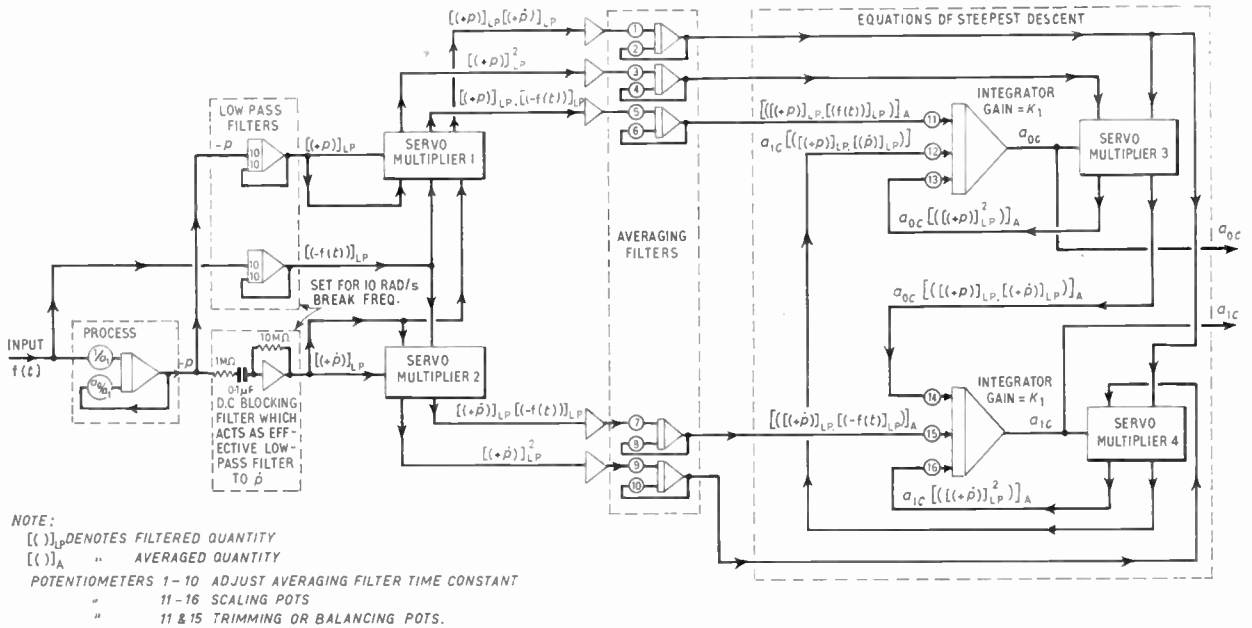


Fig. 5. Mechanization of 'least squares' parameter tracking system for a first-order process.

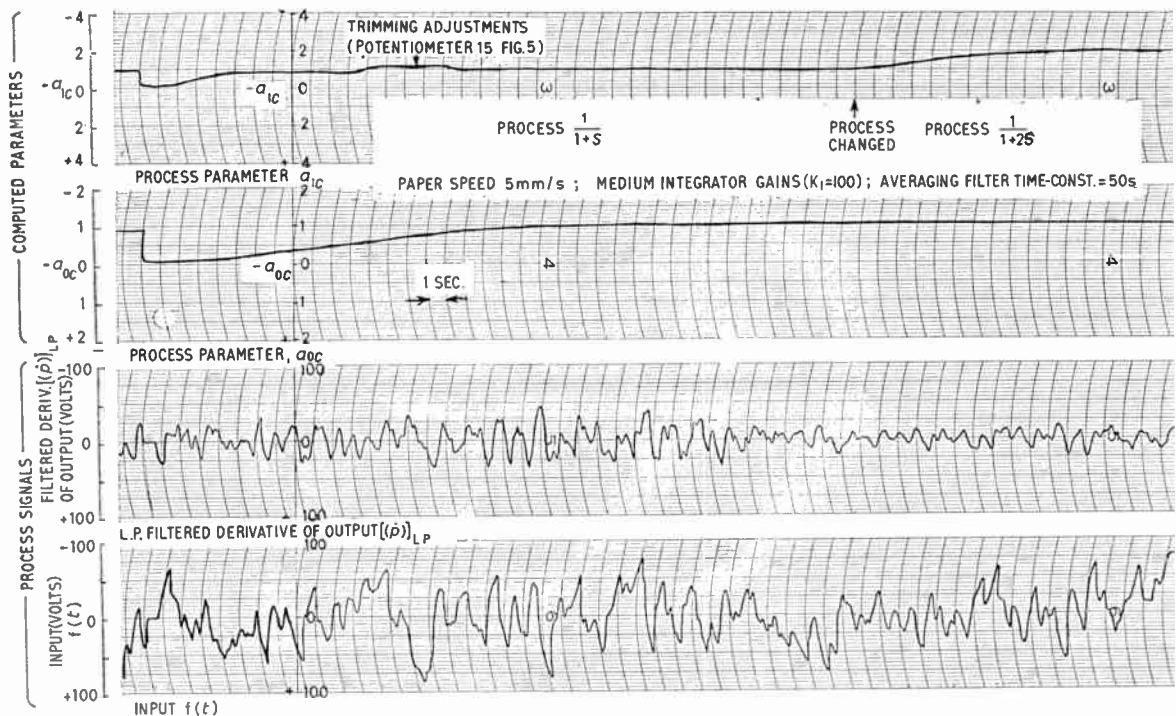


Fig. 6. Performance of p.d.c. system (least squares) for random input.

$$E^2 = E_2 = (a_{0c}p + a_{1c}\dot{p} - f(t))^2$$

The equations of steepest descent become:

$$\frac{da_{0c}}{dt} = \dot{a}_{0c} = -K \frac{\partial E_2}{\partial a_{0c}} = -K_1(a_{0c}p^2 + a_{1c}p\dot{p} - pf(t))$$

$$\frac{da_{1c}}{dt} = \dot{a}_{1c} = -K \frac{\partial E_2}{\partial a_{1c}} = -K_1(a_{0c}p\dot{p} + a_{1c}\dot{p}^2 - \dot{p}f(t))$$

where $K_1 = 2K$.

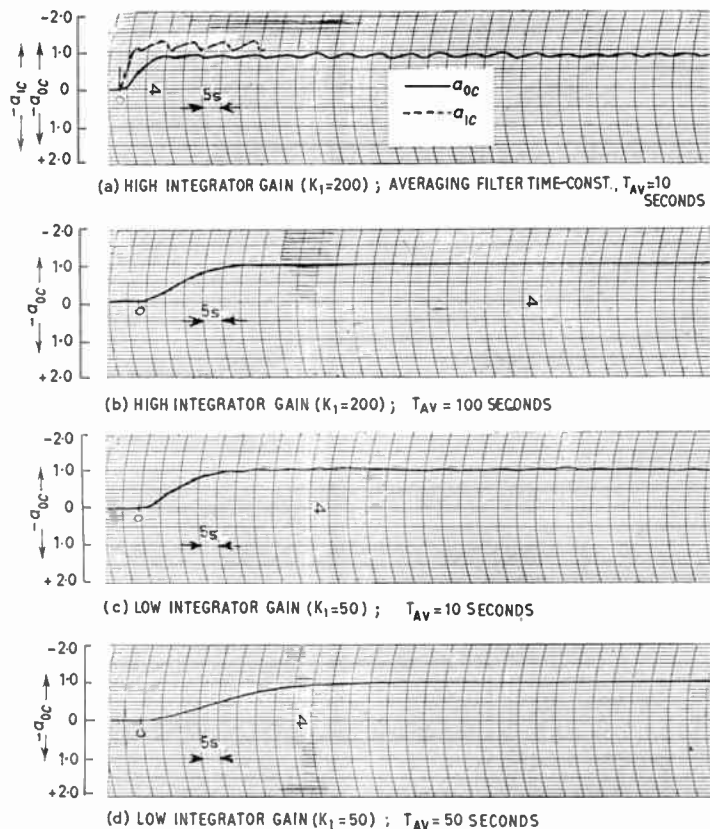
The mechanization of these equations has been carried out by the author on the analogue computing system of the Department of Electrical Engineering at Loughborough College of Advanced Technology. A brief description of this system, together with details of the major components used in the above mechanization, is contained in Appendix 4. The circuit diagram of the mechanization is shown in Fig. 5. Various additional features can be seen on this circuit diagram which require explanation.

Firstly, the input and output signals of the process are sent through a low-pass filter in order to separate out the frequency band which is of interest. This is not important when we are considering an ideal first-order process. However, if the tracking system is investigating a higher order process in order to find the first-order approximation within a particular

frequency range, or if the process signals are troubled by high-frequency noise, then such filters become necessary.

Secondly, the various multiples of the filtered input and output signals are averaged by means of a low-pass filter (i.e. filter with a large time-constant). By weighting the signals into the past,¹⁵ this device is able to reduce the sensitivity of the steepest descent system to rapid fluctuations of the error parameter surface. Although, as we have seen, the instrumentation must necessarily react to these fluctuations, it is found that by decreasing the sensitivity in this manner it is possible to increase the stability of computation of the tracked parameters a_{1c} and a_{0c} . The addition of the averaging filters successfully eliminates the tendency for the running point to oscillate about the answer point in sympathy with the movements of the error parameter surface (see Fig. 7 and Fig. 10). Unfortunately, this improvement in tracking performance is accompanied by a necessary decrease in the speed of response of the system. Consequently, both the integrator gain K_1 and the averaging time-constant will effect the speed of response of the system, and these must be selected to give the most satisfactory overall performance. The justification for the use of filtered signals in the computation is discussed in Appendix 3.

Fig. 7. Effect of integrator gain and averaging filter time constant on performance of p.d.c. system (least squares). (N.B.— $a_{1c}a_{0c}$ computation shown in Fig. 7(a). But only a_{0c} computation shown in Fig. 7(b), 7(c) and 7(d). Process input—repeated steps (see Fig. 8.)



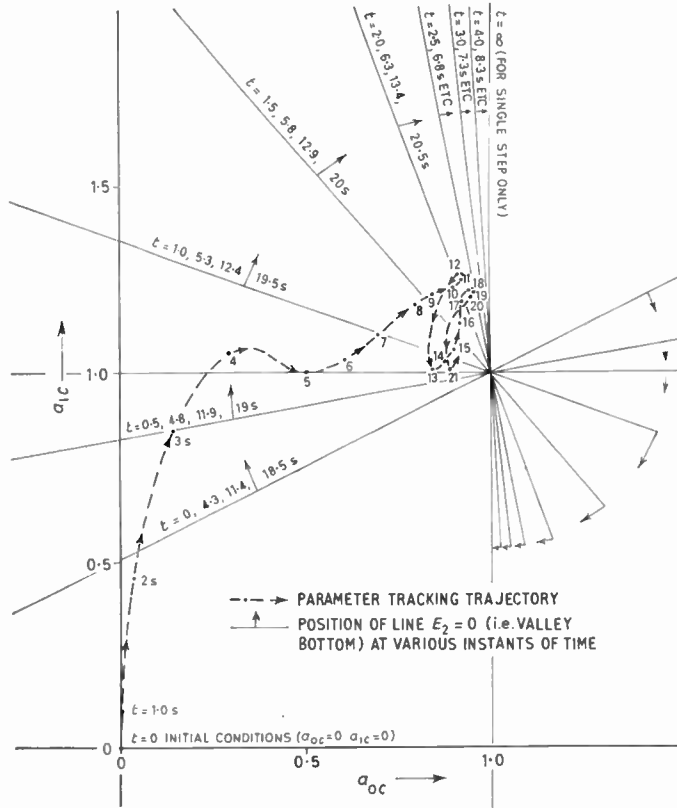
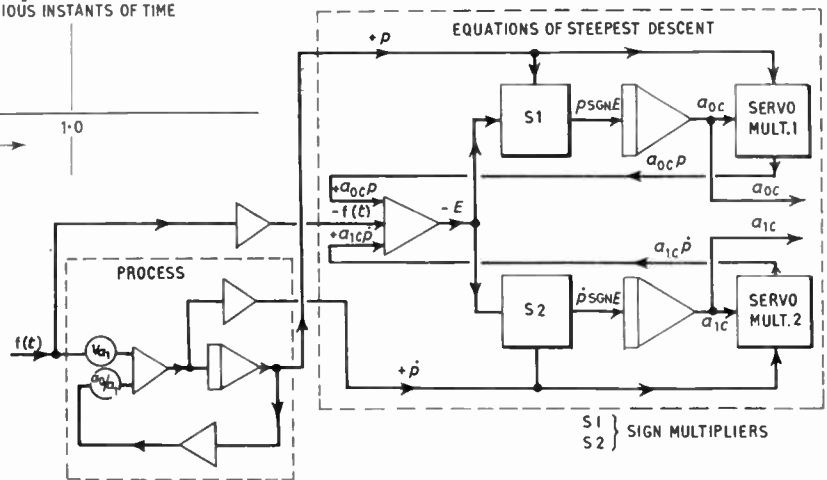


Fig. 8. Plot of Fig. 7(a) on $a_{1c} - a_{0c}$ plane.

Fig. 9. Idealized mechanization of 'least magnitude' parameter tracking system for a first order process.



Theoretically, the 'least squares' method is extendable to the detection of any number of unknowns. However, the inaccuracy incurred by virtue of the necessary increase in complexity and hardware will limit the number of unknowns which can be handled satisfactorily. The system required to track three unknown parameters is quite complicated but has been found to work reasonably well.

The performance of the parameter tracking system for random input disturbances is shown in Fig. 6 whilst an example of the effect of the integrator gain and averaging time-constant on the system response is shown in Fig. 7. Figure 8 shows the plot of Fig. 7(a) on the $a_{1c} - a_{0c}$ plane. This is interesting as it illustrates very well the descent of the variable error parameter surface.

4.2. Parameter Tracking by the 'Least Magnitude' Method

Consider once more the first-order process described by the equation

$$a_0 p + a_1 \dot{p} - f(t) = 0 \quad \dots\dots(18)$$

The magnitude of the satisfaction error will be given by

$$|a_0 c p + a_1 c \dot{p} - f(t)| = |E| = E_1 \quad \dots\dots(19)$$

Consequently the equations of steepest descent are:

$$\frac{da_{0c}}{dt} = \dot{a}_{0c} = -K \frac{\partial E_1}{\partial a_{0c}} = -K p \operatorname{sgn} E \quad \dots\dots(20)$$

$$\frac{da_{1c}}{dt} = \dot{a}_{1c} = -K \frac{\partial E_1}{\partial a_{1c}} = -K \dot{p} \operatorname{sgn} E \quad \dots\dots(21)$$

where the $\text{sgn } E \left(= \frac{E}{|E|} \right)$ is included so that the surface E_1 is considered and not the surface E .

The equations may be mechanized on the analogue computer in the manner indicated by the idealized circuit shown in Fig. 9. Here, $p \text{sgn } E$ and $\dot{p} \text{sgn } E$ are generated and put through integrators each having a gain of K . The output of these integrators supply the values of a_{0c} and a_{1c} respectively.

The various additional features which were incorporated to improve the overall performance of the 'least squares' tracking system have also been found necessary in the mechanization of the 'least magnitude' system. Similarly, the conclusions of section 4.1 as regards speed of response apply equally to this equipment.

In any practical mechanization of the system shown in Fig. 9 the running point will very rarely remain completely stationary once it has achieved the answer point. It will inevitably be subject to slight fluctuations, which can result in rapid and repeated activation of the relay element contained in the sign multiplier (see Glossary of Symbols, Appendix 1). This relay 'chatter' often leads to still greater variation in the position of the running point and, consequently, highly inaccurate and unacceptable performance. The inclusion of a small inert or attenuated zone on the E signal can help to solve this problem but it does tend to introduce a little inherent inaccuracy into the computation. Even with this precaution, however, the

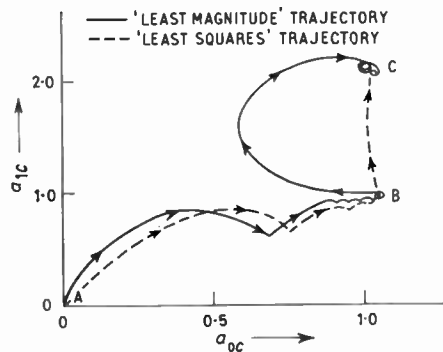


Fig. 10. Comparison of least squares and least magnitude trajectories shows marked interaction between computing channels which characterizes the least magnitude system.

Point A: First order process parameters set to $a_0 \approx 1.0$; $a_1 \approx 1.0$. Both tracking systems switched to operate. The systems perform their tracking task and converge on the point B.

Point B: Answer point: $a_{0c} \approx 1.0$; $a_{1c} \approx 1.0$. Each system's running point remains at or slightly oscillates about B until process parameter a_1 is changed to ≈ 2.0 . The systems then once more begin to track and finally converge on point C.

Point C: Answer point $a_{0c} \approx 1.0$; $a_{1c} \approx 2.0$.

'least magnitude' systems are characterized by far less inherent stability than is found in the equivalent 'least squares' systems. Considerable interaction exists between various computing channels, so that it is possible for the equipment to indicate transient fluctuations in all process parameters when only one parameter is varying (see Fig. 10).

B. G. Madden³ has developed a tracking system whose mechanization is very similar to that shown in Fig. 9. Madden investigated a second-order process having only two unknown coefficients. He required that convergence to an answer point should take place within the duration of the time derivatives of the dependent variable resulting from the application of a single unit step. As we have seen, such convergence would not occur in this period due to the indeterminate nature of the hypersurface valley bottom. Repeated fluctuations of the input function are required to force the operating point (the instantaneous values of a_{rc}) towards the answer point.

Two solutions to this problem are suggested. Firstly, tailoring of the individual integrator gains could force the operating point to intersect the line

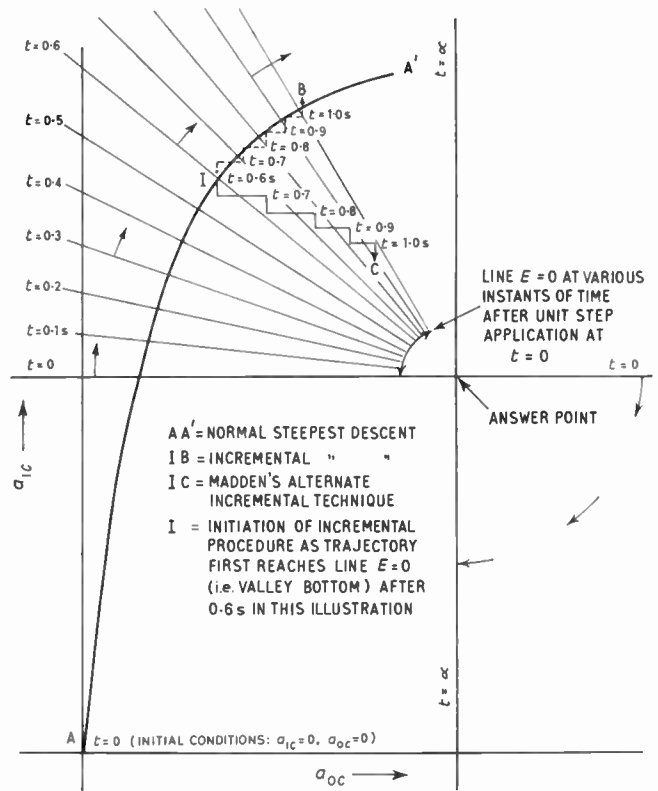


Fig. 11. Possible approximate trajectories to illustrate Madden's alternate switching method. (Steps exaggerated to emphasize principle involved.)

6. Model Reference Systems

It will be convenient at this point to mention a closely allied method of self-adaptive control known as the 'model reference system'. This procedure entails the minimization of some function of the error between an actual system transient response and that of a model having the required response characteristics, and which is subjected to the same input (see Fig. 15). The philosophy behind, and the mechanization of, such methods as these are adequately and lucidly described by several authors. Eykhoff⁸ deals with both model reference and satisfaction error parameter tracking systems, whilst Whitaker *et al.*⁹ and Clark *et al.*¹⁰ apply model reference philosophy to the actual adaptive control of aircraft. Margolis and Leondes¹¹ discuss certain types of model reference system very fully, and go on to assess the stability of such systems by means of the second method of Lyapunov.

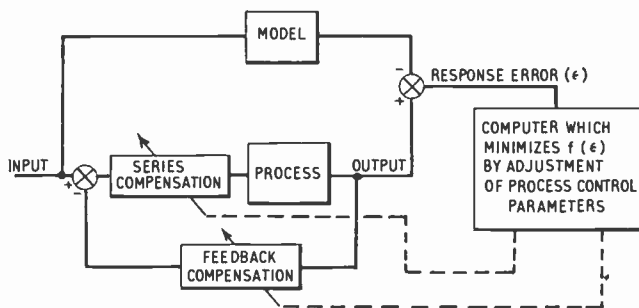


Fig. 15. Schematic diagram of a model reference adaptive system.

The model reference methods can be used in the straightforward parameter tracking role. In this application the model coefficients are adjusted to minimize the error parameter, and it is in this condition that they indicate the values of the unknown process parameters.

The aircraft autostabilization problem is concerned with the improvement of natural aircraft handling qualities by the provision of artificial stability created by an automatic control system of some kind. 'Model reference' self-adaptive control is particularly applicable to the design of the autostabilization system because of its dependence on the minimization of a function of the error between the actual and desired transient response. The 'model reference' system, in minimizing this error function, directly controls the aircraft response characteristics.

The achievement of self-adaptive control by means of the class of parameter tracking techniques discussed in this paper (satisfaction error self-adaptive control (SESAC)), requires additional instrumentation in order

to utilize the information gleaned from the tracking system. Also the system, in its basic form, contains no check on whether the desired process transient response is being achieved.

Despite such disadvantages, these methods, and in particular later 'hybrid SESAC' methods which have been developed by the author,^{13, 14} are characterized by their simplicity of mechanization, which compares very favourably with that of equivalent model reference systems. In addition, the SESAC system does not require a detailed *a priori* knowledge of the variation in the process dynamic characteristics which the model reference systems find necessary in order that suitable response error parameters may be chosen.

Although a much larger amount of work has been carried out on model reference techniques, even to the point of applying them to the actual self-adaptive control of aircraft,⁹ it is felt that the SESAC techniques, possibly with model reference trimming adjustments, have a great deal to offer in the field of aircraft autostabilization.

7. Conclusions

The techniques of parameter tracking which depend upon the minimization of functions of the 'satisfaction' error of a process have been described by the use of a particular physical interpretation of the basic mathematical principles involved. The development of these techniques is still in its infancy, and there are many problems which are still to be solved before the various methods are completely satisfactory from the point of view of both accuracy and speed of response.

The 'least squares' technique, although more complicated to mechanize than the 'least magnitude' technique, has the advantage of greater inherent stability and freedom from any noticeable interaction between separate computing channels. The very simple mechanization required to achieve steep descent of the magnitude error hypersurface at constant velocity makes such a procedure attractive. Although requiring additional instrumentation to promote convergence to the answer point, this method could prove very useful if it were possible to adapt it successfully for use with a process having any arbitrary finite forcing function. All of these particular methods of process parameter determination require a reasonably accurate assessment of the form of the process dynamic equations, in order that the computed parameters may provide a good description of the process dynamic characteristics.

A problem which has not been mentioned in any detail is the difficulty of obtaining a useful parameter estimation should uncertainty or noise appear in the measured signals. Although the low-pass filters inherent in the mechanization of the various tech-

niques may help to reduce the effect of high frequency noise, they are by no means the complete answer. A recent paper by V. S. Levadi¹⁶ discusses these effects in much greater detail and suggests a possible solution to the problem.

This paper has been concerned with the development of methods of process parameter determination which use normal analogue computing elements. Similarly, sampled data digital computation may be used to mechanize the search procedure. A number of self-adaptive control systems which use such techniques have so far been developed at Loughborough. These methods of control, which have been termed 'hybrid SESAC' techniques by the author, use the normal SESAC principle of self-adaptive control but incorporate hybrid computational methods in the determination of the process parameters. The procedures of steepest descent are replaced by the repeated solution of sets of linear algebraic simultaneous equations, whose coefficients are generated from sampled data obtained from the process input and output signals.^{13, 14}

When compared with the analogue methods which have been described, such systems can have greater accuracy and speed of response, together with the ability to track successfully many more unknown parameters. The author's 'method of multiple filters', was initially developed to improve the performance of these hybrid techniques (see Appendix 3). However, it has since become apparent that it is essential to the practical application of both the hybrid and analogue systems, because it removes the need to measure directly the higher order derivatives of the process input and output signals.

The digital store inherent in the hybrid system also provides the possibility for more sophisticated 'second generation' self-adaptive aircraft autostabilization. The store would have the secondary purpose of imparting a rudimentary 'learning capacity' to the control system, by the storage of parameters as they were obtained. These solutions would then be used again should similar environmental conditions occur in the future.

The principles underlying the analogue and hybrid methods of parameter determination mentioned here are very simple in conception and lend themselves to both manual and machine operation. Investigations into the more generalized use of these techniques for the analysis of dynamic experiments is continuing. In certain applications it is felt that because the identification procedure requires no special test input to the process, the methods can have definite advantages over the better known frequency response and correlation methods.

These and other possible developments in parameter tracking techniques and instrumentation, together

with their application to the self-adaptive autostabilization of aircraft, are at present being investigated at Loughborough.

8. Acknowledgments

The investigations described in this paper form part of a research programme being carried out in the Department of Aeronautical and Automobile Engineering of Loughborough College of Technology. The paper is published with the permission of the Head of the Department, Professor K. L. C. Legg. The author would like to express his gratitude to Messrs. D. Longley, A. C. Bajpai, D. W. Kew and J. F. Young for their help and encouragement in the preparation of this paper, and to colleagues and members of staff of the Analogue Computer Section of the Department for their invaluable assistance.

9. References

1. A. Ben Clymer, "Direct system synthesis by means of computers", *Trans. Amer. Inst. Elect. Engrs*, Pt. 1, 77, pp. 798-806 1959 (*Communications and Electronics*, No. 40, January 1959).
2. S. Fifer, "Analogue Computation". (McGraw-Hill, New York, 1961.)
(a) Vol. 2, p. 583; (b) Vol. 3, p. 835; (c) Vol. 3, p. 851.
3. B. G. Madden, "Simultaneous determination of system parameters from transient response", *Trans. Inst. Elect. Electronics Engrs on Applications and Industry*, No. 69, pp. 327-31, November 1963.
4. E. F. Beckenbach, (Ed.), "Modern Mathematics for the Engineer", p. 448. (McGraw-Hill, New York, 1900.)
5. A. Ben Clymer, T. F. Potts and G. N. Ornstein, "The automatic determination of human and other system parameters". Proceedings of Western Joint Computer Conference, Los Angeles, California, May 1961.
6. K. K. Graupe, "The analog solution of some functional analysis problems", *Trans. Amer. I.E.E.*, Pt. 1, 79, pp. 793-7, 1961 (*Communications and Electronics*, No. 52, January 1961).
7. Y. Kaya and S. Yamamura, "A self adaptive system with a variable parameter p.i.d. control", *Trans. A.I.E.E. on Applications and Industry*, No. 58, pp. 378-86, January 1962.
8. P. Eykhoff, "Some fundamental aspects of process parameter estimation", *Trans. I.E.E.E. on Automatic Control*, AC-8, No. 4, pp. 347-57, October 1963. (An excellent treatise which describes a generalized philosophy of parameter tracking systems.)
9. H. P. Whitaker *et al.*, "Design of model-reference adaptive control systems for aircraft". Instrumentation Laboratory, M.I.T., Report R.164, September 1958.
10. D. C. Clark, F. E. Pritchard and P. A. Reynolds, "Application of Self Adaptive Control Techniques to the Flexible Supersonic Transport". Society of Automotive Engineers, National Aeronautic and Space Engineering and Manufacturing Meeting, Los Angeles, California, 23rd-27th September 1963, No. 751C.
11. M. Margolis and C. T. Leondes, "A model referenced parameter tracking technique for adaptive control systems, Parts I and II", *Trans. I.E.E.E. on Applications and Industry*, No. 68, pp. 241-61, September 1963.

12. G. W. Brown, "The stability of feedback solution of simultaneous linear equations", *Amer. Math. Soc. Bull.*, Part I, 53, p. 61, January 1947 (abstract).
E. A. Goldberg and G. W. Brown, "An electronic simultaneous equation solver", *J. Appl. Phys.*, 19, No. 4, pp. 339-45, 1948.
13. P. C. Young, Discussion on "In-flight dynamic checkout", *Trans. I.E.E.E. on Aerospace*, AS-2, No. 3, pp. 1106-11, July 1964.
14. P. C. Young and C. D. Dwyer, "A Hybrid Self Adaptive Control System". (To be published. Recipient of Electronic Associates "P.A.C.E. Prize Award" for 1964.)
15. J. G. Truxal, "Control System Synthesis", p. 55 *et seq.* (McGraw-Hill, New York, 1955).
16. V. S. Levadi, "Parameter estimation of linear systems in the presence of noise". Paper presented at the International Conference on Microwaves, Circuit Theory and Information Theory, Tokyo, 7th-11th September 1964.

10. Appendix 1: Glossary of Analogue Computer Symbols

FUNCTION	SYMBOLIC REPRESENTATION	CIRCUIT DIAGRAM
HIGH GAIN DIRECT-COUPLED AMPLIFIERS		
SUMMING AMPLIFIER		
INTEGRATING AMPLIFIER		
COEFFICIENT POTENTIOMETER		
TWO-SIDED POTENTIOMETER		
SERVO MECHANICAL MULTIPLIER		
SIGN MULTIPLIER		

Reference voltage on P.A.C.E 131R Analogue Computer = 100 V, i.e. 100 V = one machine unit.

11. Appendix 2: Discussion on the Stability of 'Satisfaction Error' Parameter Determination Systems

Consider a general function of the satisfaction error of a process $E_p(t, a_{0c}, a_{1c}, \dots, a_{(k-1)c})$. E_p will be a function of time both because of its dependence upon the time dependent variables $p_r(t)$, and because it could be concerned with a non-stationary (time variable parameter) process.

Provided E_p has a lower bound $E_{p(\min)}$ (both E_1 and E_2 have a minimum value of zero), the necessary and sufficient conditions for convergence to a minimum is that dE_p/dt is always negative for $E_p > E_{p(\min)}$, i.e.

$$\frac{dE_p}{dt} < 0 \text{ for } E_p > E_{p(\min)} \quad \dots\dots(23)$$

Now,

$$\frac{dE_p}{dt} = \frac{\partial E_p}{\partial t} + \sum_{r=0}^{r=k-1} \frac{\partial E_p}{\partial a_{rc}} \cdot \dot{a}_{rc}$$

and from eqn. (17)

$$\dot{a}_{rc} = -K \frac{\partial E_p}{\partial a_{rc}}$$

Therefore

$$\frac{dE_p}{dt} = \frac{\partial E_p}{\partial t} - K \sum_{r=0}^{r=k-1} \left[\frac{\partial E_p}{\partial a_{rc}} \right]^2 \quad \dots\dots(24)$$

Hence, for convergence, from eqn. (23):

$$\frac{\partial E_p}{\partial t} - K \sum_{r=0}^{r=k-1} \left[\frac{\partial E_p}{\partial a_{rc}} \right]^2 < 0$$

i.e.

$$\frac{\partial E_p}{dt} < K \sum_{r=0}^{r=k-1} \left[\frac{\partial E_p}{\partial a_{rc}} \right]^2 \quad \dots\dots(25)$$

Now,

(a) $\frac{\partial E_p}{\partial t}$ will depend upon:

- (1) the nature of the functions $p_r(t)$
- (2) any variation in the process parameters (a_r) (i.e. non-stationary process).

(b) $K \sum_{r=0}^{r=k-1} \left[\frac{\partial E_p}{\partial a_{rc}} \right]^2$ is:

- (1) always positive
- (2) its magnitude is dependent upon $|K|$, the integrator gain, and $\left| \sum_{r=0}^{r=k-1} \left[\frac{\partial E_p}{\partial a_{rc}} \right]^2 \right|$

Although it is not apparent from inspection how condition (25) can be completely ensured, there are certain provisions that may be made which should reasonably guarantee asymptotic behaviour:

- (i) If the process under consideration has stationary or only slowly variable characteristics then any deleterious contribution to $\partial E_p/\partial t$ because (a)(2) will be small.

- (ii) K should be made as large as possible.

- (iii) $\frac{\partial E_p}{\partial a_{rc}}$, ($r = 0 \rightarrow r = k-1$), should never be allowed to go to zero simultaneously. This would be the case if the condition $E_p = 0$ was achieved and maintained for any period of time due to lack of activity at the input to the process.

12. Appendix 3: Discussion on the Justification for the Use of Filtered Signals in the Mechanization of 'Satisfaction Error' Parameter Determination Systems

Consider the process described by an equation of the form

$$\sum_{r=0}^{r=k} a_r \cdot p_r(t) = 0 \quad \dots\dots(26)$$

Performing a Laplace transformation on this equation, one obtains

$$\left[\sum_{r=0}^{r=k} a_r \cdot p_r(s) \right] - Z(s, p_r(0)_+) = 0 \quad \dots\dots(27)$$

where $Z(s, p_r(0)_+)$, $r = 0, \dots, r = k$, can be a function of the Laplace operator, s , and any initial conditions, $p_r(0)_+$, of the variables $p_r(t)$.

Multiplication of eqn. (27) by a modulating function $D(s)$ of the Laplace operator s , gives the equation

$$\left[\sum_{r=0}^{r=k} a_r \{ D(s) \cdot p_r(s) \} \right] - Z(s, p_r(0)_+) \cdot D(s) = 0 \quad \dots\dots(28)$$

and the inverse Laplace transformation of this equation may be written

$$\sum_{r=0}^{r=k} a_r \mathcal{L}^{-1} D(s) \cdot p_r(s) = \mathcal{L}^{-1} Z(s, p_r(0)_+) \cdot D(s) \quad \dots\dots(29)$$

Now, if $D(s)$ is chosen such that those terms on the right-hand side of eqn. (29) die out as time progresses, then the parameters a_r may be related by the expression:

$$\sum_{r=0}^{r=k} a_r \mathcal{L}^{-1} D(s) p_r(s) = 0$$

or

$$\sum_{r=0}^{r=k} a_r [(p_r(t))]_D = 0 \quad \dots\dots(30)$$

where $[(p_r(t))]_D$, $r = 0, \dots, r = k$, may be considered physically as the output of filters $D(s)$ as shown in Fig. 16(a).

Equation (30) may be considered valid for all time after the terms on the right-hand side have become insignificant.

As an example consider the process described by the linear differential equation

$$\sum_{n=0}^{n=N} a_n \frac{d^n p(t)}{dt^n} = \sum_{m=0}^{m=M} b_m \frac{d^m f(t)}{dt^m} \quad \dots\dots(31)$$

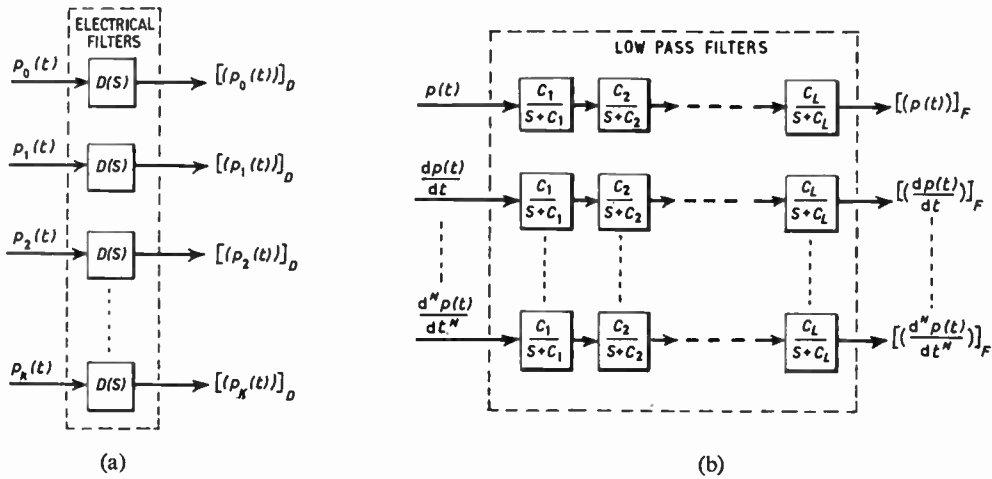


Fig. 16. Filter outputs.

with a modulating function

$$D(s) = \prod_{r=1}^{r=L} \frac{c_r}{s + c_r}$$

The equation equivalent to (28) is

$$\prod_{r=1}^{r=L} \frac{c_r}{s + c_r} \left[\sum_{n=0}^{n=N} a_n \left[s^n p(s) - \sum_{p=1}^{p=n} s^{n-p} \left(\frac{d^{p-1} p(t)}{dt^{p-1}} \right)_{0+} \right] \right] = \prod_{r=1}^{r=L} \frac{c_r}{s + c_r} \left[\sum_{m=0}^{m=M} b_m \left[s^m f(s) - \sum_{p=1}^{p=m} s^{m-p} \left(\frac{d^{p-1} f(t)}{dt^{p-1}} \right)_{0+} \right] \right] \dots\dots(32)$$

It can be shown that the inverse Laplace transformation of the terms containing initial conditions of $p(t)$, $f(t)$ and their derivatives produces functions which decay in a time which is dependent upon the filter time-constants, $1/c_r (r = 1, \dots, r = L)$. Finally, the parameters a_n and b_m may be related by the equation:

$$\sum_{n=0}^{n=N} a_n \left[\left(\frac{d^n p(t)}{dt^n} \right) \right]_F = \sum_{m=0}^{m=M} b_m \left[\left(\frac{d^m f(t)}{dt^m} \right) \right]_F \dots\dots(33)$$

where $\left[\left(\frac{d^n p(t)}{dt^n} \right) \right]_F$, $(n = 0, \dots, n = N)$ can be considered physically as the outputs of a series of low-pass filters as shown in Fig. 16(b)

similarly for $\left[\left(\frac{d^m f(t)}{dt^m} \right) \right]_F$

Equation (33) may be considered valid for $t > \epsilon$, where ϵ is a period of time immediately following the initiation of the filtration process and whose magnitude is dependent upon the filter time-constant $1/c_r (r = 1, \dots, r = L)$.

Simple theoretical calculations coupled with some

studies on the analogue computer have demonstrated the validity of equations of the form of eqn. (33), which are inherent in any practical 'satisfaction error' parameter tracking system.

A particular example of eqn. (33) is when

$$c_1 = c_2 = c_3 = \dots = c_L = c$$

Therefore

$$\prod_{r=1}^{r=L} \frac{c_r}{s + c_r} = \frac{c^L}{(s + c)^L}$$

and

$$\sum_{n=0}^{n=N} a_n \left[\left(\frac{d^n p(t)}{dt^n} \right) \right]_L = \sum_{m=0}^{m=M} b_m \left[\left(\frac{d^m f(t)}{dt^m} \right) \right]_L \dots\dots(34)$$

where the brackets $[()]_L$ indicate that the function has been filtered L times by a low-pass filter of the form

$$\frac{c}{s + c}$$

Investigations^{13, 14} have shown that by choosing $L \geq M$ or N (whichever is greater), it is possible to generate eqn. (34) from signals obtained from the successive filtration of the input and output signals, $f(t)$ and $p(t)$ by low-pass filters of the form $\frac{c}{s + c}$ (the method of multiple filters). This removes the need for sensing directly such terms as

$$\left[\left(\frac{d^n p(t)}{dt^n} \right) \right]_L, \quad (n = 1 \dots n = N), \text{ and}$$

$$\left[\left(\frac{d^m f(t)}{dt^m} \right) \right]_L, \quad (m = 1 \dots m = M)$$

which may be difficult or even impossible to obtain in practice.

**13. Appendix 4: Loughborough College of Technology
Analogue Computing System**

The analogue computing system of the Department of Electrical Engineering at Loughborough College of Technology, consists of an Electronic Associates P.A.C.E. 131.R General Purpose Analogue Computer with the following major components:

- 20 d.c. amplifiers connected for either summing or integrating operations
 - 28 d.c. amplifiers connected for summing operations only
 - 12 d.c. amplifiers for use with servo-resolvers
 - 80 helical, 10-turn coefficient potentiometers of 30 000Ω
 - 4 diode function generators
- d.c. gain: 3×10^8
- phase shift:
0.006 deg at 40 c/s
0.05 deg at 450 c/s

- 1 quarter-square electronic multiplier
- 6 servo-mechanical multipliers (each with 4 ganged pots)
 - bandwidth 13 c/s for $\pm 10V$ $p-p$ input
 - 9 c/s for $\pm 20V$ $p-p$ input
 - total dynamic error for $\pm 100V$ $p-p$ input is 0.1% at 0.2 c/s, 1.0% at 1.7 c/s
- 3 servo-resolvers
- 6 relay units
- removable pre-patch panel and patch leads plus regulated power suppliers and associated equipment (6-channel pen recorder, X-Y plotter, digital voltmeter, etc.).

Manuscript first received by the Institution on 8th July 1964, and in final form on 25th January 1965. (Paper No. 984/C80.)

© The Institution of Electronic and Radio Engineers, 1965

A Specialization of the Yanagisawa Synthesis Procedure to obtain RC Active Networks having Optimum Pole Sensitivity

By

A. G. J. HOLT, Dip.El., Ph.D.
(Associate Member)†

AND

F. W. STEPHENSON, B.Sc.
(Graduate)‡

Summary: A brief outline is given of the synthesis procedure due to Yanagisawa for obtaining a required voltage transfer function with an RC active network. The sensitivity of the networks to error in the negative impedance converter conversion factor is discussed in terms of the pole sensitivity of the network function.

The realization of networks having the optimum sensitivity is considered. For the network having the response described by the second-order function with equal ripple in pass and stop bands, this results in a network employing seven passive elements. Design equations are quoted for this structure.

A limit to the amplitude of pass-band ripple which may be obtained with a simple section designed from the equations for the seven-passive-element structure is pointed out. The method for overcoming this by a change in the circuit configuration is given, together with experimental results obtained with a specimen design.

Definitions and relationships from sensitivity theory, some properties of the elliptic function, and the evaluation of the critical values for the constant ε^2 (which determines the amplitude of the pass-band ripple) are treated in appendices.

List of Symbols

$D(p)$ voltage response | voltage excitation $\Big|_{I_2=0} = \frac{E_2}{E_1} = \frac{P(p)}{Q(p)}$

$P(p)$ numerator polynomial

$Q(p)$ denominator polynomial

$F(p)$ selected polynomial used in the synthesis procedure

y_a, y_b, Y_a, Y_b admittances of the arms of the L networks

p complex frequency variable

ω_0 frequency of transmission zero

ω_n imaginary part of pole, for high Q

σ real part of pole

θ modular angle from Tables in reference 9

k_0 multiplying constant for transfer function

$\alpha = \frac{2\sigma_c}{\omega_n}$

$Z(p)$ Zolotarev fraction

ε^2 constant determining magnitude of pass-band ripple

k conversion factor of the negative impedance converter

1. Introduction

Several papers^{1-3,12} have been written which describe the synthesis of electrical filter networks using a negative impedance converter (n.i.c.) in conjunction with resistors and capacitors. When the circuits synthesized are constructed it is found that the design performance is often not achieved because the component values and the n.i.c. conversion factor are not exactly equal to the specified values.

The sensitivity of active filter networks to these small errors has been studied by Horowitz⁴⁻⁶ who has

given expressions for the change in the pole or zero locations of the network function which are produced by small variation in element and conversion factor values. A helpful table of formulae relating to sensitivity has been compiled by Gorski-Popiel.⁷ Holt and Stephenson¹⁰ have given curves showing the effect on the responses of active filters of small variations in the n.i.c. characteristic and the element values. Sipress⁸ has obtained a method for minimizing the sensitivity of the synthesized network to changes in the converter conversion factor. This paper deals with a modification which has been found to be necessary when the Sipress method is applied to the synthesis of second-order filters having equal ripple responses in pass and stop bands. For what follows it is necessary to give a brief account of the synthesis method to which it refers.

† Department of Electrical Engineering, University of Newcastle-upon-Tyne.

‡ Formerly with Department of Electrical Engineering, University of Newcastle-upon-Tyne; now with Microelectronics Division of Electrosil Ltd.

2. Yanagisawa's Method of Synthesis

The following active RC voltage transfer function synthesis procedure was first reported by Yanagisawa.

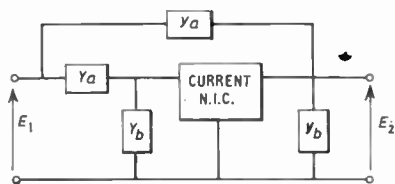


Fig. 1. Basic network.

The overall open-circuit voltage transfer function of the network in Fig. 1, where it is assumed that the n.i.c. is of the current inversion type, may be written as

$$\frac{1}{D(p)} = \frac{Q(p)}{P(p)} = \frac{E_1}{E_2} \Big|_{I_2=0} = \frac{(Y_a + Y_b) - (y_a + y_b)}{Y_a - y_a} \dots(1)$$

where the networks y_a, y_b, Y_a and Y_b are two terminal RC structures. (The terminal currents flowing into the structure are positive.) In order to synthesize $D(p)$, it is written in the modified form

$$\frac{1}{D(p)} = \frac{P(p) + Q(p) - P(p)}{P(p)} \dots\dots(2)$$

An arbitrary polynomial

$$F(p) = \prod_{i=1}^{n-1} (p - \sigma_i) \dots\dots(3)$$

is formed where the σ_i are $(n - 1)$ points on the negative real axis of p and n is the degree of $P(p)$ or $Q(p)$, whichever is the higher.

Y_a and y_a can then be determined from a partial fraction expansion of $P(p)/pF(p)$, while Y_b and y_b can be determined from a partial fraction expansion of $Q(p) - P(p)/pF(p)$. The partial fractions with positive residues are realized by Y_a, Y_b and those with negative residues by y_a, y_b respectively. Design tables for second- and fourth-order filters of this type have been given by Holt and Stephenson.¹¹

3. Sensitivity Considerations

Yanagisawa pointed out that the reasonable way of choosing the values of σ_i (eqn. (3)) had not, at the time of writing, been found. He did, however, note that the choice affected the sensitivity of the network characteristic with respect to variation in the conversion factor of the n.i.c.

Using several definitions from sensitivity theory (Appendix 1), Sipress was able to minimize the magnitude of pole sensitivity with respect to changes

in conversion factor of the n.i.c. In considering the synthesis of a transfer function of the form

$$D(p) = \frac{k_0 P(p)}{Q(p)} = \frac{k_0 P(p)}{(p + \sigma_c)^2 + \omega_c^2} = \frac{k_0 P(p)}{p^2 + 2\sigma_c p + \omega_n^2} \dots\dots(4)$$

(where $\omega_n^2 = \omega_c^2 + \sigma_c^2$, see Fig. 2), the following assumptions were made:

- (a) the degree of $D(p)$ is equal to, or less than two;
- (b) the Q of the poles is large, where Q is defined from Fig. 2 as

$$Q = \frac{\omega_c}{2\sigma_c} \dots\dots(5)$$

As a result of (b), σ_c can be neglected compared to ω_c^2 and $\omega_n \simeq \omega_c$.

An examination of the sensitivity of these poles led Sipress to observe that:

- (a) pole sensitivity with respect to changes in conversion ratio of the n.i.c. increases as the Q of the poles increases;
- (b) the minimum magnitude of pole sensitivity is $2Q$;
- (c) the minimum magnitude of S_k^p (see Appendix 1) occurs when the direction of pole movement is, approximately, directly towards the $j\omega$ axis.

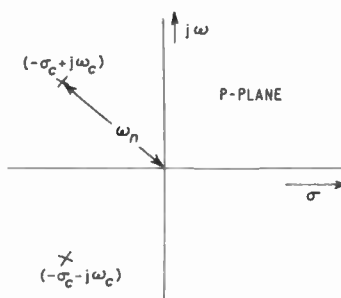


Fig. 2. Plot of pole locations for the transfer function $D(p)$.

From the above observations, Sipress concluded that the choice of

$$F(p) = (p + \omega_n) \dots\dots(6)$$

results, within a few per cent, in the best value of pole sensitivity with respect to changes in k that is possible. Furthermore, if we consider transfer functions of the form

$$D(p) = \frac{k_0(p^2 + \omega_0^2)}{p^2 + 2\sigma_c p + \omega_n^2} \dots\dots(7)$$

it enables one to derive simple expressions for the elements of the network shown in Fig. 1.

4. Realization of Optimum Sensitivity Network

$D(p)$, eqn. (7), can be realized in a seven-passive-element structure with $S_k^p = 2Q$, if

$$k_0 = \frac{\omega_n^2}{\omega_0^2} \quad (k_0 < 1) \quad \dots\dots(8)$$

and $F(p)$ is as defined in equation (6).

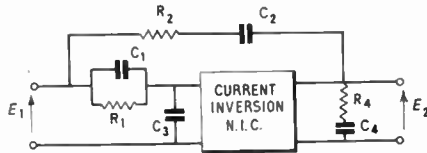


Fig. 3. Optimized low-pass network.

Following the steps of the Yanagisawa synthesis procedure, outlined in Section 2, we obtain

$$Y_a - y_a = \frac{k_0 Q(p)}{F(p)} = \frac{\left(\frac{\omega_n}{\omega_0}\right)^2 p^2 + \omega_n^2}{(p + \omega_n)} \quad \dots\dots(9)$$

A partial fraction expansion of $\frac{k_0 Q(p)}{pF(p)}$ leads to

$$\frac{Y_a - y_a}{p} = \frac{\left(\frac{\omega_n}{\omega_0}\right)^2 p^2 + \omega_n^2}{p(p + \omega_n)} = \left(\frac{\omega_n}{\omega_0}\right)^2 + \frac{\omega_n}{p} - \frac{\omega_n \left(1 + \frac{\omega_n^2}{\omega_0^2}\right)}{(p + \omega_n)}$$

Therefore

$$Y_a - y_a = \left(\frac{\omega_n}{\omega_0}\right)^2 p + \omega_n - \frac{\omega_n \left(1 + \frac{\omega_n^2}{\omega_0^2}\right) p}{(p + \omega_n)}$$

$$Y_a = \left(\frac{\omega_n^2}{\omega_0^2}\right) p + \omega_n \quad \dots\dots(10)$$

$$y_a = \frac{p \omega_n \left(1 + \frac{\omega_n^2}{\omega_0^2}\right)}{(p + \omega_n)} \quad \dots\dots(11)$$

Similarly

$$Y_b - y_b = \frac{Q(p) - P(p)k_0}{F(p)} = \frac{p^2 \left(1 - \frac{\omega_n^2}{\omega_0^2}\right) + 2\sigma_c p}{(p + \omega_n)} \quad \dots\dots(12)$$

from which

$$Y_b = \left(1 - \frac{\omega_n^2}{\omega_0^2}\right) p \quad \dots\dots(13)$$

$$y_b = \frac{\omega_n \left(1 - \frac{\omega_n^2}{\omega_0^2} - \frac{2\sigma_c}{\omega_n}\right)}{(p + \omega_n)} \quad \dots\dots(14)$$

The resultant network is shown in Fig. 3, for which the element values are:

$$R_1 = 1/\omega_n \quad \dots\dots(15a)$$

$$R_2 = 1/\omega_n(1 + k_0) \quad \dots\dots(15b)$$

$$R_4 = 1/\omega_n(1 - k_0 - \alpha) \quad \dots\dots(15c)$$

$$C_1 = k_0 \quad \dots\dots(15d)$$

$$C_2 = (1 + k_0) \quad \dots\dots(15e)$$

$$C_3 = (1 - k_0) \quad \dots\dots(15f)$$

$$C_4 = (1 - k_0 - \alpha) \quad \dots\dots(15g)$$

where

$$k_0 = \frac{\omega_n^2}{\omega_0^2} \quad \text{and} \quad \alpha = \frac{2\sigma_c}{\omega_n}$$

If we let

$$k_0 = \frac{2 \left(1 - \frac{\sigma_c}{\omega_n}\right)}{\left[1 + \left(\frac{\omega_0}{\omega_n}\right)^2\right]}$$

and leave $F(p)$ as above, then the synthesis leads to a six passive-element structure. However, the pole sensitivity is greater than in the seven-element case.

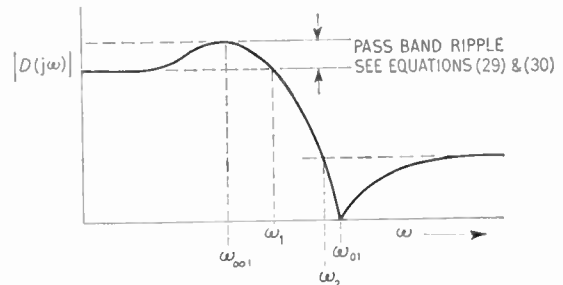


Fig. 4. Second-order low-pass response.

5. Limitation to the Application of the Technique

The design equations (15a-g) have been used to produce filters having a magnitude response which performs a Chebyshev variation in both pass and stop bands (see Fig. 4). These are often known as 'elliptic' or 'Cauer parameter' filters, and a few properties of the filters are given in Appendix 2.

Sipress has listed the element values for the two networks in terms of the coefficients of the transfer function (5).

In using these a limit has been found to the amount of pass-band ripple which can be attained using a simple section. This is illustrated in Fig. 5 and can be explained as follows. It will be seen that both C_4 and R_4 will assume negative values if $(k_0 + \alpha) > 1$.

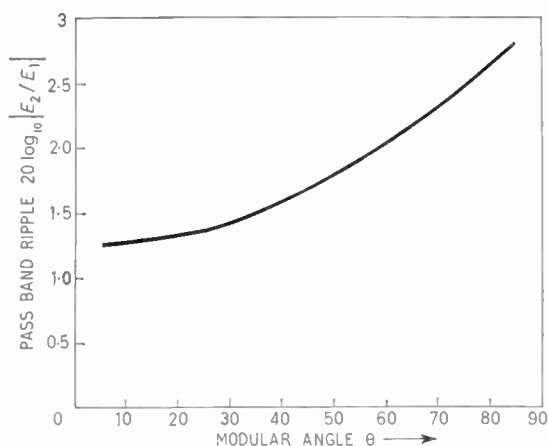


Fig. 5. Curve showing minimum ripple amplitude against modular angle θ for y_b positive.

Since

$$k_0 = \frac{\omega_n^2}{\omega_0^2} \quad \text{and} \quad \alpha = \frac{2\sigma_c}{\omega_n}$$

$$\left(\frac{\omega_n^2}{\omega_0^2} + \frac{2\sigma_c}{\omega_n} \right) > 1 \quad \dots\dots(16)$$

The elliptic function can be written as

$$D^2(p) = \frac{1}{1 + \varepsilon^2 Z^2(p)} \quad \dots\dots(17)$$

where, from Glowatski's tables for the second-order case,

$$Z(p) = \frac{p^2 + \left(\frac{a_1}{a_2}\right)^2}{p^2 + \left(\frac{1}{a_1 a_2}\right)^2} \quad \dots\dots(18)$$

a_1 and a_2 being the tabulated coefficients for a selected modular angle, θ .

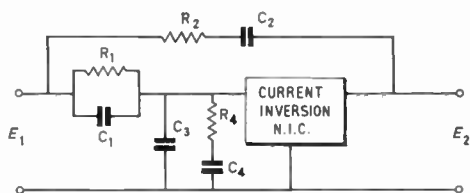


Fig. 6. Modified low-pass network having y_b moved to left side of the negative impedance converter.

Since equation (11) is simply another way of expressing the second-order function used in Sipress' equation (5), it is possible to relate the inequality, equation (10), to ε^2 which enables the critical value of ripple to be evaluated for each modular angle (see Appendix 3). Below the critical value of ripple, the function

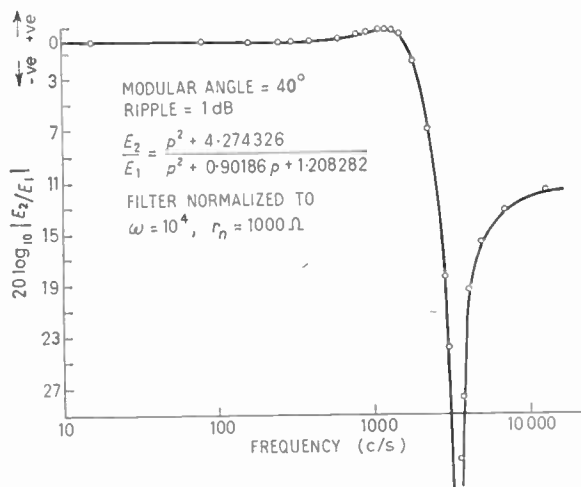


Fig. 7. Experimental results for circuit in Fig. 8.

cannot be synthesized in the form of Fig. 3 unless one uses a polynomial $F(p)$ which is different from $(p + \omega_n)$, i.e. $F(p) = (p + \omega_s)$ where $\omega_s \neq \omega_n$.

The appearance of negative elements in the synthesis can be overcome by moving the elements R_4 and C_4 , which make up y_b , to the left-hand side of the n.i.c. This change yields the circuit configuration of Fig. 6 for a low-pass network.

Typical experimental results for a network designed for 1 dB amplitude of pass-band ripple, a transmission zero at 3300 c/s and a minimum attenuation of 10.5 dB in the stop band, are shown in Fig. 7. The specification corresponds to a modular angle θ of 40 degrees. Figure 8 shows the circuit with the component values. The normalized transfer function is

$$D(p) = \frac{E_2}{E_1} = \frac{p^2 + 4.274326}{p^2 + 0.90186p + 1.208282} \quad \dots(19)$$

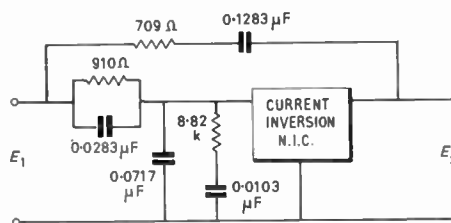


Fig. 8. Low-pass network showing component values.

6. Conclusions

It is clear that networks yielding the second-order function having equal ripple in pass and stop bands may be designed by the Yanagisawa technique, employing the Sipress polynomial optimization, for any amplitude of pass-band ripple. When the ripple

required for a given modular angle is less than the limiting value obtained from Fig. 5 the passive components in y_b must be moved to the left-hand side of the n.i.c.

7. Acknowledgments

The authors have pleasure in thanking Professor R. L. Russell, Professor of Electrical Engineering in the University of Newcastle-upon-Tyne, for his interest and for the use of the facilities of the Department. It is also a pleasure to acknowledge occasional, but stimulating discussions with Mr. D. Maclean of Messrs. Barr and Stroud, Glasgow, and Dr. W. Saraga and his colleagues at Associated Electrical Industries Research Laboratories, Woolwich. Thanks are also due to the Welwyn Electric Company for financial support.

8. References

1. J. G. Linvill, "RC active filters", *Proc. Inst. Radio Engrs*, **42**, pp. 555-64, March 1954.
2. T. Yanagisawa, "RC active networks using current-inversion type negative-impedance converters", *Trans. I.R.E. on Circuit Theory*, CT-4, pp. 140-4, September 1957.
3. B. K. Kinariwala, "Synthesis of active networks", *Bell Syst. Tech. J.*, **38**, p. 1269, September 1959.
4. I. M. Horowitz, "Optimization of negative-impedance conversion methods of active RC synthesis", *Trans. I.R.E. CT-6*, pp. 293-303, September 1959.
5. I. M. Horowitz, "Exact design of transistor RC band-pass filters with prescribed active parameter insensitivity", *Trans. I.R.E.*, CT-7, pp. 313-20, September 1960.
6. I. M. Horowitz, "Optimization design of single stage gyrator-RC filters with prescribed sensitivity", *Trans. I.R.E.*, CT-8, pp. 88-94, June 1961.
7. J. Gorski-Popiel, "Classical sensitivity—a collection of formulas", *Trans. I.E.E.E.*, CT-10, pp. 300-2, June 1963.
8. J. M. Sipress, "Synthesis of Active RC Networks". Polytechnic Institute of Brooklyn, Electrical Engineering Department, Dissertation, June 1960.
9. E. Glowatzki, "Sechsstellige Tafel der Cauer-Parameter". (Verlag der Bayerischen Akademie der Wissenschaften, Munchen, 1955.)
10. A. G. J. Holt and F. W. Stephenson, "The effects of errors in the element values and converter transfer characteristic on the responses of active RC filters", *The Radio and Electronic Engineer*, **26**, No. 6, pp. 449-57, December 1963.
11. A. G. J. Holt and F. W. Stephenson, "Design tables for active filters having 2nd- and 4th-order Chebyshev responses in pass and stop bands", *Proc. Instn Elect. Engrs*, **111**, pp. 1807-20, November 1964.
12. F. H. Blecher, "Applications of synthesis techniques to electronic circuit design", *Trans. I.R.E. on Circuit Theory*, CT-7, Special Supplement, pp. 79-91, August 1960.

9. Appendix 1:

Definitions and Required Relationships from Sensitivity Theory

Certain definitions and relations from sensitivity theory were used by Sipress in his study of the

polynomial $F(p)$. Consider the transfer function $D(p)$ of a network

$$D(p) = \frac{k_0 \prod_{i=1}^n (p - p_i)}{\prod_{j=1}^m (p - p_j)} = \frac{A(p) + kB(p)}{C(p) + kE(p)} \dots\dots(20)$$

A, B, C, E are polynomials and are independent of the parameter k . It can be shown that

$$S_k^D(p) = S_k^{k_0} - \sum_{i=1}^n \frac{S_k^{p_i}}{(p - p_i)} + \sum_{j=1}^m \frac{S_k^{p_j}}{(p - p_j)} \dots(21)$$

where $S_k^D(p)$, the sensitivity of D to changes in k , is defined as

$$S_k^D(p) = \frac{d(\ln D(p))}{d(\ln k)} = \frac{dD(p)/D(p)}{dk/k} \dots\dots(22)$$

and $S_k^{p_i}, S_k^{p_j}$ the pole (zero) sensitivity, or the sensitivity of the pole p_j (or zero p_i) to changes in k , are defined as

$$S_k^{p_j} = \frac{dp_j}{d(\ln k)} = \frac{dp_j}{dk/k} \dots\dots(23)$$

$$S_k^{p_i} = \frac{dp_i}{d(\ln k)} = \frac{dp_i}{dk/k} \dots\dots(24)$$

respectively. Use of the above definitions led Sipress to the results referred to in Section 3.

10. Appendix 2:

Some Properties of the Elliptic Functions

$D(p)$, as defined in eqn. (7) is obtained from

$$D(p) = \frac{1}{1 + \epsilon^2 Z^2(p)}$$

(see eqn. (17)). Here ϵ^2 is an arbitrary constant which determines the magnitude of the pass-band ripple (Fig. 4).

$Z(p)$ is the Zolotarev fraction,⁹

$$Z(j\omega) = \frac{\prod_{v=1}^{n/2} (\omega_{0v}^2 - \omega^2)}{\prod_{v=1}^{n/2} (\omega_{\infty v}^2 - \omega^2)} \quad \text{for even } n \dots(25a)$$

$$Z(j\omega) = \frac{\omega \prod_{v=1}^{(n-1)/2} (\omega_{0v}^2 - \omega^2)}{\prod_{v=1}^{(n-1)/2} (\omega_{\infty v}^2 - \omega^2)} \quad \text{for odd } n \dots(25b)$$

and the zeros and poles of the function are determined from the formulae

$$\left. \begin{aligned} \omega_{0v} &= \text{sn} \left(\frac{2v-1}{n} K, k_1 \right) \\ \omega_{\infty v} &= 1/k_1 \omega_{0v} \end{aligned} \right\} \text{for even } n \dots\dots(26a)$$

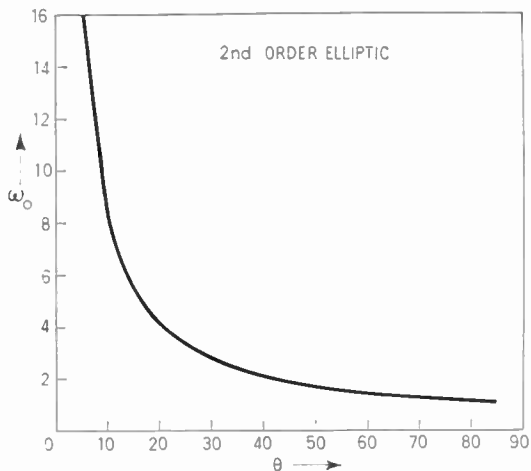


Fig. 9. Variation of ω_0 with modular angle θ for second-order elliptic function.

$$\left. \begin{aligned} \omega_{0v} &= \operatorname{sn}\left(\frac{2v}{n}K, k_1\right) \\ \omega_{\infty v} &= 1/k_1 \omega_{0v} \end{aligned} \right\} \text{for odd } n \dots\dots(26b)$$

In eqns. (26a) and (26b), K is the full type-I elliptic integral, with the modulus

$$k_1 = \frac{\omega_1}{\omega_2} \dots\dots(27)$$

Figure 4 illustrates a typical second-order response curve.

The determination of $D(p)$ has been greatly aided by the Glowatzki tables,⁹ which present parameters of the Zolotarev fraction from the first to the twelfth degree, for values of the modular angle θ ($= \arcsin k_1$) from 1 deg to 90 deg. From these tables it is found that

$$\omega_{0v} = \frac{a_m}{a_n} = \operatorname{sn}\left(\frac{m}{n}K, \theta\right) \dots\dots(28a)$$

$$\omega_{\infty v} = 1/a_m a_n = -1/k \operatorname{sn}\left(\frac{m}{n}K, \theta\right) \dots\dots(28b)$$

$$m = 1, 3 \dots (n-1) \text{ for even } n$$

$$m = 0, 2 \dots (n-1) \text{ for odd } n$$

the values of a_m and a_n being listed in the tables.

Having thus obtained $Z(j\omega)$ and hence $Z^2(p)$, the final form of $D(p)$ will depend upon the choice of ϵ^2 , which determines the pass-band ripple.

If

$$P = 20 \log_{10} x \dots\dots(29)$$

where P is the required pass-band ripple for a given modular angle θ in a second-order function, then

$$\epsilon^2 = \frac{(x^2 - 1)}{a_1^8} \dots\dots(30)$$

If we let

$$Z^2(p) = \frac{R^2(p)}{S^2(p)}$$

then

$$D^2(p) = \frac{S^2(p)}{S^2(p) + \epsilon^2 R^2(p)} \dots\dots(31)$$

from which $D(p)$ can be formed by taking the square root of $S^2(p)$ (which is always of the form $(p^2 + \omega_0^2)^2$), and forming the denominator function from the left half-plane zeros of $[S^2(p) + \epsilon^2 R^2(p)]$.

Figure 9 shows the variation of infinite rejection point (ω_0) against modular angle (θ) for a second-order function. Figure 10 shows rejection between pass and stop bands against modular angle for various values of pass-band ripple.

11. Appendix 3:

Evaluation of Critical Values of ϵ^2

From eqn. (18),

$$Z(p) = \frac{p^2 + (a_1/a_2)^2}{p^2 + (1/a_1 a_2)^2}$$

Let

$$(a_1/a_2) = X, \quad (1/a_1 a_2) = Y$$

Therefore

$$Z(p^2) = \frac{(p^2 + X^2)^2}{(p^2 + Y^2)^2} = \frac{R^2(p)}{S^2(p)} \dots\dots(32)$$

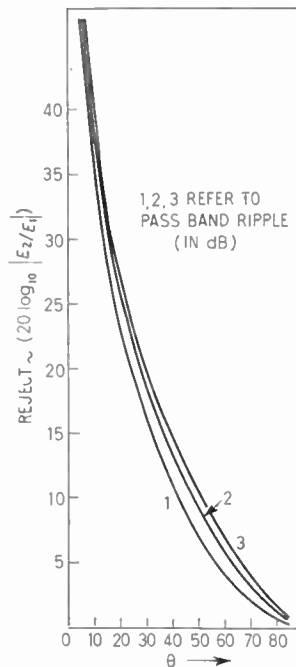


Fig. 10. Variation in rejection between pass and stop bands with modular angle θ for second-order elliptic function.

Thus, from (32) and (31) we obtain

$$D^2(p) = D(p) \cdot D(-p) = \frac{(p^2 + Y^2)^2}{(p^2 + Y^2)^2 + \epsilon^2(p^2 + X^2)^2}$$

$$= \frac{(p^2 + Y^2)^2}{(1 + \epsilon^2)p^4 + 2p^2(Y^2 + \epsilon^2 X^2) + (Y^4 + \epsilon^2 X^4)}$$

Therefore

$$D(p) \cdot D(-p) = \frac{(p^2 + Y^2)^2(1/1 + \epsilon^2)}{\left\{ p^4 + p^2 \frac{2(Y^2 + \epsilon^2 X^2)}{(1 + \epsilon^2)} + \frac{(Y^4 + \epsilon^2 X^4)}{(1 + \epsilon^2)} \right\}}$$

.....(33)

Forming the function from the left half-plane poles we obtain

$$D(p) = \frac{H(p^2 + Y^2)}{p^2 + 2\beta p + \gamma} \quad \text{.....(34)}$$

where

$$\beta = \left\{ \frac{\left(\frac{Y^4 + \epsilon^2 X^4}{1 + \epsilon^2} \right)^{\frac{1}{2}} - \left(\frac{Y^2 + \epsilon^2 X^2}{1 + \epsilon^2} \right)^{\frac{1}{2}}}{2} \right\} \quad \text{.....(35)}$$

$$\gamma = \left(\frac{Y^4 + \epsilon^2 X^4}{1 + \epsilon^2} \right)^{\frac{1}{2}} \quad \text{.....(36)}$$

and H is a constant.

It will be seen that eqn. (34) represents the same function as eqn. (7) where

$$\beta = \sigma$$

$$\gamma = \omega_n^2$$

$$Y = \omega_0$$

Further, we let

$$H = k_0$$

This latter choice is important for although not affecting the shape of the response, it plays no small part in the pole sensitivity.

We can now express the inequality in eqn. (16) as

$$\frac{\gamma}{Y^2} + \frac{2\beta}{\gamma^{\frac{1}{2}}} > 1 \quad \text{.....(37)}$$

The formidable task of evaluating the critical value of ϵ^2 was greatly reduced by use of a digital computer.

Evaluation of ϵ^2

For a given value of θ , the coefficients a_1 and a_2 can be obtained from the Glowatzki tables.⁹ One is thus able to express β , γ and Y in terms of ϵ . Substitution of these expressions into eqn. (37) produces an inequality in terms of ϵ , i.e. the condition becomes $\phi(\epsilon) > 1$ where $\phi(\epsilon)$ is same function of ϵ .

A digital computer can be used to increase ϵ from zero, in increments of 10 (say), until $\phi(\epsilon)$ just exceeds unity. ϵ can then be decreased in smaller increments (say 1.0) until $\phi(\epsilon)$ falls just below unity. The incremental changes in ϵ can be altered in the above fashion until the required accuracy is obtained.

Manuscript first received by the Institution on 13th April 1964 and in revised form on 9th December 1964. (Paper No. 985.)

© The Institution of Electronic and Radio Engineers, 1965

A Technique for the Transmission of Digital Information over Short Distances using Infra-red Radiation

By

A. T. DAVIES, (*Graduate*)[†]

Summary: The paper describes a means of transmitting digital information over limited distances, using a gallium arsenide diode as an infra-red source. At the transmitter parallel binary characters are converted to serial form, and used to pulse-modulate the diode. Different widths of pulses represent logical one, and logical zero. Mirrors are employed to confine the energy into a nearly parallel beam, for transmission to the receiver, where the serial pulse train is restored to parallel form. The data may be sent out at speeds up to 100 characters/second.

1. Introduction

The introduction of gallium arsenide (GaAs) diodes as light emitting sources two years ago in the U.S.A., has made possible a convenient method of communication over limited distances. Papers¹ have been written describing how infra-red radiation from the diodes can be modulated by video and sound signals.

This paper describes a data link which uses similar diodes to convey digital information over short distances at the National Physical Laboratory. The link will be invaluable for setting up temporary connections between computers and remote peripheral equipment.

The logical and practical designs of the transmitter and receiver are discussed in detail, and a description of the optical system is included. No analysis is given of the operation of the light emitting diode, because a discussion of the theory of these devices has already been published.²

2. The Transmitter Logic

Data are applied to the transmitter in the form of parallel eight-binary digit characters or words, and are controlled by the N.P.L. standard interface.³ The interface comprises a set of standard connections and control logic used to join together a wide range of data processing equipment at the laboratory. The link is terminated in the standard interface to facilitate its use with this existing equipment.

Consider the three element counter in Fig. 1. The state of this counter is monitored by an AND gate, the output of which is connected to both the interface RESET input, and the gated oscillator. When the counter is at zero, the AND gate provides a signal to inhibit the oscillator and reset the interface, which then indicates that the transmitter is ready to accept a new word.

[†] Autonomics Division, National Physical Laboratory, Teddington, Middlesex.

When a word is applied to the transmitter, a stimulate signal is also applied to the input (STIM J) to produce a positive-going voltage step at J. This step reads the data into the shift register and also fires the 90- μ s monostable circuit. The resulting 90- μ s pulse is inserted before each word by means of an OR gate, and is transmitted to synchronize a counter in the receiver.

The trailing edge of the 90- μ s pulse is delayed by 50 μ s, and applied through an OR gate to another monostable (30/60 μ s). This monostable generates a 30- μ s or 60- μ s pulse, depending on whether the serial output from the shift register is a 'zero' or a 'one'; the width of the pulse is thus determined by the first digit of the data word. The 30/60 μ s width pulse is applied to the OR gate and thence to the transmitter, and the delay of 50 μ s provides separation between the 90- μ s synchronizing pulse and the first digit of the data.

The trailing edge of each digit pulse is used to trigger the three-element counter, which produces a pulse to shift up the contents of the shift register in order to present the next digit of the data word to the variable-width monostable.

While the counter is not at zero, the clamp is removed from the gated multivibrator, and this produces pulses at 1 ms intervals which repeatedly trigger the 30/60- μ s monostable. This causes the counter and shift register to transmit the remaining digits.

When the counter has counted eight pulses, the AND gate detects zero to produce an output, this clamps the gated oscillator and resets the interface, thereby indicating the transmitter is ready for a new word.

The transmitted waveform is shown in Fig. 3, A. If the READY K, and STIM J are interconnected, the system will run freely at its maximum speed; this feature is useful for checking purposes.

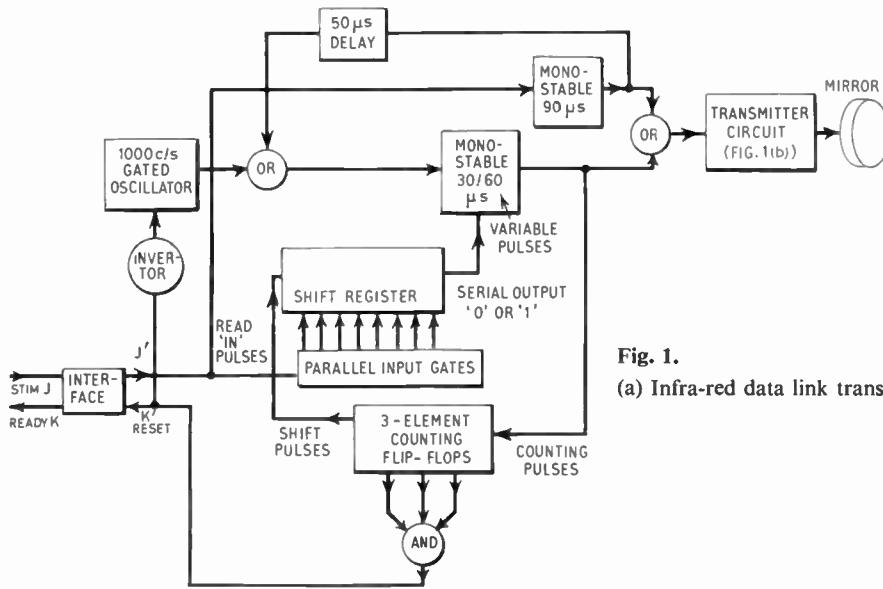


Fig. 1. (a) Infra-red data link transmitting logic.

2.1. Transmitter Circuit

A power amplifier is mounted adjacent to the mirror system, and is connected to the logic circuit via a coaxial line. This arrangement avoids switching relatively high current pulses into the coaxial line in situations where the mirrors are remote from the terminating points.

The circuit of Fig. 1(b) switches current pulses of 700 mA through the gallium arsenide diode. These pulses have a rise-time of less than 0.1 μs.

3. The Receiver Logic

The receiver logic circuit is shown in Fig. 2.

The word pulse train from the detector head amplifier is re-shaped by a Schmitt trigger circuit, and appears as shown in Fig. 3, A, as a replica of the transmitted waveform.

The waveform is applied to the serial input of a shift register, and to a 45-μs monostable circuit. The trailing edge of the 45-μs pulse is used to shift up the contents of the shift register. A 30-μs digit pulse ends before the register is shifted and is interpreted as a 'zero': a 60-μs pulse is, of course, interpreted as a 'one'.

The synchronizing pulse is detected as follows. The trailing edge of the 45-μs monostable fires a further 30-μs monostable (Fig. 3, C). This is differentiated and inverted (Fig. 3, D) and compared in an AND gate with the input (Fig. 3, A). The AND gate output is shown in (Fig. 3, E). The output signal appears only when the 90-μs pulse is received, and

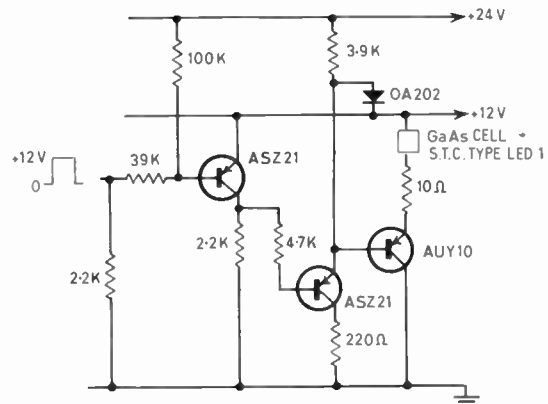


Fig. 1. (b) Infra-red data link transmitter.

resets the three-element counter to zero at the beginning of each word.

The 90-μs pulse is detected as a 'one' but this is shifted right through the register, and is finally lost at the far end.

The leading edges of the 45-μs pulses from the monostable are counted in the counting circuit; after eight edges have been received the counter returns to zero, and an output from the AND gate resets a bistable which was previously set when the 90-μs synchronizing pulse was detected.

The output from the bistable is used to indicate that data have been received and are ready to be read out.

3.1. Receiver Circuit

The solar cell detector which is sensitive to the energy of 0.9 μm has rather a slow response; to reduce

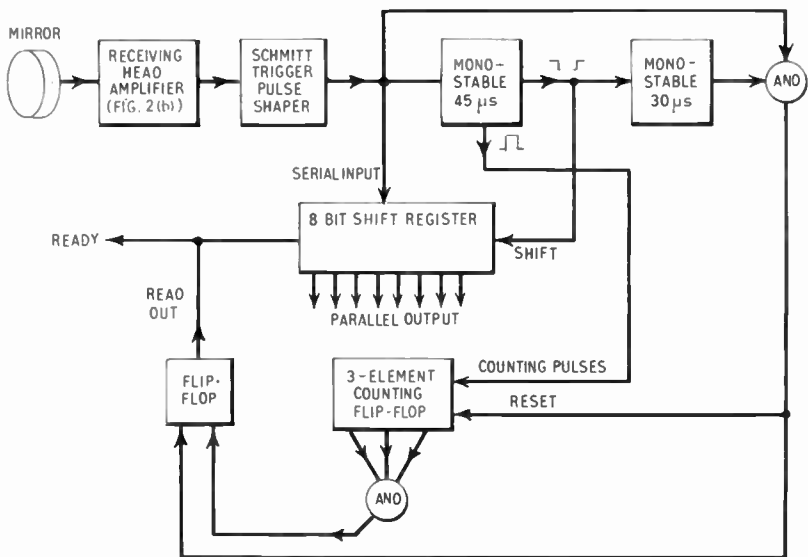


Fig. 2. (a) Infra-red data link receiving logic.

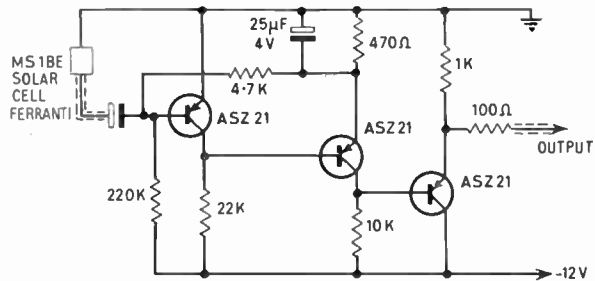


Fig. 2. (b) Infra-red data link receiving amplifier.

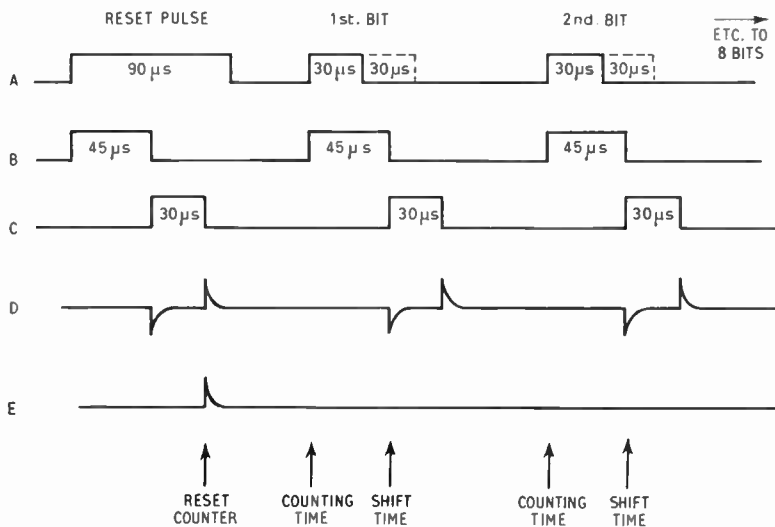


Fig. 3. Waveforms in the receiver logic.

Modifications to the Goonhilly Earth Station

The new satellite *Early Bird* differs from *Telstar* and *Relay* in many respects, and all the earth stations which took part in the earlier experiments have required considerable modifications. Goonhilly, the British Post Office earth station, was out of service for several months before the satellite was put into orbit in April.

The prime requirement of an earth station is its high-gain, narrow-beam steerable aerial which must be capable of tracking moving satellites with great accuracy. The optimum frequency range for broadband radio transmission between satellites and the earth is in the 1000–10 000 Mc/s range, and there has been a recent international agreement that the frequency for transmission between the earth and the satellite should be in the 6000 Mc/s region, and that for the satellite to ground direction frequencies near 4000 Mc/s should be used. Consequently a high-powered 6000 Mc/s transmitter is required, preceded by a frequency modulator which raises the input baseband signals (multi-channel telephony or television) to an intermediate frequency; between the modulator and the transmitter is a transmitter drive unit which converts from the intermediate frequency to the s.h.f. frequency.

In the satellite-to-ground direction a very sensitive low-noise receiver, such as a maser or parametric amplifier, is necessary to amplify the very low signal levels from the satellite. This is followed by a further s.h.f. amplifier and then a down-converter from s.h.f. to intermediate frequency; finally a frequency demodulator extracts the baseband information. These transmit and receive sequences must be in operation simultaneously for telephony transmission.

The transmitter and low-noise receivers must be fitted as close to the aerial feed as possible to keep waveguide losses to a minimum and at Goonhilly the transmitters are carried in a turntable cabin that turns, but does not tilt, with the aerial; the low-noise amplifiers are in very small cabins high up in the aerial backing structure.

For tracking, the aerial must either be programmed in its movements, which pre-supposes an accurate foreknowledge of the satellite orbit, or there can be an auto-follow system. At Goonhilly the system is basically a programmed tracking scheme to which is added an auto-correction unit to take out the effects of wind gusts or any very small errors in the original computation.

AERIAL MODIFICATIONS

The aerial at Goonhilly uses an 85 ft (26 m) diameter paraboloidal reflector with a centre feed, i.e. the feed is

located at the focus of the paraboloid. As a result of the experience gained over the past two years the design has been modified to give improved performance.

The reflector has been rebuilt and now consists of 24 adjustable stainless steel petals surrounding a 25 ft (7.5 m) diameter paraboloid. The reflector profile tolerances are determined by the required radiation patterns, which must be such that the levels of side-lobes do not result in interference to or from terrestrial radio-relay systems and other satellites; the reduction in gain caused by profile imperfections must also be acceptable. To meet these requirements, the individual petals of the reflector are constructed of panels made to a tolerance of ± 0.025 in (± 0.635 mm) over 99% of their surface. Alignment of one panel relative to another is such that the surface of the complete reflector is within ± 0.1 in (± 2.54 mm) of the 'best fit' paraboloid over 99% of its surface. The loss in gain due to surface imperfections is estimated to be 0.3 dB at 6000 Mc/s and 0.1 dB at 4000 Mc/s. The angular aperture of the reflector has been reduced from 180 deg to 140 deg; this eased the design of the primary feed so that more efficient illumination of the reflector could be obtained.

Careful consideration has been given to the design of the feed-support structure to minimize its deleterious electrical effects. Aperture blocking, produced by the structure intercepting the main beam, is kept small by making the legs of the structure as transparent as possible. The structure may also shade the dish from the feed illumination so that transmitted energy is scattered; this energy appears as increased side radiation with consequent reduction of power in the wanted direction. When used for reception, noise from the hot earth is scattered by the structure into the feed and the system noise temperature is increased. Shadowing is minimized by having the legs of the structure as near to the rim of the dish as possible. Loss in gain due to aperture blocking and feed shadowing should not exceed 0.26 dB. The increase in system noise temperature due to these effects should be less than 1 deg K.

The new reflector surface has been fitted on top of the original surface. The central 25 ft diameter paraboloid, although manufactured in four quadrants, was machined as one piece to very high accuracy. Each of the surrounding 24 petals has its own stiff backing girder structure carrying accurately machined trays, and these, in turn, bear the stainless steel reflector membrane. The position of the membrane on the backing structure can be adjusted to give accurate control of the shape of each petal, and the petals, when

in position in the reflector bowl, are carried on jacks to permit adjustment of the assembled bowl. The additional weight on the front of the aerial is 120 tons because of these modifications, and to balance this a lead counterbalance has been added. The total gross weight of the rotating part of the modified aerial is about 1100 tons.

Preliminary measurements indicate that the net gain of the aerial is comparable to that of the giant horn aeriels used in the American and French earth stations, but because the aerial does not require a radome, which would increase the system noise temperature in rain, a consistent performance can be expected in all weather conditions.

Further additions to the aerial structure include two new maser cabins fitted behind the reflector where the two lower tripod legs meet the reflector surface, and a staircase that provides easy access to all working areas.

Primary Feed

The primary feed at the focus of the reflector is required to transmit up to 10 kW of radio energy at a frequency of 6000 Mc/s and to receive simultaneously signals at 4000 Mc/s having the very low level of about a micromicrowatt. The dual requirement of transmitting and receiving at different frequencies necessitates the use of a coaxial configuration of apertures to obtain the best aerial efficiency. The feed therefore consists of an open-ended coaxial waveguide having a hollow inner conductor. The lower-frequency signals, used for reception, are carried in the outer coaxial waveguide and the high-frequency signals are transmitted through the inner tube.

A dish is mounted on the outside of the waveguide to reduce rearward radiation from the feed and spill-over past the rim of the reflector. It also provides a means of shaping the feed radiation diagram, and obtaining high aerial efficiency and low noise.

The coaxial waveguide configuration with its circular inner tube is transformed along the length of the feed into separate rectangular waveguides for connection to the main waveguide feeder runs.

Waveguide Feeders

In normal terrestrial microwave systems the losses of the waveguide feeders between the aerial and the transmitters and receivers are not normally of very great importance. In long-range satellite systems, however, such as *Early Bird*, the losses in the waveguides must be kept to a minimum to both conserve the energy collected by the aerial during reception and to avoid wasting power during transmission. Losses have been more than halved by re-engineering the waveguide transmission lines on the aerial and making use of low-loss over-moded guides. To realize the full advantages of over-moded waveguide transmission, special waveguide components were developed to preserve mode purity and to absorb any unwanted modes.

Aerial Control System

The basic control system at Goonhilly uses predictions, prepared in the U.S.A., of the position of satellite throughout the usable parts of its orbit. For tracking *Telstar* and *Relay* these data are produced for one-minute intervals in time in Cartesian co-ordinates referred to the aerial. The Goonhilly computer then

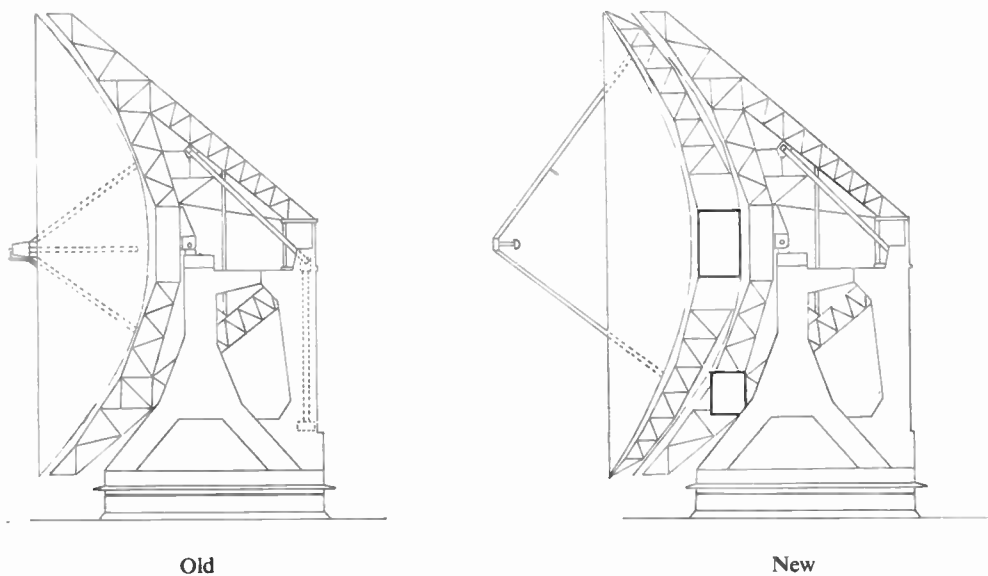


Fig. 1. Modifications to aerial structure.

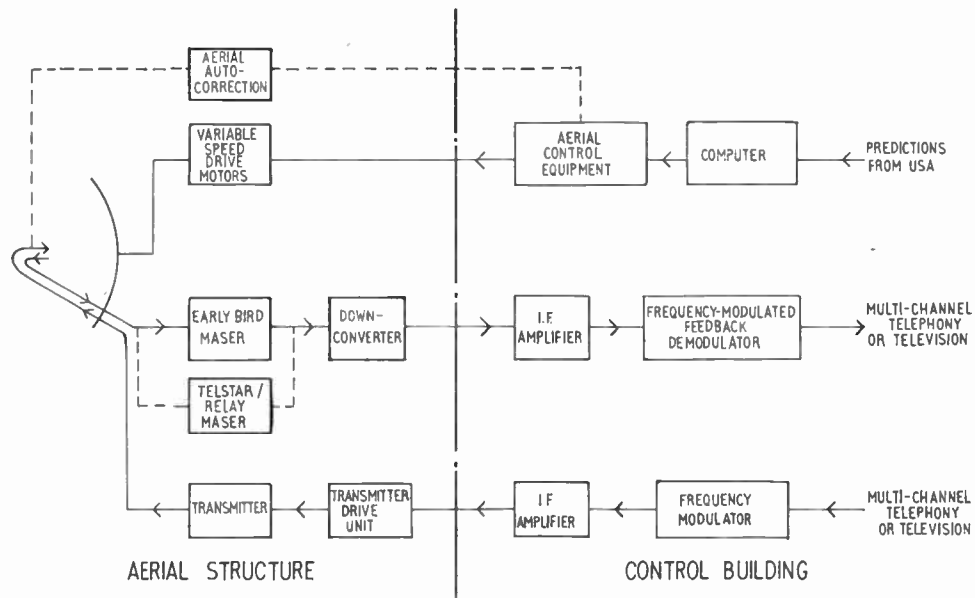


Fig. 2. Simplified schematic diagram of Goonhilly Radio Station.

checks for feasibility, makes allowance for the refraction of radio waves at low angles of elevation, converts from Cartesian co-ordinates to corresponding elevation and azimuth angle positions of the aerial, and interpolates down to one second intervals in time. This is punched on to a paper 'control tape' which can be stored until required, and about 1500 feet is necessary to control the aerial for one hour when tracking *Telstar*. About one hour is required in its preparation. *Telstar* and *Relay* require aerial tracking speeds of a few degrees per minute, but to follow satellites in orbits which may pass almost overhead the control system can operate at aerial speeds of up to 120 degrees per minute in azimuth and 30 degrees per minute in elevation.

Although *Early Bird* has in fact been launched into a perfect synchronous orbit, i.e. it is stationary with respect to the Earth, there was the possibility that its plane would be inclined by a few degrees to the equator, thus making it appear to trace out a tall, thin figure-of-eight once a day. The required tracking speeds would, however, be very much lower than those of *Telstar* and *Relay*, in fact less than one or two degrees per hour for most of the time. The control system was therefore modified so that, when required, steering data could be read from the control tape once per minute instead of once per second. In consequence, a simplified computing program enables a 300-ft control tape for twelve hours tracking of *Early Bird* to be prepared in less time than is required for one hour's operation with *Telstar*. Because of the perfect orbit, these control facilities are not at present required.

Vernier Tracking Facilities

Small steering errors due to wind gusts or imperfect predictions are corrected by swinging the aerial beam independently of the motion imparted to it by the aerial mount. A beam-swing mechanism, controlled automatically by error signals, moves the aerial feed about the true focus of the paraboloid, setting the beam accurately on the satellite. The tracking equipment includes an error-sensing unit of the conical-scan type in which the aerial feed rotates about an axis slightly offset from its own axis, scanning the aerial beam conically. When the satellite is off the scanning axis, but still within the beam, the beacon signal from the satellite is amplitude modulated at the scan frequency. Error signals in two orthogonal planes, derived from the amplitude and phase of the superimposed modulation, control the beam-swing mechanism to bring the scanning beam into track with the satellite. This part of the system is therefore an auto-follow system which continuously minimizes small steering errors.

The scan speed is about 1000 rev/min and the eccentricity of the scanning feed 0.15 in, resulting in an angular offset of the beam of 0.02 deg, one-tenth of the beamwidth. The deterioration in aerial gain due to offsetting the beam for scanning is only 0.13 dB which allows the high aerial efficiency to be retained, an essential feature in working to long range satellites. Although the magnitude of the scan is so small, adequate tracking sensitivity is obtained by employing a high-gain tracking receiver with an output band-

width limited to 2 c/s. The pull-in range of the conical-scan sensor is 0.2 deg. It is very unlikely that errors will accumulate to this magnitude faster than the auto-follow system can correct them.

Monitoring and control facilities are incorporated at a control console in the main equipment building one-quarter mile from the aerial. Provision is made for manual as well as for automatic control of the mechanism. Standby plant, where provided, is switched manually or automatically.

TRANSMITTING EQUIPMENT

Standard frequency modulating equipment, of the type used in normal line-of-sight microwave radio links, accepts the input multi-channel telephony or television signals, and produces a frequency-modulated 70 Mc/s output. The deviation employed is several times greater than the standard adopted in normal terrestrial circuits. Further intermediate frequency amplification occurs before the modulated signal is transmitted over coaxial cables between the control building and the aerial site.

Because of the greater orbital height of *Early Bird*, as compared with *Telstar* and *Relay*, some increase in the power of the signals transmitted from earth stations may be desirable. A new water-cooled travelling wave tube, having a clover-leaf slow wave structure and a ceramic output window has been specially developed that can supply 8 kW of power at the *Early Bird* frequency, or 5 kW when required for *Telstar*.

New auxiliary low power driving stages of the transmitter enable it to be switched to either the European or American frequency assignment for *Early Bird* or to the *Telstar* transmit frequency.

RECEIVING EQUIPMENT

Reception of very weak signals from satellites depends upon the use of a pre-amplifier having an extremely low level of internal noise. The principal type of amplifier in use in the various earth stations is the travelling wave ruby maser. The maser requires an operating temperature only a few degrees above absolute zero, and this is achieved by immersing the device in a bath of liquid helium. The original installation at Goonhilly incorporated the first fully operational travelling wave maser made in Britain, and this was used in all the experiments with *Telstar* and *Relay*.

The operating frequencies for the *Early Bird* satellite are sufficiently different from those of *Telstar* to require considerable modification to the maser, and an entirely new maser has been installed, incorporating developments since 1962. The new design has a greater gain and bandwidth, but the greatest improve-

ment lies in the reductions of the internal noise level to less than half its previous value, and an improvement in stability achieved by using a lightweight superconducting magnet (immersed in the liquid helium bath) instead of a heavy external permanent magnet. The use of a larger Dewar vessel to hold the liquid helium should increase the operating life to about two days.

Monitoring and control circuits have been built into the new equipment to overcome possible interruptions caused by the failure of auxiliary equipment. Another complete maser will be installed later in 1965 to provide a main and standby receiving channel.

The maser is followed by a low-noise travelling wave tube which provides further amplification at microwave frequencies and is then down-converted in frequency to 70 Mc/s. An all solid-state pre-amplifier follows this and then conventional i.f. amplifiers for transmission back to the control building.

Because the carrier/noise ratio over the satellite link is so low, conventional discriminator-type frequency demodulators cannot be used, and an f.m. negative-feedback demodulator is used instead. In this type of receiver the instantaneous frequency of the incoming signal is continuously tracked and the noise bandwidth is limited by a filter of narrower passband than that occupied by the whole deviation range of the r.f. carrier.

A paper "Application of parametric amplifiers in satellite communications" by H. N. Daghli and D. Chakraborty which describes the parametric amplifiers used at Goonhilly, is being given at the Symposium on "Microwave Applications of Semiconductors" in London (30th June to 2nd July).

TEST FACILITIES

An improved design of power measuring equipment has been developed to enable a sample of the transmitted power launched into space to be measured at the vertex of the aerial. The device is not affected by temperature changes, and is sufficiently sensitive and compact to be used as a hand-held radiation monitor. In addition, a miniature transmitter has been installed at the vertex that operates on the same frequency as the transmitter in *Early Bird*. The aerial, therefore, has a satellite simulator built into it, and the whole of the earth station equipment can be checked under realistic conditions without pointing the aerial to an earth-bound distant checking station.

Equipment has also been provided that can inject an edge-of-band pilot signal at various points in the transmission path to ensure that the station is functioning correctly and to provide a ready means of fault localization.

This article is based on information received from the British Post Office.

Tolerances in Automatic Landing:

An analysis of the effect of equipment tolerances, changes in aircraft configuration and variations in wind conditions

By

M. G. HENLEY, B.Sc. †

Presented at a meeting of the Radar and Navigational Aids Group in London on 21st October 1964.

Summary: To ensure that production systems will perform an automatic landing with consistent accuracy, it is necessary to analyse the variations that may be expected in the landing performance. The system discussed is the B.L.E.U. single channel automatic landing system which utilizes ground-based radio aids to provide aircraft position information to the autopilot.

The critical landing parameters are discussed, together with the factors which contribute to variations in these parameters. The methods used to determine the errors are analysed and the criteria needed to assess whether or not the errors are acceptable are established.

It is found that variations in wind conditions make a significant contribution to the total errors and that changes in the aircraft configuration also add to the overall variation. The effect of equipment tolerances varies widely with the landing parameter under consideration so that it is not necessarily possible to improve performance significantly by tightening equipment specifications.

Should it be necessary to reduce the probability of an unacceptable performance, restrictions on the allowable wind conditions and on the aircraft weight and centre of gravity position must be considered.

1. Introduction

In the past, the acceptance of an automatic pilot for an aircraft has been obtained by demonstrating that the performance of one system, including radio aids where relevant, in one aircraft is satisfactory. Although it was recognized that variations in performance would occur with different combinations of autopilot units, experience shows that the variations obtained from any set of autopilot units in any aircraft of the same type are acceptable. It has not been necessary, therefore, to assess the variations in performance which will occur with different combinations of equipment.

However, when considering an automatic landing, normal variations in performance may or may not be acceptable as the limits on permissible variations are very definite compared with those that apply during normal cruise and auto-approach flight. Although many thousands of successful automatic landings have been carried out in a programme extending over several years, it is necessary to establish that the standard production systems will perform the manoeuvres with consistent accuracy before clearance can

be given for regular use in low visibility weather conditions.

The limits to be applied can be defined in terms of aircraft position and velocity at touch-down. It is obviously essential for the aircraft to land on the runway and in such a manner that the undercarriage is not over-stressed, that no other part of the aircraft strikes the ground, and that the aircraft remains on the runway for the whole of the landing run.

When carrying out trials to ensure that these criteria are met, it is necessary, unless a very large flying programme is envisaged, to calculate the effect of all parameter variations on performance.

2. The B.L.E.U. System of Automatic Landing

The system referred to in this paper is the B.L.E.U. single channel system which utilizes two ground-based radio aids, the instrument landing system and the leader cable system, together with a radio altimeter. ‡ The signals from these radio systems are fed into an autopilot which controls the aircraft by means of electric servomotors driving the elevator, aileron, rudder and throttle control runs.

† S. Smith and Sons (England) Ltd., Aviation Division, Bishops Cleeve, Cheltenham, Gloucestershire.

‡ J. S. Shayler, "Radio guidance elements of the B.L.E.U. automatic landing system for aircraft", *J. Brit.I.R.E.*, 21, p. 17, January 1961.

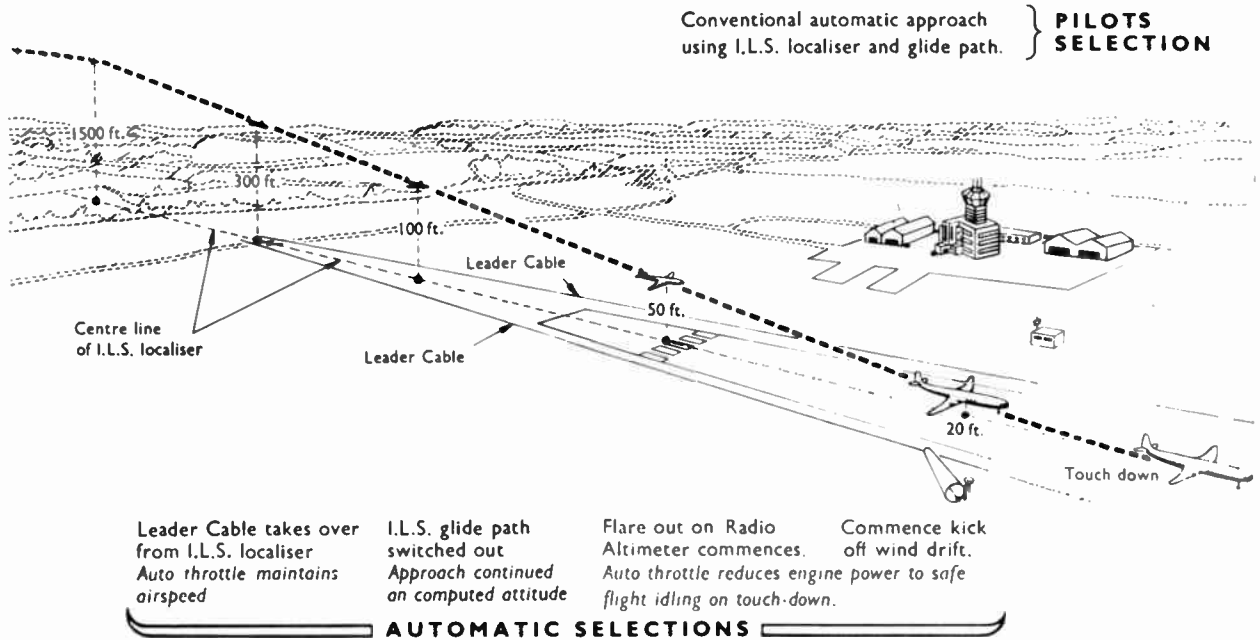


Fig. 1. Automatic approach using i.l.s. localiser and glide path.

The autopilot itself operates on the rate/rate principle in which the rate of control surface deflection is proportional to the rate of change of aircraft attitude. This type of control is achieved by using three mutually-perpendicular rate gyroscopes mounted on a platform which is maintained level by means of servomechanisms. The datum for each axis is defined by a monitor; a simple pendulum mounted fore-and-aft is used for the pitch plane, another pendulum mounted athwartships for the roll plane and the compass system for azimuth. Commands fed into the autopilot are met by moving the platform relative to the aircraft. Heading changes are brought about by tilting the platform in the roll axis, the rudder channel being used to suppress sideslip. Tilting the platform in the pitch axis will cause the aircraft to climb or dive as required. The autothrottle sub-system maintains the aircraft at a constant selected airspeed by adjusting the position of the throttles.

This is the first automatic landing system to be put into quantity production and has, in fact, been developed from equipment which was not originally designed with automatic landing in mind. The reliability needed is obtained by careful engineering, simplicity in design, and the use of reliable components. It should be noted that the second generation of equipment, which is to be used for automatic landing on scheduled passenger carrying flights, has been designed from the start to meet even more stringent performance and reliability criteria.

Using the system described above, an automatic

approach and landing is carried out as follows (see Fig. 1). The aircraft is flown at a constant barometric height, usually between 1000 and 2000 feet and on a heading suitable for intercepting the inbound localizer beam of the i.l.s. This is known as the 'track' phase during which the autopilot guides the aircraft on the localizer beam and holds it there. The range is chosen so that the aircraft is below the glide path. As the aircraft is inbound it will eventually intersect the glide path beam, and, when this happens, the pilot selects 'glide' phase. The aircraft is then automatically controlled to follow the i.l.s. path and the barometric height lock is disconnected.

The autopilot now controls the aircraft both in pitch and azimuth to follow the i.l.s. beams and, during this phase, the pilot primes for an automatic landing. This consists of pulling a knob and the whole of the remaining sequence switching and aircraft manoeuvring is completely automatic, the pilot needing only to monitor the progress of the landing from his flight instruments.

At a height of approximately 300 feet, as the aircraft enters the coverage of the leader cable system, the leader cable phase commences and the azimuth signal into the autopilot is switched automatically from the i.l.s. localizer to leader cable, the aircraft continuing to follow the i.l.s. glide path in pitch. At a height of approximately 100 feet the i.l.s. glide path signal into the autopilot is disconnected and the aircraft is controlled to a mean pitch datum which was computed automatically as the aircraft flew down the glide path.

This is known as the 'attitude' phase and continues to a height of approximately 50 feet, the actual height being dependent on the aircraft type. The 'flare' phase then commences during which the aircraft is flared along a flight path computed from the radio altimeter height signal. The throttles are also closed at a constant rate to the safe flight idling revolutions of the engines.

At approximately 20 feet 'land' phase commences in which the leader cable azimuth control is disconnected, the wings are levelled and rudder is applied to yaw the aircraft towards the pre-set runway heading, thus eliminating any drift angle due to a cross-wind.

After touch-down the autopilot is disconnected and the steering of the aircraft along the runway, the complete closure of the throttles and the application of the brakes are performed manually by the pilot.

To summarize the manoeuvre, control in azimuth is obtained first from the i.l.s. localizer, then from the leader cable and finally the aircraft is yawed on to the runway heading to remove drift. Control in pitch is obtained first from the i.l.s. glide path and finally from the radio altimeter, there being an interim period where no external control is applied. The throttle closure during the 'flare' phase can be carried out either automatically or manually, but only the completely automatic case is considered in this paper.

3. Consideration of the Problem

As stated above, it is necessary for certain conditions to be satisfied if the landing is to be considered satisfactory. These conditions are best assessed in terms of the following touch-down parameters:

Azimuth plane

- (i) heading error;
- (ii) bank angle;
- (iii) rate of change of heading;
- (iv) crab angle (the angle between the heading of the aircraft and its velocity relative to the ground);
- (v) lateral displacement;
- (vi) a combination of lateral displacement and lateral velocity.

Pitch plane

- (i) rate of descent;
- (ii) pitch attitude;
- (iii) loss of airspeed;
- (iv) touch-down scatter.

The causes of the variations in these parameters arise from three different sources, as follows:

(a) *Tolerances in the individual units.* These can be sub-divided into those attributable to the autopilot

and those attributable to various other systems employed to give signals to the autopilot, such as the airborne radio receivers and the radio altimeter system (Fig. 2). The total tolerance of a unit is dependent on manufacturing tolerances, tolerances due to temperature variations and tolerances due to variations in power supplies.

(b) *Changes in the aircraft configuration.* Variations in the landing weight and the position of the centre of gravity of the aircraft affect the performance.

(c) *Variability of the wind conditions.* Headwind, crosswind, wind shear and turbulence all contribute to the variations in performance.

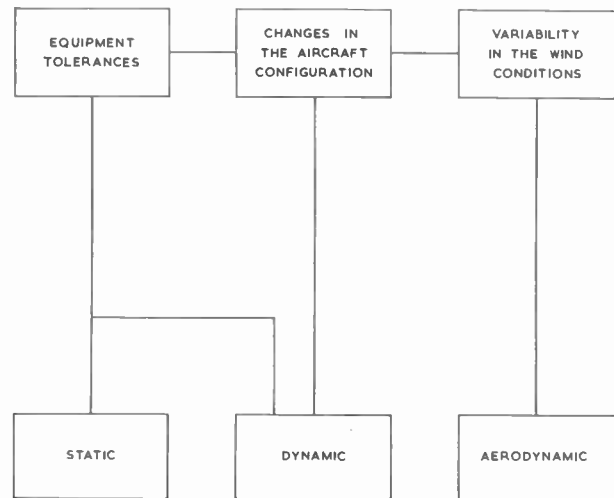
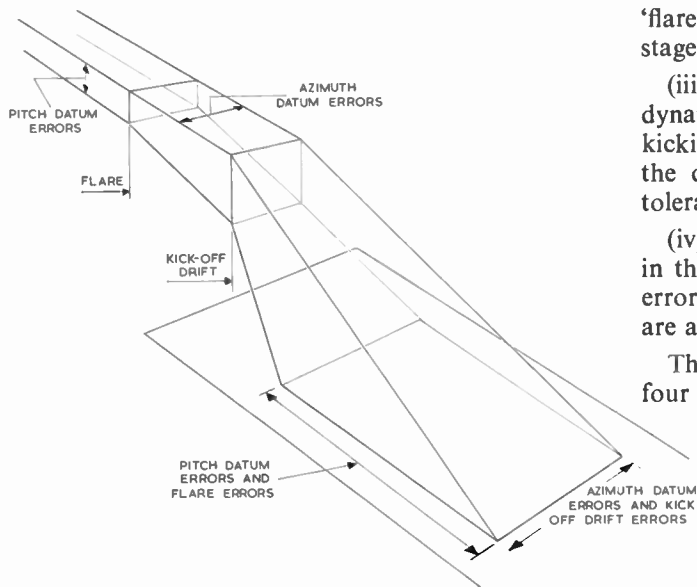


Fig. 2. Inter-relationship of tolerances.

For the purpose of analysis, the errors arising from the above variations are divided into static, dynamic and aerodynamic. Static errors are caused by the datum errors and the thresholds in the equipment together with misalignment of the leader cable and i.l.s. glide path systems. Dynamic errors are caused by the variations in the sensitivity of the airborne radio, tolerances on the autopilot gearings and changes in the aircraft configuration. Aerodynamic errors are due to the wind conditions encountered.

During the approach phases the aircraft is being flown to a datum in the pitch and azimuth planes until the commencement of the final landing manoeuvres (Fig. 3). From then on the aircraft is first flared nose up and then any drift is removed. The analysis, therefore, divides into two stages for each of the pitch and azimuth planes; in the first stage the displacement errors on the approach are determined and in the second the effects of the errors occurring during the landing manoeuvres are assessed for each of the touch-down parameters.



'flare' phase and are not, therefore, considered at this stage.

(iii) *Kick-off-drift errors.* These arise from the dynamic and aerodynamic errors occurring during kicking-off drift. As the leader cable is disconnected the dynamic errors depend only on the autopilot tolerances.

(iv) *Flare errors.* All sources of error contribute in this phase and, as stated above, the aerodynamic errors occurring during the Glide and Attitude phases are also included.

The analysis used to obtain the errors in each of the four stages is now discussed.

Fig. 3. Factors affecting approach and landing.

In calculating the displacement on the approach both the static and aerodynamic errors are taken into account, but any dynamic errors have been ignored. These can be caused by bends in the beam, 'noise' on the beam, variations in the sensitivity of the airborne radio and the tolerances of the autopilot gearings. It is difficult to include any imperfections in the beam in this kind of theoretical analysis and, in particular, beam bends are a function of the individual site. For the purpose of this paper, therefore, the radio beams are assumed to be of adequate quality and in this case the remainder of the dynamic errors on the approach are considered to be negligible.

During the landing manoeuvres the dynamic and aerodynamic errors are evaluated together with any additional static errors which do not occur during the approach.

The analysis of the variables consists, therefore, of four parts and these are each considered separately.

(i) *Azimuth datum errors.* The azimuth datum errors are calculated from the static and aerodynamic errors occurring during the leader cable phase. It is assumed that any errors occurring when on i.l.s. localizer beam in the 'track' phase are removed during the leader cable phase.

(ii) *Pitch datum errors.* These are the displacement errors due to the static errors which occur from the top of the 'glide' phase, down through the 'attitude' phase, to the commencement of the 'flare' phase. The aerodynamic errors will affect the pitch datum errors, but for convenience of analysis they are included in the

4. Analysis of the Landing Variables

4.1. Azimuth Datum Errors

During this stage the aircraft is, in the lateral plane, under the control of the leader cable system, the signal from the leader cable receiver being used to generate a bank demand for steering the aircraft through the aileron channel of the autopilot. (Table 1.) The autopilot tolerances are specified in terms of allowable variations in the various individual units comprising the system. The total maximum errors are extremely unlikely to occur and a more realistic addition of

Table 1

Typical azimuth datum errors

Source of Error	Standard Deviation (feet)
Autopilot	5
Leader cable beam misalignment	2
Leader cable receiver	0.5
Siting of leader cable aerial	2.5
Wind shear	5
Turbulence	4

errors is obtained by assuming appropriate probability distributions for the errors and summing the variances. For this purpose rectangular distributions have been assumed for the manufacturing errors. In addition, it is assumed that the temperature errors vary linearly with temperature and that there is a rectangular probability distribution of temperature.

The same assumptions are made about the effects of power supply variations. Therefore, in computing the variance of the total error the variance of the three independent contributions, i.e. manufacturing, temperature variations and power supply variations are added. A typical figure for the standard deviation of the lateral displacement due to autopilot datum errors is of the order of 5 feet.

There are two sources of error to consider for the lateral displacement due to datum errors in the leader cable system. The first of these is the leader cable beam misalignment due to a steady displacement error between the beam centre and the runway centre line. The beam is monitored just beyond the runway threshold and a failure warning is operated in the event of this error exceeding 6 feet. It is assumed that the distribution of this error is normal with a standard deviation of 1.8 feet. The second datum error is in the leader cable receiver itself. There are two separate datum setting errors, a.c. and d.c. respectively, which are assumed to have rectangular distributions each having a standard deviation of 0.4 feet.

There is an additional error to those above due to the siting of the leader cable aerial at a distance from the aircraft centre of gravity. Under crosswind conditions, the centre of gravity will be displaced from the beam centre. The aerial is normally mounted forward of the centre of gravity and, assuming a standard deviation of 6 knots for the cross-wind, a standard deviation for the aerial drift effect can be of the order of 2 to 3 feet.

The final source of error for positioning the aircraft laterally whilst under leader cable control is due to the effects of wind. Turbulence and wind shear both cause errors due to the inability of the autopilot to correct the aircraft heading without incurring a lateral displacement from the beam centre. Standard deviations of the order of 4 and 5 feet respectively due to turbulence and wind shears are typical. The above errors are now added statistically to give a standard deviation for the azimuth datum errors.

4.2. Pitch Datum Errors

In the longitudinal plane the aircraft approaches the runway under control of the glide path beam until a height of about 100 feet is reached, below which the autopilot provides an attitude lock until the start of the flare.

The statements made previously on the effects of temperature and supply variation on the autopilot tolerances are also applicable here. The standard deviation for the longitudinal displacement due to elevator channel datum errors during 'glide' phase is of the order of 15 feet.

As in the lateral plane there are two sources of error to consider for the longitudinal displacement

Table 2
Typical pitch datum errors

Source of Error	Standard Deviation (feet)
Autopilot	15
Glide path beam misalignment	38
Glide path receiver	14
Wind shear	17

due to datum errors in the glide path system. (Table 2) The first of these is the glide path beam misalignment due to a steady displacement error between the effective beam centre line and the nominal centre. A maximum error of $\frac{1}{2}$ deg is allowed and, to be consistent with the leader cable calculations, it is assumed that the distribution of this error is normal, with a standard deviation of 0.1 deg. The second datum error is in the glide path receiver and an estimate of the standard deviation of the glide path error is 0.038 deg. The corresponding standard deviations for the longitudinal displacements are approximately 38 and 14 feet respectively. The above errors are now summed statistically to obtain a standard deviation for the pitch datum errors, excluding those due to wind effects.

4.3. Kick-off-drift Errors

During the kick-off-drift phase all external lateral control is removed and the aircraft is yawed on to the runway heading.

The kick-off-drift performance depends on the magnitude of the drift angle being removed and the autopilot control gearings. These gearings have overall tolerances consisting of individual tolerances on the components which make up any particular gearing. As in the case of the datum errors, the autopilot tolerances again depend on manufacturing errors and temperature and electrical supply variations.

To determine the dependence of the azimuth landing variables on the autopilot gearings an analogue computer is used. The kick-off-drift performance depends on the initial conditions at the commencement of the manoeuvre and these are expressed in terms of heading error, heading error rate and lateral velocity. From the computer it is possible to determine how the landing variables depend on each control gearing in turn, the remaining gearings having their nominal values. The dependence of the landing variables on the maximum permissible tolerances allowed and on the time of duration of the manoeuvre can then be determined.

Each of the landing variables is directly proportional to the initial drift angle when landing in a steady

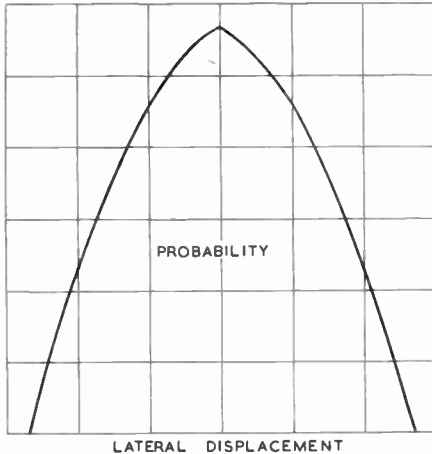


Fig. 4. Probability of the lateral displacement at touchdown being greater or less than the median value.

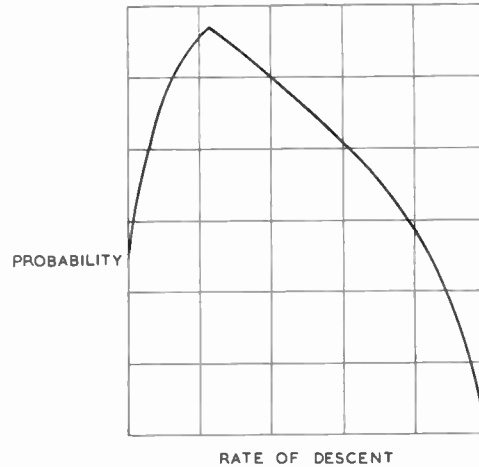


Fig. 5. Probability of the rate of descent at touchdown being greater or less than the median value.

wind. There is, therefore, a probability of having to remove a given drift angle. A typical model for the steady wind normal to the runway takes the form of a restricted normal distribution with a standard deviation of 6 knots and a maximum value of 18 knots. The time at which the aircraft touches down after initiation of the kicking-off-drift manoeuvre depends on the flare manoeuvre and the height at which the manoeuvre is commenced. The variation in this time is a function of the flare gearings, together with their associated tolerances, the aircraft configuration and the wind conditions.

With the above assumptions, the standard deviations for the azimuth landing variables arising from the kicking-off-drift errors can now be calculated for any particular aircraft type.

4.4. Flare Errors

During the 'flare' phase the radio altimeter signal is used to compute a flight path which will flare the aircraft exponentially to the ground.

The dependence of the longitudinal landing variables on the autopilot gearings during this manoeuvre is again determined by an analogue computer, in a manner similar to that for the kick-off-drift manoeuvre. The flare performance also depends on the dynamic behaviour of the aircraft, and this is a function of the landing weight, centre of gravity position and approach speed. In addition, turbulence and wind shear affect the performance and also determine the initial conditions at the commencement of flare. For this reason wind effects from the commencement of 'glide' phase have been included in this part of the analysis, and consequently were omitted during the pitch datum error work, as already explained. A typi-

cal model for the wind takes the form of a restricted normal distribution with a 9 knot headwind mean and a standard deviation of 6 knots, limited to 27 knots head and 9 knots tail. The lack of symmetry is to compensate for the likely alignment of the runway in use into the prevailing wind. The amount of turbulence present, both horizontal and vertical, is scaled to the strength of the wind.

With the above assumptions, the standard deviations for the pitch landing variables arising from the flare errors can now be calculated for any particular aircraft type.

4.5. Total Errors

The displacement errors arising from the azimuth and pitch datum errors can now be combined with the errors occurring in each of the landing variables during the kick-off-drift and flare manoeuvres respectively. The total errors in each of the landing variables arising from equipment tolerances, variations in the aircraft configuration and wind conditions are thus obtained.

In the azimuth plane the errors are, in general, approximately normally distributed even though the individual errors are not. However, because the performance in the pitch plane does not vary evenly about the mean, the distributions of the total longitudinal errors are skew (Figs. 4 and 5).

5. Results

From the dispersions of the errors the actual errors associated with different probability levels are obtained. The mean time between failure of the equipment is such that the probability of a fault occurring in a single channel automatic landing

system of the type discussed is, during the restricted time of an automatic landing, of the order of 1 in 10^5 . The performance variations which can occur are, therefore, examined at this probability level and the results so obtained are discussed below. In addition, the errors obtained for the landing parameters can be allocated between the different categories of equipment tolerances, variations in aircraft configuration and wind conditions.

6. Discussion of Results

The results obtained for each of the variables are now considered separately. It will be seen that the criteria by which the errors for the landing variables are judged depend in some cases on the particular aircraft type being considered. When considering these results the assumptions made regarding the adequacy of the radio beams must be borne in mind. Noisy beams will obviously degrade the overall performance.

6.1. Heading Error

The analysis for the heading error shows the error to be small even when associated with low levels of probability and it would, in general be acceptable at the 10^{-5} probability level. By far the biggest contribution to the error comes from the wind conditions and the autopilot only contributes a comparatively small amount. The equipment tolerances can, therefore, be considered to be satisfactory. Very little improvement would in fact be obtained by tightening the equipment tolerances affecting this parameter.

6.2. Bank Angle

Whether the bank angle is acceptable or not depends on the aircraft geometry, as it is essential that the wing tip does not touch the ground. The bank angle error is small and would in most cases be acceptable. Should it be marginal for a particular aircraft, modifications to the equipment would be worth considering as, in this case, a large proportion of the error comes from the autopilot.

6.3. Heading Rate

A large heading rate at touch-down is undesirable and landings with a residual drift angle, but a small rate of change of heading, are preferable to landings with all drift removed but a high heading rate. The rates of change of heading which emerge from this analysis are caused mainly by the wind conditions rather than by equipment and are considered to be acceptable.

6.4. Crab Angle

As this angle determines the side load on the undercarriage it should be as small as possible at touch-down. However, crab angles up to 5 deg are normally acceptable and the probability of this value being exceeded is negligibly small.

6.5. Lateral Displacement

The allowable error here is dependent on the width of the runway and the width of the aircraft undercarriage. With the assumptions made, there is only a very small probability of an aircraft with say, a 40 feet wheelbase, touching down on the edge of a 200 feet wide runway.

6.6. Lateral Displacement plus Lateral Velocity

A more important landing criterion than the lateral displacement alone is that the lateral displacement plus the displacement arising from a lateral velocity lasting for, say, 5 seconds should not exceed a given value. A typical value for this is 75 feet and the extremes of this criterion allow the aircraft to touch down, either on a line parallel to the runway centre but displaced 75 feet from it with zero lateral velocity, or to touch down on the centre line with a lateral velocity of 15 feet per second. Again, with the assumptions made, there is only a very small probability that this criterion will be exceeded.

6.7. Rate of Descent at Touch-down

When considering the rate of descent at touch-down light landings are unimportant and the distance of the touch-down point from the threshold becomes of greater significance. The acceptable rate of descent in heavy landings depends upon the ultimate load in an undercarriage member and so is a function of the aircraft type. The rate of descent at the appropriate probability level must, therefore, be judged for each aircraft application. The majority of the variation is attributable to wind shear and turbulence so that, should it be necessary to reduce the risk of a heavy landing, this could be achieved by a restriction on the range of wind conditions in which an automatic landing is carried out. This would normally consist of restricting the permissible maximum headwind and so would not be a drawback during landings in low visibility where winds are normally light or non-existent.

6.8. Pitch Attitude

There will be some mean pitch attitude associated with the mean touch-down performance. In addition there will be two limiting attitudes, one nose up and one nose down to ensure that the main wheels touch first and so the results must be assessed for the particular aircraft under consideration. Over half the total variation of pitch attitude is due to the aircraft configuration and so, should it be desirable to limit the variation in pitch attitude, this could be achieved by limiting the landing weight and centre of gravity range of the aircraft.

6.9. Airspeed Loss

The ratio of the loss of airspeed to the approach airspeed at touch-down provides a measure of how

near the aircraft is to the stall. If there is an unacceptable probability of too large an airspeed loss this can be corrected by increasing the approach speed.

6.10. Touch-down Scatter

The longitudinal scatter of the touch-down point must be assessed from both the probability of under-shooting and overshooting the runway. The touch-down point will depend on the position of the glide-path origin and this is normally 1000 feet from the runway threshold. The probability of the aircraft either landing in the undershoot area or landing too far down the runway is a function of the aircraft configuration so that this variation will have to be assessed for each aircraft type. However, wind conditions again play a large part and, if the probability of an unacceptable performance is too high, this can be improved by limiting the wind conditions in which the automatic landing is carried out.

7. Conclusions

The results arrived at in this paper are, in the main, based on theoretical considerations, and depend on the accuracy of the assumptions made. Some experimental flight trials are needed, therefore, to confirm these results and the flying must be carried out on radio beams of adequate quality.

However, it is evident that, with this type of system, variations in wind conditions play a large part in contributing towards the total variations in the landing parameters. Where necessary these effects can be reduced by specifying the range of wind conditions under which the system is required to work. When designing autopilots for automatic landing, therefore, consideration must be given to ensuring that the control laws chosen will enable the system to cope adequately with the wind conditions likely to be encountered.

The variations in the aircraft landing weight and centre of gravity position affect certain of the landing

parameters so that the errors in these parameters can, if necessary, be reduced by suitably restricting the aircraft landing configuration.

The effects of noisy beams have not been considered, but it is evident that the radio equipment static tolerances have only a small effect on the variation in the performance of the automatic landing.

In several cases the autopilot tolerances have very little effect on the total variations and this emphasizes the fact that production tolerances should not be made tighter than is necessary from the performance point of view, especially at the expense of complexity, as this can reduce reliability. However, this type of analysis is a useful method for determining which of the autopilot tolerances, if any, need improving in a given set of circumstances.

It is seen then, that several quite distinct sources of error contribute to the total variations, equipment tolerances only being responsible for a proportion of them. However, the analysis shows that the total variations are normally comparatively small and it is suggested that, in general, these are acceptable for the risk level associated with the equipment. Nevertheless, each aircraft installation must be considered individually and, should it be necessary to improve the performance for any particular landing parameter, careful consideration must be given to the best method of achieving this.

8. Acknowledgment

The author wishes to acknowledge the useful discussions on this subject which have been held with the Blind Landing Experimental Unit of the Royal Aircraft Establishment, Bedford.

Manuscript received by the Institution on 15th October 1964. (Paper No. 987/RNA 43.)

© The Institution of Electronic and Radio Engineers, 1965

DISCUSSION

Under the chairmanship of Mr. R. W. Lord

Mr. T. W. Prescott: It is an essential part of system design that an overall analysis be made to assess the performance capable of being achieved by a production system when used under all the different environmental conditions that are met in service. To meet the stringent safety standards of an automatic landing system, rightly demanded by the civil certificating authorities, system reliability is achieved by the use of equipment redundancy techniques which allow square roots and even cube roots to be taken. No such easy way out is available in assessing system performance.

Mr. Henley has considered one particular system built to a 10^{-5} safety criterion, and it appears at first sight that

wind, and not equipment tolerances, accounts for most of the errors in performance. Before the equipment manufacturers become too complacent let me say that obviously for a civil system, which calls for a 10^{-7} safety criterion, improvements have to be made, and are being made, to the form of control used to lessen the effects of wind changes. Therefore the effects of equipment tolerances become much more important. It is a complicated business, however, because modifications to improve one part of the system may have repercussions elsewhere, so that continuous assessment of performance is necessary. Such a performance study has been under way for some time and many discussions have taken place between interested

parties. However, the time is now ripe for the problem to be discussed more openly and I should like to thank Mr. Henley for taking the initiative in this respect. One detailed criticism of the paper is that the dynamic errors on the approach have been neglected in the analysis and these can have a significant effect on landing performance, and incidentally these errors are caused mainly by equipment tolerances and imperfections.

Mr. M. G. Henley (*in reply*): Mr. Prescott's statement is an excellent summary of the present situation, and I agree that with an improvement in the control laws to lessen the effects of wind, equipment tolerances become more important. This applies to the second generation of automatic landing equipment which has been excluded from the paper. It is certainly true that the dynamic errors on the approach have been omitted in the paper; hence the qualification regarding beams of 'adequate quality'.

Mr. P. F. Cook: Mr. Henley has referred more than once to the assumption that the existence of a suitable i.l.s. beam was necessary in his calculations. Would he care to define more precisely what the suitable characteristics of this beam have to be?

Secondly, in the calculations which were done on the dispersion of the touch down point, no reference was made to the radio altimeter. It is suggested that the performance of this device could have an effect on this parameter.

Mr. Henley (*in reply*): The definition of a suitable i.l.s. beam is outside the scope of this particular analysis, and it has been assumed that the beam bends and noise on the beam are such that the effect of them is negligibly small. Whether a particular installation is satisfactory may well depend on local site conditions as well as the particular

aircraft and autopilot combination under consideration. Work is still proceeding to obtain a satisfactory definition.

Datum errors in the radio altimeter and noise on the radio altimeter signal have been ignored, but it is considered that the effect of these will be negligibly small.

Mr. I. A. Watson: How has the effect of wind shear been estimated in the pitch axis, in particular how was a standard deviation (S ft) deduced?

Have all the figures been estimated for one aeroplane only? Was this a small one?

Mr. Henley (*in reply*): At entry to flare a longitudinal displacement due to wind shear has been given as having a standard deviation of 17 feet. As explained in the paper this source of error is not actually used in the final computation of the longitudinal touchdown scatter as the wind effects are continuous throughout the approach and land phases. The effects of wind are taken into account in the analogue computer studies. These commence at 'glide' phase and have the wind conditions varied throughout the approach.

The actual figure of 17 feet for the standard deviation in the longitudinal scatter due to wind shear at commencement of flare is obtained from the displacement of the aircraft from the beam centre line in the 'attitude' phase. Knowing the time constant of the pitch monitor, which itself senses the change of ground speed due to the wind shear, the pitch displacement is found. From a knowledge of the pitch displacement and the duration of the attitude phase the horizontal scatter about the nominal intersection of the glide path with the flare height is found.

The figures have been estimated for one aeroplane only. It was not a particularly small one.

A Constant Impedance Voltage-controlled Phase-shift Network

By

W. D. RYAN, M.Sc., Ph.D. †

AND

W. FLECK, M.Sc.

(Associate Member) ‡

Summary: A voltage-controlled phase-shift network is presented in which a continuous change in phase of up to 60 deg per section may be obtained at constant impedance in the h.f. and v.h.f. range. Theoretical and experimental results are compared for two typical circuits, operating at 1 Mc/s and 80 Mc/s, which have an insertion loss of less than 1 dB, and a bandwidth of about 10%.

1. Introduction

V.h.f. aerial arrays may be steered by the adjustment of the phase of the signal from the individual elements. In the past, this has been done by physically changing the values of the components involved, either locally or through mechanical couplings. Recently some attention has been given to purely electronic systems usually employing non-linear elements in the phase-shift sections. For example, Swarner¹ has described a transmission line system using variable-capacitance junction diodes which gives a change in phase of 45 deg at 300 Mc/s with an insertion loss of less than one decibel. At higher frequencies, Hardin² has investigated a system based on the termination of a transmission line with pure reactance using junction diodes and directional couplers and reports phase shifts up to 180 deg with low insertion loss. Of the lumped parameter devices, Doherty³ describes a ladder network with voltage-variable capacitors and Pawley⁴ develops a bridged-T network. In both cases it would appear to be difficult to maintain the image impedance of the sections constant with change in phase. An interesting modulation technique is described by Vogt⁵ which employs variable-capacitance diodes in the bridge arms of balanced modulators.

2. The Phase-Shift Network

The present system employs variable-capacitance diodes and is based on the properties of the lossless lattice network shown in Fig. 1. For this section, the characteristic impedance Z_0 and the propagation constant $\gamma = \alpha + j\beta$ may be obtained from,

$$Z_0^2 = Z_A Z_B \quad \text{.....(1)}$$

and

$$\tanh^2(\gamma/2) = Z_A/Z_B \quad \text{.....(2)}$$

In order to maintain Z_0 constant when Z_A and Z_B are changed, the product $Z_A Z_B$ must remain constant. Z_A and Z_B must also be pure reactances for minimum insertion loss and must be of opposite sign to give a real Z_0 . These conditions are satisfied by the $L-C$ lattice of Fig. 1(b), if the ratio $L_1/C_1 = Z_0^2$ is kept constant. To do this, all four elements in the network must be varied simultaneously. The realization of a variable inductance with similar characteristics to the variable capacitance employed is difficult and it is therefore preferable that all four elements be capacitive. This may be done, in a given frequency range, by replacing the inductors by quarter-wave sections with capacitive terminations, as shown in Fig. 2. Thus, if $Z_{0\pi}$ is the characteristic impedance of the quarter-wave π -section, then

$$Z_{0\pi} = \omega_0 L_2 = 1/\omega_0 C_2 \quad \text{.....(3)}$$

and the effective inductive reactance $\omega_0 L_1$ at the input terminals of the section due to the terminating capacitor C_r , is given by,

$$\omega_0 L_1 = Z_{0\pi}^2 \omega_0 C_r \quad \text{.....(4)}$$

The requirement that Z_0 remain constant is now satisfied if the ratio C_r/C_1 is constant, or,

$$C_r = kC_1 \quad \text{.....(5)}$$

For operation in an unbalanced line, the lattice section must be transformed into an unbalanced network. A relation between the lattice and its equivalent bridged-T section has been obtained by Bode.⁶ Comparing the basic lattice of Fig. 1(a) with the unbalanced bridged-T section shown in Fig. 3, we have

$$Z_B = Z_1 + 2Z_2 \quad \text{.....(6)}$$

and

$$1/Z_A = 1/Z_1 + 2/Z_3 \quad \text{.....(7)}$$

It is convenient to assume that Z_1 is the impedance of the capacitor C_2 , in which case $Z_3/2$ becomes the impedance of inductor L_2 in series with the parallel combination of C_2 and C_r , and $2Z_2$ becomes the difference in impedance between C_1 and C_2 . Thus

† Department of Electrical Engineering, The Queen's University of Belfast.

‡ Department of Physics, College of Technology, Belfast.

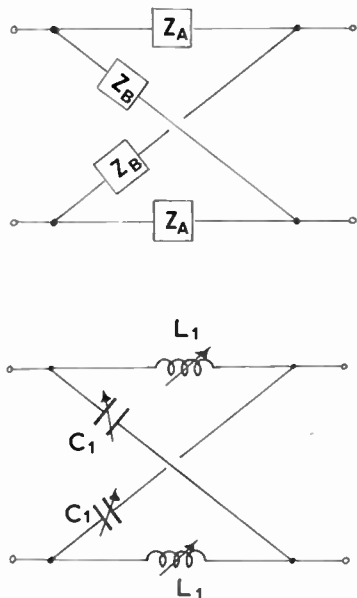


Fig. 1. The basic lattice phase-shift network.

$$Z_1 = 1/j\omega_0 C_2 \quad \dots\dots(8)$$

$$Z_2 = 1/2j\omega_0 C_1 - 1/2j\omega_0 C_2 \quad \dots\dots(9)$$

$$Z_3 = 2j\omega_0 L_2 + 2/j\omega_0 (C_2 + C_r) \quad \dots\dots(10)$$

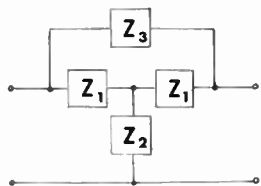


Fig. 3. Bridged-T network.

At a given operating angular frequency ω_0 , the constant negative capacitive reactance $-1/2j\omega_0 C_2$ may be obtained in practice by an inductor L such that,

$$j\omega_0 L = -1/2j\omega_0 C_2 \quad \dots\dots(11)$$

or

$$L = 1/2\omega_0^2 C_2 = L_2/2 \quad \dots\dots(12)$$

from (3).

This procedure leads to the circuit of Fig. 4, in which, for constant Z_0 at ω_0 , $C_r = kC_1$. In theory k may assume any value but in practice it is necessary to use similar, if not identical, diodes for C_r and C_1 in order to maintain the ratio C_r/C_1 constant. Hence k must be of the form n/m where n and m are integers. The choice of k is also influenced by its effect on the values of the other circuit elements and on the variation of the characteristic impedance and phase shift of the network with frequency. At the same

time n and m should be small to keep the number of diodes required to a minimum.

3. Characteristic Impedance and Phase Shift at ω_0

At ω_0 , the derived bridged-T network is an exact equivalent to the original lattice section in which

$$Z_A = j\omega_0 L_1 = jZ_{0\pi}^2 \omega_0 C_r \quad \dots\dots(13)$$

and

$$Z_B = 1/j\omega_0 C_1 \quad \dots\dots(14)$$

Thus

$$Z_0^2 = Z_A Z_B = Z_{0\pi}^2 C_r / C_1 = k Z_{0\pi}^2 \quad \dots\dots(15)$$

and

$$C_2 = \sqrt{k} / \omega_0 Z_0 \quad \dots\dots(16)$$

$$L_2 = Z_0 / \sqrt{k} \cdot \omega_0 \quad \dots\dots(17)$$

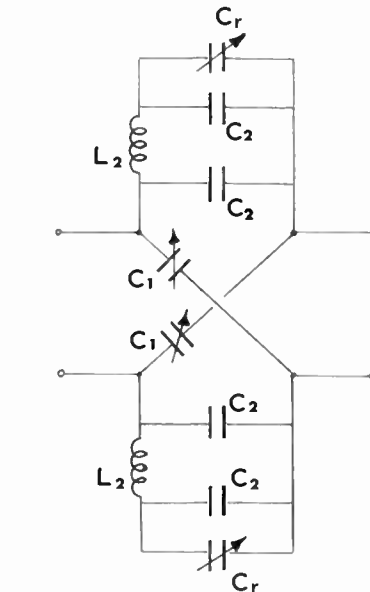


Fig. 2. Lattice with quarter-wave sections.

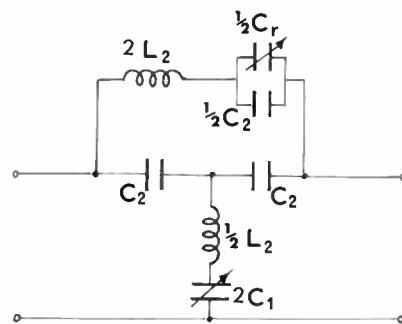


Fig. 4. Constant-impedance phase-shift network.

Similarly, at ω_0 , the phase shift ϕ may be obtained from

$$\begin{aligned} \tanh^2(\gamma/2) &= Z_A/Z_B \\ &= -\omega_0^2 Z_{0\pi}^2 C_r C_1 \quad \dots\dots(18) \end{aligned}$$

Thus, from (3), we obtain

$$\tan^2(\beta/2) = C_r C_1 / C_2^2 = k(C_1/C_2)^2 \quad \dots\dots(19)$$

or

$$\tan(\beta/2) = \sqrt{k} \cdot C_1/C_2 \quad \dots\dots(20)$$

The total change in phase $\Delta\phi$, corresponding to C_1 taking the limiting values C_a and C_b , is then given by

$$\begin{aligned} \Delta\phi &= 2 \tan^{-1} \sqrt{k} \cdot C_a/C_2 - 2 \tan^{-1} \sqrt{k} \cdot C_b/C_2 \\ &= 2 \tan^{-1} \frac{\sqrt{k}(C_a - C_b)/C_2}{1 + k \cdot C_a C_b / C_2^2} \quad \dots\dots(21) \end{aligned}$$

Normally the values of C_a and C_b are determined by the variable-capacitance diodes employed in the circuit, while the value of k is fixed by the factors discussed above. The value of C_2 required for maximum change in phase may now be obtained by equating $\partial(\tan \Delta\phi/2)/\partial C_2$ to zero. This gives

$$C_2 = \sqrt{k C_a C_b} \quad \dots\dots(22)$$

Inserting this value of C_2 into (21),

$$\Delta\phi_{\max} = 2 \tan^{-1} \frac{\sqrt{C_a/C_b} - \sqrt{C_b/C_a}}{2} \quad \dots\dots(23)$$

The maximum change in phase is thus seen to be a function of the ratio of the maximum to the minimum

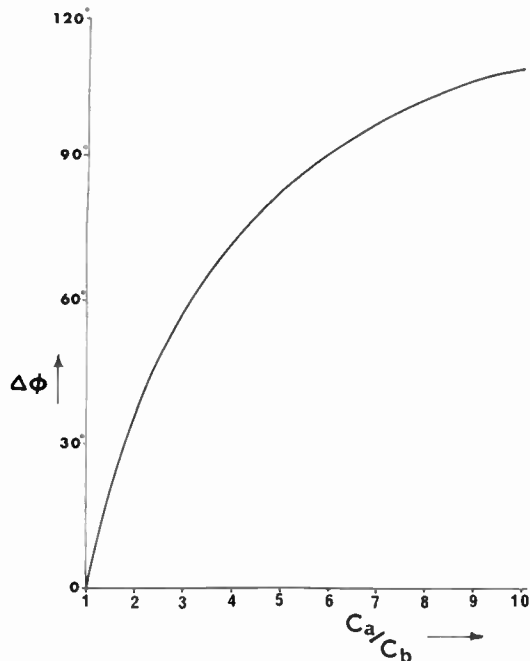


Fig. 5. The maximum change in phase as a function of the ratio of the maximum to minimum value of the variable capacitance.

value of the variable capacitance only and independent of the value of k and is plotted against C_a/C_b in Fig. 5.

Variable-capacitance diodes rarely exhibit a useful ratio of maximum to minimum capacitance much greater than three. It is possible that some improvement in this ratio may result from the addition of inductors in series with the diodes though this may cause a reduction in the bandwidth of the system. Thus a total difference in phase shift of about 60 deg per section may be expected using typical variable-capacitance junction diodes as the variable elements.

4. Characteristic Impedance and Frequency as a Function of Frequency

If $Z_0(\omega)$ is the characteristic impedance of the phase-shift section at ω , then

$$\begin{aligned} Z_0^2(\omega) &= \frac{1}{\omega^2 C_2^2} \cdot \frac{\omega^2 L_2 C_2 - C_2 / (C_2 + k C_1)}{\omega^2 L_2 C_2 - C_2 / (C_2 + k C_1) - 1} \times \\ &\quad \times (\omega^2 L_2 C_2 - C_2 / C_1 - 1) \quad \dots\dots(24) \end{aligned}$$

This becomes, using (15) and (16),

$$(Z_0(\omega)/Z_0)^2 = \frac{1}{k} \cdot \frac{(f^2 - \lambda)(f^2 - \mu)}{f^2(f^2 - \lambda - 1)} \quad \dots\dots(25)$$

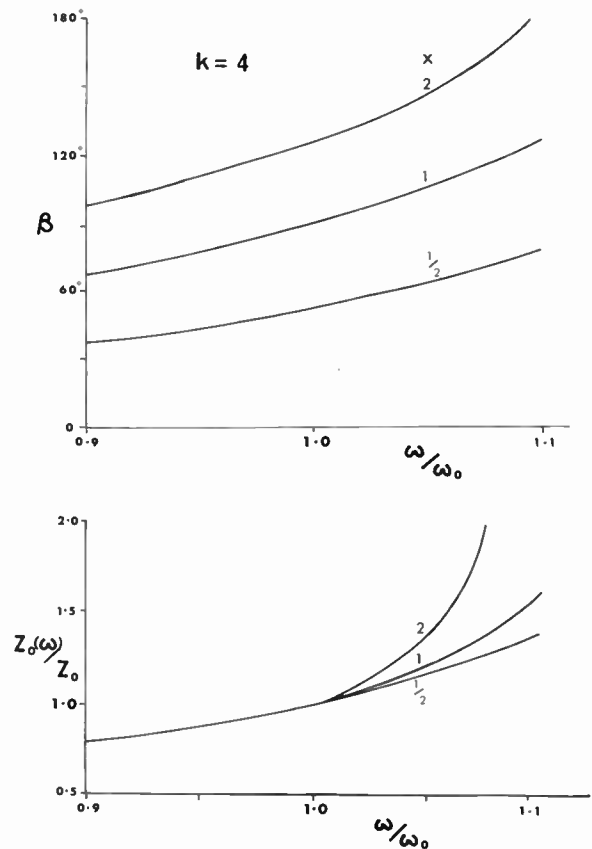


Fig. 6. Variation of phase shift and impedance with frequency for $k = 4$.

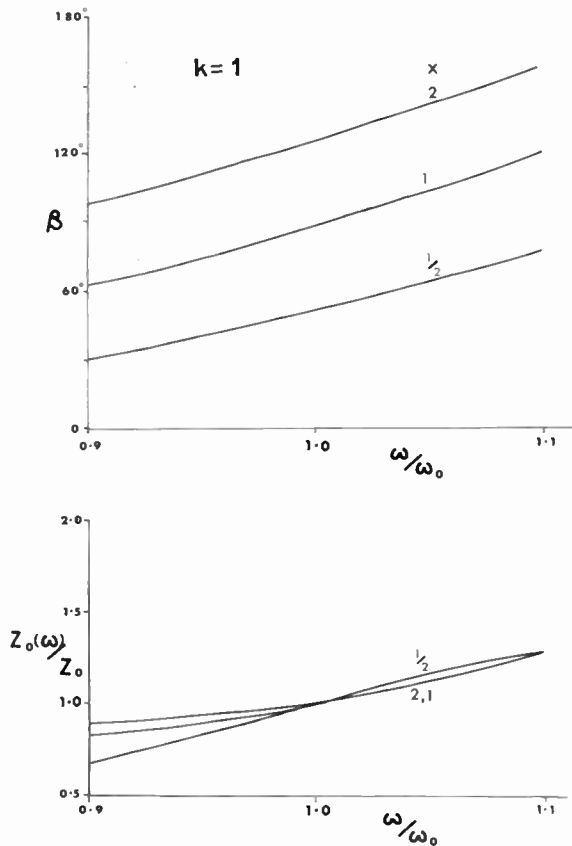


Fig. 7. Variation of phase shift and impedance with frequency for $k = 1$.

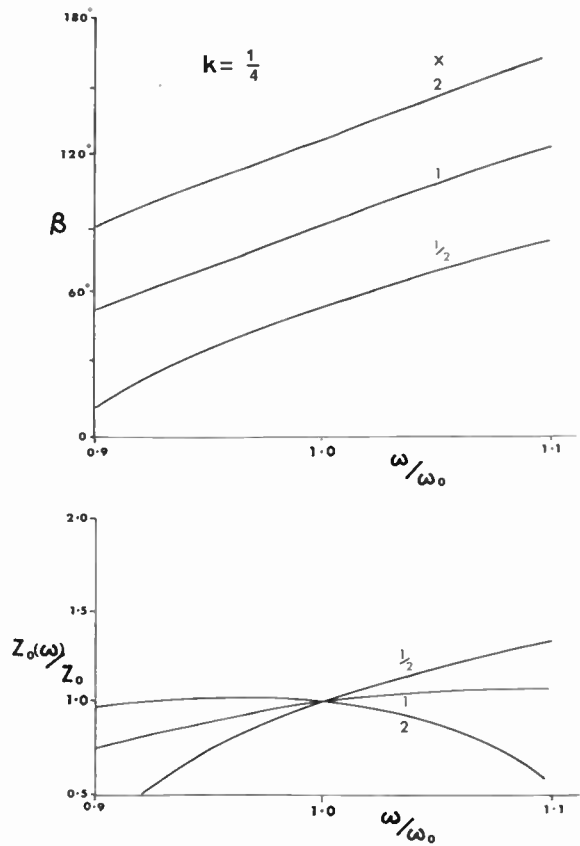


Fig. 8. Variation of phase shift and impedance with frequency for $k = 1/4$.

where

$$\begin{aligned} \lambda &= 1/(1+x\sqrt{k}) \\ \mu &= 1+\sqrt{k}/x \\ f &= \omega/\omega_0 \\ x &= \omega_0 Z_0 C_1 \end{aligned}$$

In the same way, the effect of k , C_1 and ω on the phase shift of the section may be obtained from,

$$\tan^2\left(\frac{\beta}{2}\right) = \frac{(f^2 - \lambda)}{(f^2 - \lambda - 1)(f^2 - \mu)} \dots\dots(26)$$

Values of $Z_0(\omega)/Z_0$ and β are plotted against relative frequency $f = \omega/\omega_0$ for $k = 4, 1$, and $1/4$ and $x = 2, 1, 1/2$, (the latter corresponding to C_1 having an effective capacitance range of 4 : 1) in Figs. 6, 7, and 8. It can be seen that the value of k has a profound effect on the variation of characteristic impedance and phase shift with frequency, and that the changes are a minimum for $k = 1$. This requires the variable capacitance in the shunt arm of the phase shift network to be four times that in the bridge arm, needing a minimum of four diodes, two in series and two in parallel. By choosing $k = 2$, only three diodes are

required and the effective bandwidth of the circuit is not greatly reduced. This value of k was therefore used in the following practical circuits.

5. A Phase-shift Network Operating at 1 Mc/s

In order to test the principles of the circuit, it was decided to construct a model having a characteristic impedance of about 1000 Ω , operating at a frequency of 1 Mc/s. The influence of the various circuit elements on the performance of the phase-shift network could then be studied free from the effects of stray capacitance and lead inductance which may be expected at higher frequencies. Variable-capacitance diodes with relatively large values of capacitance are required and it was found that voltage-reference or Zener diodes could be selected having a capacitance range of 225 pF to 75 pF corresponding to an optimum value of C_2 of 180 pF and a characteristic impedance of 1250 Ω for $k = 2$. The complete circuit is shown in Fig. 9, where the bias resistors have been chosen to have a value high compared with the circuit impedance and at the same time to give roughly the same voltage drop due to leakage current which in any event is small with reverse-biased silicon diodes.

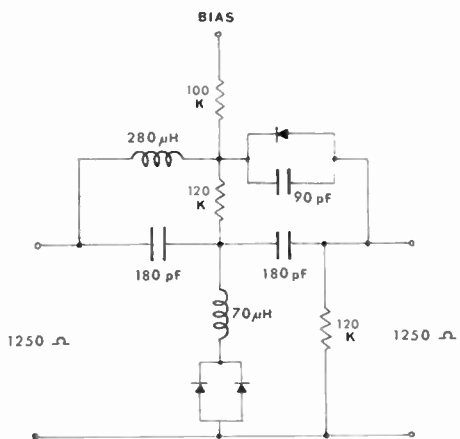


Fig. 9. Phase-shift network for operation at 1 Mc/s.

The network was first tested by measuring the open and short circuit terminal impedances from which the image impedances and the propagation constant could be found. Initial measurements indicated that some trimming of the circuit element values was necessary in order to maintain Z_0 constant with change in applied bias.

Figure 10 shows the variation in image impedance with tuning capacitance for one port of the untrimmed network. There is a corresponding variation at a different level for the other port. It can be seen that the effect is principally a variation of the image impedance coupled with the introduction of spurious stop regions where the image impedance becomes imaginary. It was found empirically that the image impedance variation could be reduced considerably by adjusting the two capacitors C_2 until the network was symmetrical, indicated by the two image impedances being equal in value. Generally this resulted in the impedance level differing from the design value. A further adjustment to the bridge arm inductor ($2L_2$) then gave the required value of Z_0 . The variation in Z_0 for the corrected network is shown in Fig. 11 and the corresponding phase characteristic in Fig. 12.

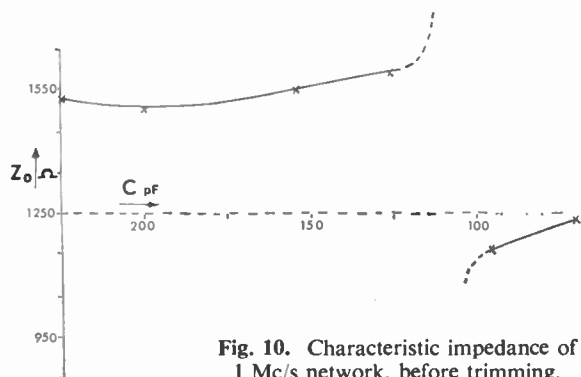


Fig. 10. Characteristic impedance of 1 Mc/s network, before trimming.

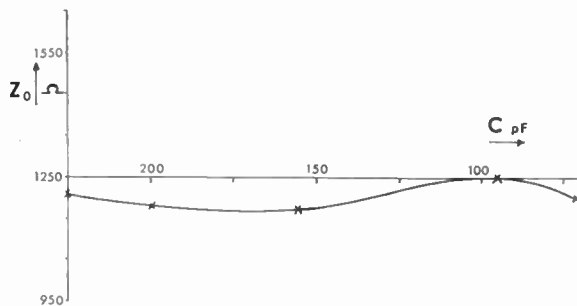


Fig. 11. Characteristic impedance of 1 Mc/s network, after trimming.

The overall difference in phase is 61 deg and the attenuation constant of the order of 0.5 dB. Insertion measurements gave substantially similar results.

6. An 80-Mc/s Phase-shift Network

Additional problems arise when the network is modified for operation at 80 Mc/s. With lumped elements, lead inductance and stray capacitance must be taken into account. To minimize these effects, the value of k must again be chosen to be close to unity. This may be seen from Table 1, where the values of the fixed components for a 50-Ω network are given for $k = 4, 1,$ and $1/4$. The inductor $L_2/2$ must be $0.025 \mu\text{H}$ for $k = 4$ and the capacitor $C_2/2$ has to be 10 pF for $k = 1/4$. A value of $k = 2$ was again selected and the final circuit is shown in Fig. 13. The lead inductance of the series-connected diodes was

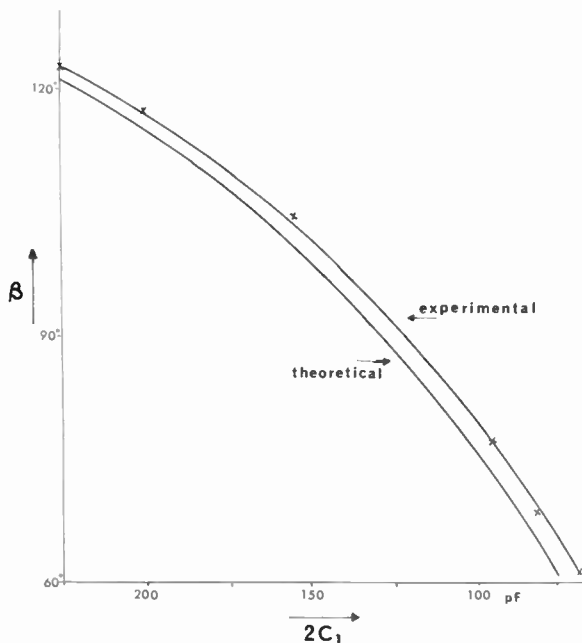


Fig. 12. Predicted and measured phase shifts for the 1 Mc/s circuit.

Table 1
Values of fixed components for 80 Mc/s phase-shift network

	4	$\frac{k}{l}$	1/4
C_2 (pF)	80	40	20
$C_2/2$ (pF)	40	20	10
$2L_2$ (μ H)	0.10	0.20	0.40
$L_2/2$ (μ H)	0.025	0.05	0.10

compensated by the additional capacitor and the lead inductance of the single diode provided the required value of 0.035 μ H for $L_2/2$. The trimming procedure was identical to that employed in the 1-Mc/s model.

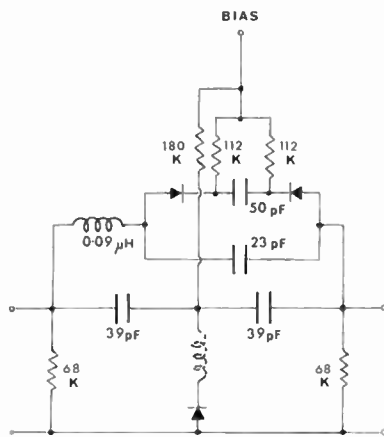


Fig. 13. Phase-shift network for operation at 80 Mc/s.

The phase and impedance characteristics of the circuit are shown in Fig. 14 where it can be seen that a total difference in phase shift of 53 deg may be obtained for a bias voltage change of 10 V, the impedance remaining within $\pm 10\%$ of the nominal value over the operating range. The bandwidth was found to extend from 70 Mc/s to 85 Mc/s and the insertion loss to be less than 1 dB.

7. Conclusion

It has been shown that it is possible to obtain a continuous phase shift of up to 60 deg per section at constant impedance in an unbalanced line using a lumped-parameter bridged-T network in which the variable elements are voltage-controlled variable-capacitance diodes. The network may be employed at frequencies in the h.f. and v.h.f. range with small insertion loss and reasonable bandwidth. Application at higher frequencies may be limited by the effect of stray inductance and capacitance and it is possible that distributed systems may be preferred in this case.

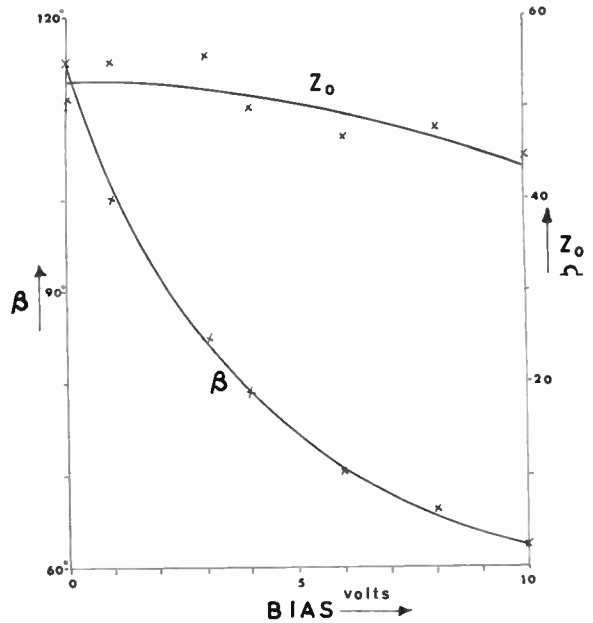


Fig. 14. Phase and impedance characteristics at 80 Mc/s.

While a phase shift of 60 deg per section may be sufficient for many applications, additional phase shift may be obtained by cascading sections or possibly by the addition of inductance in series with each of the diodes.

8. Acknowledgment

The authors would like to acknowledge the support of the Department of Scientific and Industrial Research in providing the necessary apparatus for this work.

9. References

1. W. G. Swarner, "A Voltage-controlled Radio-frequency Phase-shifter", Antenna Laboratory Report No. 903-5, Ohio State University, August 1959.
2. R. H. Hardin, E. J. Downey and J. Munushian, "Electronically variable phase shifters utilizing variable-capacitance diodes", *Proc. Inst. Radio Engrs*, 48, pp. 944-5, May 1960.
3. W. H. Doherty, "Operation of a.m. broadcast transmitters into sharply-tuned antenna systems", *Proc. Inst. Radio Engrs*, 37, pp. 729-34, July 1949.
4. M. G. Pawley, "A wide-range phase control with constant attenuation by adjustable impedance in a resistance-loaded bridged-T network", *J. Res. Nat. Bur. Stand.*, 45, pp. 193-200, September 1950.
5. G. Vogt, "Electronic method for steering the beam and polarization of h.f. antennas", *Trans. I.R.E. on Antennas and Propagation*, AP-10, pp. 193-200, March 1962. See also "An analogue polarization follower for measuring the Faraday rotation of satellite signals", *The Radio and Electronic Engineer*, 28, No. 4, pp. 269-78, October 1964.
6. H. W. Bode, "Network Analysis and Feedback Amplifier Design", p. 266 (Van Nostrand, New York, 1945).

Manuscript received by the Institution on 18th November 1964. (Paper No. 988.)

© The Institution of Electronic and Radio Engineers, 1965

SUBJECT INDEX

Papers and major articles are denoted by printing the page numbers in bold type.

Absorption-type Ferrite Modulator, Couple-wave, Description of the	129	The Generation of a Selected Harmonic or Sub-harmonic by means of a Single Externally-driven Switch	247
Accelerating Medical Progress through Medical Engineering	159	Hybrid Positive and Negative Parameter Delay-line Synthesis	255
AERIALS AND ARRAYS:		Pulse Response of Delay Lines. I: Constant- <i>k</i> Delay Lines	271
Effect of a Linear Phase Taper on the Near Field of an Ultrasonic Multi-element Array	207	Specialization of the Yanagisawa Synthesis Procedure to obtain RC Active Networks having Optimum Pole Sensitivity	362
Enhancing the Angular Resolution of Incoherent Sources	21	Civil Service Commissioners recognize I.E.R.E. qualifications	20
Least-Squares Array Processing for Signals of Unknown Form	213	Cold Cathode Tubes and their Applications (<i>Symposium paper published</i>) :	
Modifications to the Goonhilly Earth Station ...	374	Impedance Characteristics of Glow-discharge Tubes in the Frequency Range 200 c/s-70 Mc/s ...	313
Multiplicative Processing Antenna Systems for Radar Applications	53	Colour Blindness	197
Discussion	49	COMMUNICATIONS:	
Multiplicative Receiving Arrays (Discussion) ...	49	Lincomex System for High Frequency Radio Telephony	172
Optimum Line and Crossed Arrays for the Detection of a Signal on a Noise Background	101	Modifications to the Goonhilly Earth Station ...	374
The Possibility of an Interaction Anomaly in Acoustic Receiving Arrays and Radio Arrays	113	Multi-channel Open-wire Carrier Telephone System (Discussion)	254
A Radar Receiving Array with I.F. Multiple-beam Forming Matrix	277	Technique for the Transmission of Digital Information over Short Distances using Infra-red Radiation	369
Recording and Analysis of Seismic Body Waves using Linear Cross Arrays	33	"Components and Materials Used in Electronic Engineering" Conference	133
Statistical Optimization of Antenna Processing Systems	117	COMPUTERS:	
Technique for the Time-transformation of Signals and its Application to Directional Systems ...	135	British Joint Computer Conference, 1966	134
Annual General Meeting of the Institution ...	3, 20, 84	A Computer Program for Analysing Networks containing Three-terminal Active Devices characterized by their Two-port Parameters	85
Anode Structures for Cold-cathode High-power Magnetrons	93	Large Capacity Magnetic Film Stores—A Design Approach	161
Apparatus for Automatic Quantitative Analysis of Electrolytes by Controlled Potential Coulometry	307	A Light Absorption Detector for a Computer Controlled Film Scanner	325
"Application of Microelectronics", Symposium ...	20, 262	CONFERENCES AND SYMPOSIA:	
<i>Ariel 1</i> Anglo-American satellite	344	Colloquium on "Techniques of Memory Circuits" ...	70, 133
Associated Electrical Industries Ltd.	100	British Joint Computer Conference	134
Astronautical Congress, Sixteenth Annual	70	Conference on "Components and Materials Used in Electronic Engineering"	133
Automatic Landing, Tolerances in	378	Conference on "Medical Physics"	262
Avalanche Mode, Transistor Parameters in the ...	27	National Inspection Conference on "Engineering Inspection in the Future"	330
B.L.E.U. single channel automatic landing system ...	378	Conference on "Non-metallic Thin Films"	262
British Joint Computer Conference, 1966	134	Conference on "Optics in Space"	134
British Standards Institution	6	Society of Motion Picture and Television Engineers, 98th Conference	134
Carrier Telephone System, Multi-channel Open-wire (Discussion)	254	Conference on "Thermionic Electrical Power Generation"	70
Changes in N.B.S. Radio Broadcasts	291	Conference on "U.H.F. Television"	133, 134, 330
Cinematography		Sixteenth Annual Astronautical Congress	70
98th Society of Motion Pictures and Television Engineers Conference	134	Symposium on "Applications of Microelectronics" ...	20, 262
CIRCUIT TECHNIQUES:		Symposium on "Cold Cathode Tubes and their Applications" (<i>Paper</i>)	313
High-speed Tunnel Diode Counter	199	North Eastern Symposium on "Electronic Control Systems for Industry"	198
Progress in Electromechanical Filters	173	International Aerospace Instrumentation Symposium	262
Transistor Crystal Oscillators and the Design of a 1-Mc/s Oscillator Circuit Capable of Good Frequency Stability	229	Symposium on "Microwave Applications of Semiconductors"	134, 198, 292
CIRCUIT THEORY:			
A Computer Program for Analysing Networks containing Three-terminal Active Devices characterized by their Two-port Parameters	85		
Constant Impedance Voltage-controlled Phase-shift Network	387		

SUBJECT INDEX

Symposium on "Modern Techniques for Recording and Processing Seismic Signals" (<i>Papers</i>)	33, 297	Electronic Drawing:	
Symposium on "The Operation of Electronic Equipment under Conditions of Severe Electrical Interference" (<i>Paper</i>)	149	Correction to report published in September 1964 issue of <i>The Radio and Electronic Engineer</i>	20
Symposium on "Signal Processing in Radar and Sonar Directional Systems" (<i>Papers</i>)	21, 33, 49, 53, 101, 117, 135, 143, 207, 213, 223, 277	Engineering Industry Training Board	5
Constant Impedance Voltage-controlled Phase-shift Network	387	"Engineering Inspection in the Future" Conference	330
CONTROL ENGINEERING:		Engineering Institutions Joint Council	
"Electronic Control Systems for Industry" Symposium	198	Size of membership	4
Determination of the Parameters of a Dynamic Process	345	Petition for Royal Charter	84
CORRECTION:		Engineering Profession:	
"Instruction in Electronic Drawing for Students of Radio and Electronic Engineering" (p. 199, <i>The Radio and Electronic Engineer</i> , September 1964).	20	National Prosperity and the Engineer	3
Coulometry, Apparatus for Automatic Quantitative Analysis of Electrolytes by Controlled Potential	307	Recognition of I.E.R.E. qualifications by Civil Service	20
Council of Engineering Institutions (<i>see</i> Engineering Institutions Joint Council)		Enhancing the Angular Resolution of Incoherent Sources	21
Council on Scientific Policy	344	EXHIBITIONS:	
Coupled-wave Description of the Absorption-type Ferrite Modulator	129	East African Institution of Engineers' Radio and Electronics Show	70
Cranfield College of Aeronautics		International Television and Radio Show	133, 330
Advanced course on "Microwave Laboratory Practice"	198	London Components Exhibition	133
Aerospace Instrumentation Symposium	262	Paris Components Exhibition	70, 133, 329
Delay-line Synthesis, Hybrid Positive and Negative Parameter	255	S.I.M.A. Exhibition in Moscow	70
Delay-lines, Pulse Response of: I. Constant- <i>k</i> Delay Lines	271	Experimental Frame Difference Signal Generator for the Analysis of Television Signals	71
Design Principles and Rôle of a Comprehensive Unit System of Electronic Equipment, with particular reference to the Harwell 2000 System	185	Ferrite Modulator, Coupled-wave Description of the Absorption-type	129
Determination of the Parameters of a Dynamic Process	345	Film Scanner, A Light Absorption Detector for a Computer Controlled	325
Discussion on "Multi-channel Open-Wire Carrier Telephone System"	254	Flight Test Instrumentation Symposium (<i>see</i> International Aerospace Instrumentation Symposium)	
Discussion on "Multiplicative Receiving Arrays"	49	Generation of a Selected Harmonic or Sub-harmonic by means of a Single Externally-driven Switch	247
<i>Early Bird</i> communications satellite	261, 374	Glow-discharge Tubes in the Frequency Range 200 c/s-70 Mc/s, Impedance Characteristics of	313
East African Institution of Engineers		Goonhilly Earth Station, Modifications to the	374
Radio and Electronics Show	70	Graduateship Examination, November 1964, Pass Lists (Overseas)	128
EDITORIALS:		Harwell 2000 Unit System of Electronic Equipment	185
Sir Winston Churchill, K.G. 1874-1965	69	Hayes Memorial Medal, Norman W. V.	
International Exhibitions	133	Award to Australian author	71
Colour Blindness	197	High-definition Q-band River Radar, Performance Calculations for	263
On Station	261	High-Power V.L.F. Radio Station for N.A.T.O.	47
An International Outlook for Engineers	329	High-speed Tunnel Diode Counter	199
EDUCATION :		Honours, Her Majesty's New Year	20
Post Graduate Courses: Quantum Electronics, and Microwave Laboratory Practice	198	Dissolution	20
Effect of a Linear Phase Taper on the Near Field of an Ultrasonic Multi-element Array	207	Hybrid Positive and Negative Parameter Delay-line Synthesis	255
Electromechanical Filters, Progress in	173	Impedance Characteristics of Glow-discharge Tubes in the Frequency Range 200 c/s-70 Mc/s	313
ELECTRON DEVICES:		Impurity Monitor for Liquid Metal Circuits, The Rhometer: A Continuous	331
Anode Structures for Cold-cathode High-power Magnetrons	93	Indian <i>Proceedings</i>	329
Impedance Characteristics of Glow-discharge Tubes in the Frequency Range 200 c/s-70 Mc/s	313	Infra-red Radiation, A Technique for the Transmission of Digital Information over Short Distances using	369
Transistor Parameters in the Avalanche Mode	27	Institute of Physics and The Physical Society	
"Electronic Control Systems for Industry" North Eastern Symposium	198	Conference on "Optics in Space"	134
		Conference on "Non-Metallic Thin Films"	262
		INSTITUTION:	
		Council	1
		Local Sections and Divisions	2
		Annual General Meeting	3, 20, 84
		Presidential Address of Colonel G. W. Raby	3, 84
		<i>List of Members, 1964</i>	20

New Premium for Television Reception	20	Transistorized Rocket-borne Proton Magnetometer and associated Data Processing Equipment ...	9
Recognition of qualifications by Civil Service ...	20	Mechanism of Interference Pick-up in Cables and Electronic Equipment with special reference to Nuclear Power Stations	149
Stand at Paris Components Exhibition	70	MEDICAL ELECTRONICS:	
Dinner	198	Accelerating Medical Progress through Medical Engineering	159
Joint Symposium on "Microwave Applications of Semiconductors"	134, 198	Medical Physics Conference	262
Karachi Section Committee, 1965	198	Meetings	
London Meeting on Military Electronics	198	International Radio Consultative Committee, Oslo, 1966	197
North Eastern Symposium on "Electronic Control Systems for Industry"	198	Institution London Meeting on Military Electronics	198
Overseas Sections' activities; new divisions in Canada and France	329	Microelectronics, Symposium on Applications of	20, 262
Premiums and Awards, 1964	330	"Microwave Applications of Semiconductors" Symposium	134, 198
Instrument Society of America		Outline programme and synopses of papers	292
Aerospace Instrumentation Symposium	262	Microwave Laboratory Practice Course	198
Interaction Anomaly in Acoustic Receiving Arrays and Radio Arrays, The Possibility of an	113	Military Electronics	
INTERFERENCE:		The Impact of Electronics on the Army's Repair Organization: paper given at London Meeting ...	198
Mechanism of Interference Pick-up in Cables and Electronic Equipment with special reference to Nuclear Power Stations	149	Ministry of Technology	
I.F. Multiple-beam Forming Matrix, A Radar Receiving Array with	277	Joint Symposium on "Electronic Control Systems for Industry"	198
International Aerospace Instrumentation Symposium	262	"Modern Techniques for Recording and Processing Seismic Signals" (<i>Symposium papers published</i>):	
International Exhibitions	133	The Recording and Analysis of Seismic Body Waves using Linear Cross Arrays	33
International Outlook for Engineers	329	Seismic Recording Techniques in Oil Prospecting ...	297
International Radio Consultative Committee Meeting in Oslo, 1966	197	Modifications to the Goonhilly Earth Station	374
<i>Journal:</i>		Montefiore Foundation Prize	262
Back copies	262, 330	Mullard Space Science Laboratory	344
Karachi Section		Multi-channel Open-wire Carrier Telephone System (Discussion)	254
Committee for 1965	198	Multiplicative Processing Antenna Systems for Radar Applications	53
Large Capacity Magnetic Film Stores—A Design Approach	161	Discussion	49
Least-Squares Array Processing for Signals of Unknown Form	213	Multiplicative Receiving Arrays (Discussion)	49
Lectures and Courses		N.A.T.O., High-power V.L.F. Radio Station for National Bureau of Standards, U.S.	47
Cranfield College of Aeronautics course "Microwave Laboratory Practice"	198	Changes in radio broadcasts	291
University of Southampton course "Quantum Electronics"	198	National Electronics Research Council	7, 84, 261
Light Absorption Detector for a Computer Controlled Film Scanner	325	<i>N.E.R.C. Review</i>	261
Linear Phase Taper on the Near Field of an Ultrasonic Multi-element Array, The Effect of a	207	National Inspection Conference on "Engineering Inspection in the Future"	330
Lincompex System for High Frequency Radio Telephony	172	National Prosperity and the Engineer	3, 84
Liquid Metal Circuits, The Rhometer: A Continuous Impurity Monitor for	331	Near Field of an Ultrasonic Multi-element Array, The Effect of a Linear Phase Taper on the	207
<i>List of Members, 1964</i>	20	Nuclear Power Stations, Mechanism of Interference Pick-up in Cables and Electronic Equipment with special reference to	149
Local Sections		Obituary	
Karachi Section Committee 1965	198	Sir Winston Churchill	69
North Eastern Section Symposium on "Electronic Control Systems for Industry"	198	Of Current Interest	344
Magnetic Film Stores—A Design Approach to Large Capacity	161	Oil Prospecting, Seismic Recording Techniques in On Station	297
Magnetrons, Anode Structures for Cold-cathode High-power	93	"Operation of Electronic Equipment under conditions of Severe Electrical Interference" (<i>Symposium paper published</i>):	261
MEASUREMENTS:		The Mechanism of Interference Pick-up in Cables and Electronic Equipment with special reference to Nuclear Power Stations	149
Apparatus for Automatic Quantitative Analysis of Electrolytes by Controlled Potential Coulometry	307	"Optics in Space" Conference	134
The Rhometer: A Continuous Impurity Monitor for Liquid Metal Circuits	331	Optimum Line and Crossed Arrays for the Detection of a Signal on a Noise Background	101
		Oscillators and the Design of a 1-Mc/s Oscillator Circuit Capable of Good Frequency Stability, Transistor Crystal	229

Technique for the Transmission of Digital Information over Short Distances using Infra-red Radiation ...	369	Transistorized Rocket-borne Proton Magnetometer and Associated Data Processing Equipment ...	9
"Techniques of Memory Circuits" Colloquium ...	70, 133	Transmission of Digital Information over Short Distances using Infra-red Radiation ...	369
TELECOMMUNICATIONS:		Tunnel Diode Counter, A High-speed ...	199
World link-up at East African Electronics Show ...	70	Ultrasonic Multi-element Array, The Effect of a Linear Phase Taper on the Near Field of an ...	207
U.K.-Belgium Submarine Cable: Provision of Submerged Transistor Repeaters ...	100	Unit System of Electronic Equipment with particular reference to the Harwell 2000 System, The Design Principles and Rôle of a Comprehensive ...	185
Seastations for Air Traffic Control ...	344	United Kingdom Automation Council British Joint Computer Conference, 1966 ...	134
TELEVISION:		U.K.-Belgium Submarine Cable: Provision of Submerged Transistor Repeaters ...	100
An Experimental Frame Difference Signal Generator for the Analysis of Television Signals ...	71	University College, London Space Research Section of Physics Department ...	344
Conference on "U.H.F. Television" ...	133, 134, 330	Use of Quantizing Techniques in Real Time Fourier Analysis ...	143
98th S.M.P.T.E. Conference ...	134	Vernier satellite tracking system at Goonhilly earth station ...	376
International Television and Radio Show ...	133, 330	Voltage-controlled Phase-shift Network, A Constant Impedance ...	387
Uncertainty on colour standards ...	197	WAVEGUIDES:	
International Radio Consultative Committee meeting in Oslo, 1966 ...	197	Coupled-wave Description of the Absorption-type Ferrite Modulator ...	129
Television Society Joint Conference on "U.H.F. Television" ...	134	Yanagisawa Synthesis Procedure to Obtain RC Active Networks having Optimum Pole Sensitivity, A Specialization of the ...	362
Telstar communications satellite ...	374		
"Thermionic Electrical Power Generation" Conference	70		
Thin Films, Conference on Non-Metallic ...	262		
Time-transformation of Signals and its Application to Directional Systems, A Technique for the ...	135		
Tolerances in Automatic Landing ...	378		
Transistor Crystal Oscillators and the Design of a 1-Mc/s Oscillator Circuit Capable of Good Frequency Stability ...	229		
Transistor Parameters in the Avalanche Mode ...	27		

INDEX OF PERSONS

Names of authors of papers published in the volume are indicated by bold numerals for the page reference.

Authors of papers which are given in abstract form are denoted by A.

Contributors to discussion are indicated by D.

Anderson, C. W. M. 254D	Davies, D. E. N. 49D	Krause, G. 328A
Ansari, I. A. 198	Davies, R. D. 312A	Ksienski, A. 49D, 53, 126D
Ansari, S. H. 198	de Bruyne, P. 325	Kürzl, A. 296A
Atkinson, Major-General L. H. ... 198	Dehn, R. 331	Kwiatkowski, W. 296A
Avinor, M. 271	Deval, S. 294A	
Aziz, S. A. 198	Dolbear, D. W. N. 297	Lange-Hesse, G. 328A
	Dunstan, E. M. 330	Levin, M. J. 142D, 213, 222D
Baldock, G. S. 142D	Duthie, R. L. 330	Limb, J. O. 328A
Bapat, Y. N. 330	Dyson, A. A. 84	Lindemann, F. A. 69
Bassett, H. G. 85	Eames, A. R. 331	Lord, R. N. 26D, 125D, 141D, 385D
Basu Mallick, S. 296A	Edwards, D. B. G. 330	
Baxandall, P. J. 229	Engel, J. 260A	McCartney, B. S. 45D, 52D
Bedford, L. H. 261	Fairbrother, L. R. 85	Mackenzie, G. H. 254D
Benes, L. 196A	Fleck, W. 387	Maddock, I. 84
Benjamin, R. 45D, 125D, 141D, 212D, 228D, 290D	Froom, J. 294A	Marte, G. 68A
		Massey, Sir Harrie 344
Benny, A. H. 293A	Galpin, R. K. T. 184D	Meinke, H. H. 312A
Benson, F. A. 313, 324D	Gambling, W. A. 84, 296A, 330	Melchior, H. 260A
Bessho, T. 328A	Garbrecht, K. 293	Metzger, E. 260A
Biggi, V. 196A	Garlick, N. L. 84	Miller, C. H. 68A
Birch, J. 184D	Garner, R. H. 84	Milne, K. 45D, 126D, 330
Birgels, P. 68A	Gissing, J. G. 293A	Miyauchi, K. 196A
Bisby, H. 185	Grimley, W. K. 112D, 148D, 212D	Molz, K. F. 126D
Bishai, A. M. 328A	Groves, G. V. 344	Morgan, C. Grey 324D
Bishop, K. G. 254D	Hall, G. 307	Mountbatten of Burma, The Earl 7
Bishop, M. J. 207	Halliday, A. G. 49D	Munro, A. 254D
Blommendaal, R. 49D, 212D	Hanna, F. F. 328A	
Blythe, J. M. 142D	Harcourt, R. W. 294A	Nicholls, N. S. 142D
Bonyhard, P. I. 161	Harrison, D. 149	
Booth, A. D. 199	Harvey, G. C. W. 182D	Pacák, M. 196A
Börner, M. 173, 182D	Heap, B. C. 295A	Partom, Y. 271
Boyd, R. L. F. 344	Heaps, H. S. 101, 112D, 143, 148D	Partridge, S. J. 184D
Bradsell, P. 126D, 142D, 290D		Parvulescu, A. 223
		Pavey, N. A. D. 295A
Bradshaw, M. W. 313	Heeks, J. S. 294A	Payne, J. B. 291D
Burd, A. N. 330	Heinlein, W. 296A	Perring-Thoms, P. 20
Burgess, P. H. G. 330	Helszajn, J. 129	Persson, D. R. 312A
Burrows, K. 9	Henley, M. G. 378, 386D	Pichafroy, S. 277
Burry, L. F. 295A	Henning, H. B. 312A	Ponsonby, J. 142D
Bhawalkar, D. D. 330	Herbison-Evans, D. 45D	Poorter, T. 323D
	Hinton, L. J. T. 295A	Potok, M. H. N. 296A
Caputi, W. J. 135, 141D	Holt, A. G. J. 362	Prescott, T. W. 385D
Carré, B. A. 330	Howson, D. P. 247	Properjohns, F. J. F. 20
Carter, W. S. 161	Hurbin, P. 277	
Chakraborty, D. 312A	Hyde, F. J. 294A	Raby, Colonel G. W. 3, 84
Chapman, C. T. 182D		Renwick, Sir Robert 20
Churchill, Sir Winston 69	Ikeda, Y. 93	Roberts, D. A. E. 295A
Clarke, A. C. 261	Ito, S. 68A	Roucaché, R. 68A
Clay, C. S. 223, 228D		Rusby, J. S. M. 113
Cook, P. F. 386D	James, J. R. 296A	Ryan, W. D. 387
Cooke, H. F. 293A	James, M. 84	Ryle, M. 26D, 125D
Cooper, D. C. 52D	Johnson, R. H. 141D	
Cox, R. J. 84	Jones, C. I. 255	Sajid, H. 198
Croncy, J. 125D, 330		Salomon, J. 277, 290D
Cross, T. A. 84	Kapur, Major-General B. D. ... 84	Sandbank, C. P. 294A
	Kay, L. 207, 212D	Schell, A. C. 21, 26D
Daglish, H. N. 312A	Keitel, G. H. 26D	Schott, E. 328A
Dardenne, J. 196A	Kelly, S. 182D	Schwarz, H. F. 84
Darlington, Rear-Admiral Sir	Kenyatta, J. 70	Seitzer, D. 260A
Charles R. 20, 84	Khan, Lt. Cdr. M. T. 198	Seppen, J. M. G. 263
Davies, A. T. 369	Kiano, J. G. 70	

Seyler, A. J. 71	Toker, C. 294 A	Watson, I. A. 386 D
Shah, S. 198	Tsukada, K. 328 A	Whiteway, F. E. 33, 45 D
Shaw, E. 49 D	Tucker, D. G. 49 D	Whitfield, G. R. 142 D
Shearman, E. D. R. ... 141 D, 228 D	Tunis, C. J. 330	Willcock, P. W. 143, 148 D
Sherman, J. W. 330	Ueda, O. 196 A	Williams, E. 84
Shurmer, H. V. 294 A	Uhlir, A. 296 A	Williams, E. M. 255
Skolnik, M. I. 49 D, 142 D, 212 D, 290 D, 330	van Kessel, T. J. 196 A	Williams, J. S. 330
Smith, R. C. 330	van Schooneveld, C. ... 126 D, 148 D	Wilson, K. 295 A
Stephenson, F. W. 362	Vevers, Colonel J. 20	Withers, M. J. 51 D
Strutt, M. J. O. 260 A	Viswanathan, T. R. 199	Woodward, P. M. ... 51 D, 125 D
Süsskind, C. 93	Vogt, G. F. 142 D, 330	Wreathall, W. M. 330
Swamy, M. N. S. 27	Wadden, C. 101	Young, G. O. 26 D, 49 D, 117, 125 D, 142 D, 222 D
Taylor, D. 70	Wallis, P. R. 222 D, 330	Young, P. C. 345
Taylor, G. A. 84	Walters, L. C. 50 D, 112 D	Zakaria, H. 183 D
Tenenholtz, R. 293		Zworykin, V. K. 159
Thompson, J. L. 8, 20, 84		

INDEX OF ABSTRACTS

This index classifies under subject headings the abstracts published throughout the volume in "Radio Engineering Overseas" and the summaries of papers read at the Symposium on "Microwave Applications of Semiconductor Devices".

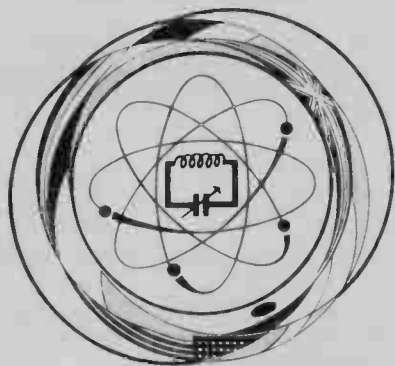
Aerials	
Determining the influence of reflector distance on a horn antenna. F. F. Hanna and A. M. Bishai	328
Circuit Techniques	
High-speed microwave switches using silver-bonded diodes in the II-Gc region. Kazuhiro Miyauchi and Osamu Ueda	196
A path difference type microwave discriminator. Sadao Ito	68
The properties of parametric frequency multipliers which are driven by modulated signals. P. Birgels	68
A pulse frequency demodulator. L. Beneš	196
A valve generator for producing pulses with very steep rise times. G. Marte	68
Communications	
Compatible single-sideband modulation. T. J. van Kessel	196
Design of a frequency storage device. V. Biggi and J. Dardenne	196
High efficiency amplification using width modulated pulses. C. H. Miller	68
Information rate and reliability of transmission of binary signals with a d.c. content when subjected to distortion in wide-band systems. J. Engel	260
Methods for improving the signal/noise ratio in television transmission systems. G. Krause	328
Sinewave interference in double-FM (FM-FM). E. Metzger	260
Computer Techniques	
Analysis of an Esaki diode memory cell by analog simulation. Teruhiko Bessho and Keiichi Tsukada ...	328
A hybrid circuit for nanosecond pulses to reduce the write noise in a magnetic film store. D. Seitzer ...	260
Ionospheric Phenomena	
Ionization variations in the mid-latitudes of the ionosphere and the variation of the usable frequencies for long distance short wave propagation with 27-day period as the effect of solar wave radiations. G. Lange-Hesse and E. Schott	328
Measurements	
An electronic microvoltmeter with a contact modulator. M. Pacák	196
Semiconductor Circuits*	
Applications of parametric amplifiers and satellite communications. H. N. Daghish and D. Chakraborty	312
Broad-band p-i-n diode switches in the range 7 to 16 Gc/s. N. A. D. Pavey	295
Broad-band varactor frequency multiplier chains—fundamental problems and realization. A. Kürzl ...	296
Calculation of the mixer conductance and noise of a tunnel diode mixer using the static diode characteristic. H. Melchior and M. J. O. Strutt	260
An investigation into the effects of charge storage on the efficiency of a varactor diode doubler. B. C. Heap	295
p-i-n diode modulators for the K and Q frequency bands. L. F. Burry and L. J. T. Hinton	295
Parametric amplifiers in radio astronomy. R. D. Davies	312
Parametric multi-port networks for microwave signal processing. H. B. Henning	312
An S-band tunnel-diode mixer. S. Basu Mallick and W. A. Gambling	296
A sampler-quantizer for television waveforms. J. O. Limb	328
A survey of possible applications of tunnel diodes in antenna systems. H. H. Meinke	312
Transient analysis of varactor bridge doublers. A. Uhlir	296
A tunnel diode oscillator with wide tuning range (0.7–4.9 Gc/s). D. R. Persson	312
Up-converter type transmitter for radio link. W. Kwiatkowski	296
Wideband coaxial variable attenuators using p-i-n diodes. J. R. James and M. H. N. Potok	296
Semiconductor devices*	
Acoustic amplification in semiconductors. H. W. Harcourt, J. Froom and C. P. Sandbank	294
Advances in microwave transistors and diodes. H. F. Cooke	293
The application of instabilities in semiconductors to microwave oscillations and amplification. J. S. Heeks and C. P. Sandbank	294
The development and properties of microwave p-i-n diodes. J. G. Gissing	293
Evaluation of high quality varactor diodes. D. A. E. Roberts and K. Wilson	295
Intrinsic frequency limitations for semiconductor microwave devices. H. V. Shurmer	294
Silicon variable capacitance diodes for use at low temperatures. A. H. Benny	293
Varactor diode measurements. F. J. Hyde, S. Deval and C. Toker	294
Television	
Transistor television receivers: 10 papers in <i>L'Onde Électrique</i>	68

* The titles of papers included in the Symposium on "Microwave Applications of Semiconductors" and listed under these headings do not comprise the full programme of that Symposium.

JOURNALS FROM WHICH ABSTRACTS HAVE BEEN TAKEN DURING THE FIRST HALF OF 1965

Annales de Radioélectricité (France)
Archiv der Elektrischen Übertragung (Germany)
Nachrichtentechnische Zeitschrift (Germany)
L'Onde Électrique (France)
Philips Technical Review (Holland)

Proceedings of The Institution of Radio and Electronics Engineers Australia
Review of the Electrical Communication Laboratory, N.T.T. (Japan)
Slaboproudý Obzor (Czechoslovakia)



Salon International des Composants Electroniques

THE BRITISH ELECTRONICS INDUSTRY

at the Paris Components Show, Porte de Versailles,
Paris, 8-13 April, 1965.

Over 60 companies belonging to the British Electronics industry are taking part in this year's Paris Components Show and in the associated "Salon International de L'Electroacoustique". Details of some of their exhibits are given in this "Paris Components Show Preview".

A.B. METAL PRODUCTS LTD.
Abercynon, Glamorgan.

ALLÉE 61
STAND 12

The company is showing its latest developments, some of which are shown in the adjoining photograph.

Top left: Mark III v.h.f. tuner using neutralized triode input and fitted with 'memory fine tuner'.

Top right: $\frac{1}{2}$ -wave transistorized tuner.

Centre: digital and binary switches, available as a 1-pole 10-way edge control switch and as a binary coding device

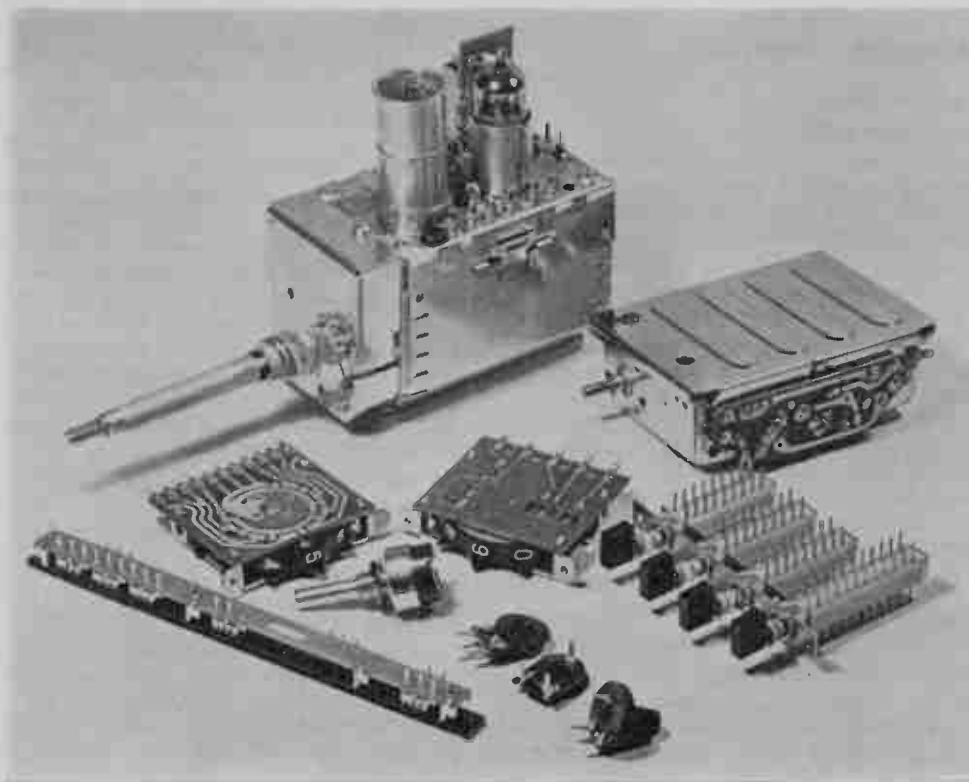
adaptable to various codes.

Bottom left: CK switch, which is a simple form of light action slider switch using a double row of contacts for printed circuit use.

Bottom right: '400' switch—a multi-purpose push-button switch available in a multitude of spacing where each button is capable of being fitted with up to eight changeover contacts.

Near the centre: Type 89, 1 watt wirewound potentiometer.

Lower centre: Types 83 and 84 composition type preset potentiometers for printed circuit use.



BELLING & LEE LTD. ALLÉE 20
Great Cambridge Road, Enfield, Middlesex. STAND 161

Among the many items to be shown will be a new range of double coaxial connectors (Pattern 22) which is contained within standard BNC shell sizes. The inner screen can be used to provide an independent path to the normal 'earth' return or, by application of an out-of-phase feedback signal, to achieve a low shunt capacitance in the circuit. Two intermateable types are available for cable diameters of 0.25 in (6.35 mm) and 0.325 in (8.26 mm) respectively. Both types mate with standard BNC's giving through connection on the outer screen.

A new range of removable contact units is intermateable with the existing Pattern 102 types. The gold-plated contacts are supplied separately for insertion into the diallyl phthalate mouldings after making the wire connections. Contact terminations fully meet the relevant I.E.C. and MIL specifications or alternatively connections may be soldered. Contacts are easily removed by means of the simple extractor tools supplied.

Based on metric standards a new series of 4 mm banana plugs and panel sockets include a specially designed plug with a snap-on handle slim enough to fit the recessed head of Belling-Lee 'Continental' terminals, single and twin stacking plugs with shrouded side entry for the cable, and newly styled panel sockets with round and square flanges.

Shielded enclosures of various sizes which can be provided for easy assembly on site are to be shown. These are based on a range of interchangeable metal construction modules, each measuring 2.24 x 1.12 m (7' 4" x 3' 8"). Exacting performance requirements are met with a typical attenuation figure of 100 dB from 100 kc/s to 1000 Mc/s. The special wedge type door design is supplemented by modules providing ventilation (by fan or window) and a penetration module for taking power and services into the enclosure. A comprehensive range of filters can be supplied. Half and quarter modules are available for intermediate sizes.

THE BRITISH ELECTRIC RESISTANCE CO. LTD. ALLÉE 32
Queensway, Enfield, Middlesex. STAND 143

The following products will be shown:

The Universal 'Bercotrol', a solid state electronic power regulator which can be used to supply controlled voltage, current, power, speed, temperature, brightness, etc., by means of the phase angle control of thyristors.

The Education 'Bercotrol', a teaching and demonstration apparatus to show the principles of the smooth variation of power, current and voltage by phase angle control of thyristors.

The Model 31A 'Regavolt', a very small variable transformer with a diameter of only 7.5 cm, which when mounted on a suitable heat sink will handle a power of 250 watts.

C.V.S. voltage stabilizers, having all solid state voltage detection and control circuits which provide an extra high speed correction rate of up to 147 volts per second to within $\pm 0.2\%$ accuracy and may be used in giving accurate voltage control for computers, calculating machines, automatic welding machines, television transmission and studio equipment, etc.

COLVERN LTD. ALLÉE 55
Spring Gardens, Romford, Essex. STAND 61

The display will include the following:

Seven types of multi-turn potentiometers from a small preset/manual control to a precision 40 turn model with a unique end stop mechanism and including the new 'Dialpot' with integral watch-type dial.

Precision potentiometers in various sizes from 08 synchro to the largest of the well proved cam-corrected potentiometers giving linear and special function outputs, including sine/cosine with an accuracy of $\pm 0.05\%$.

COSMOCORD LTD. ELECTRO-
Eleanor Cross Road, ACOUSTIC
Waltham Abbey, Essex. SECTION

A new range of pick-up cartridges is being presented. These include the following:

(1) G.P. 91 Mono Crystal Cartridge which has high compliance and extended frequency range and is stated to play stereo records without damaging the record.

(2) The G.P. 94 Stereo Ceramic has high compliance, extended frequency range and 15 deg tracking angle. It is intended to supply this cartridge with high capacitance elements.

The Company's recently formed Instrument Division is producing a range of vibration meters and associated ceramic-type accelerometers suitable for readings up to 1000 g over a very wide frequency and temperature range, together with a range of bearing analysers for machine tool monitoring. Both these devices are also produced incorporating limit switching devices which automatically stop a test or process in the event of an overload condition.

Also available is a wide range of a.c. millivoltmeters of particular interest to electronic circuit designers and manufacturers because of a very high input impedance of 100 M Ω .

Two really portable oscilloscopes are included in the range of instruments, the display being on a 1 in diameter cathode-ray tube and can be operated from any 6 or 12 V d.c. source.

E.M.I. ELECTRONICS LTD. ALLÉE 36
Hayes, Middlesex. STAND 156

A wide range of metal-ceramic sealed components will be publicly exhibited for the first time. These components are used in insulators for various parts of microwave valves, in waveguide windows for electronic devices and in several other engineering applications. Glass parts of vacuum enclosures are the first to fail during the high temperature working which is required for modern techniques. This has led to the use of ceramic components, which can withstand very high temperatures.

A new addition to the Company's range of plug-in klystrons, also on display, is the low-voltage type R.9678 which operates in the Ku-band. This has a typical power output of from 30 mW to 60 mW over the frequency range of 12 Gc/s to 18 Gc/s. It is also useful in X-band between 8 Gc/s and 10 Gc/s.

Latest cathode-ray tube being exhibited is the 5 in diameter oscilloscope tube type MX 58. This is an exact replacement for the D13-22GH and is notable for high screen brightness and high sensitivity. A separate mesh screen ensures freedom from raster distortion and radial deflection plate pins keep plate capacitances to a minimum.

A comprehensive range of photomultiplier tubes will be shown. These special valves are suitable for a variety of applications including photometry, spectroscopy, spectrophotometry, and gamma-ray spectrometry. Tube diameters range from approximately 1 in (28 mm) to 12 in (300 mm) and offer spectral coverage from approx. 1200 Å to 12 000 Å. Electron gains of up to 10^9 are available with very low dark currents.

Camera tubes being shown range from 4½ in image orthicon—type 7295 and 7389—with a superior grey scale, freedom from microphony and high signal/noise ratio, to the unique ½ in vidicon with separate mesh brought out adjacent to the target. This gives a very rigid construction with resolution capabilities of the 1 in tube.

ERIE RESISTOR LTD.
1 Heddon Street, London, W.1.

ALLÉE 20
STAND 175

Among the large range of components will be the following more recent developments:

'Monobloc' ceramic capacitors combining stability, reliability and miniaturization.

'Microcap' and 'Weecon' ceramic capacitors, offering high volumetric efficiency.

Radio frequency and low pass filters comprising a pi-circuit in single feedthrough form, yielding a 50 dB attenuation at 70 Mc/s and beyond, with capacitance up to 1.5 microfarad and working voltages up to 1.5 kV d.c.

U.h.f. planar tube u.h.f. capacitors, for bypassing and decoupling in u.h.f. circuitry; these annular capacitors fit directly over the anode, grid or cathode of planar type electronic tubes.

Ultrasonic microphones, ruggedly built for industrial control systems, operating at frequencies 35 kc/s to 45 kc/s with high receiving sensitivity.

Diodes. New diodes include high p.i.v. ratings, both in single and series versions, the latter in moulded packages.

Full wave doubler rectifiers, giving smooth rectification in module form for p.c. boards.

Metal oxide film resistors, various ratings, combining reliability with small size.

Resistor-capacitor networks. These passive circuits offer reliability and miniaturization in module form, with resistances up to 100 000 ohms and capacitances up to 10 nF. Close tolerances can be specified. The standard finish is dipped, with terminal spacings 1.9 mm.

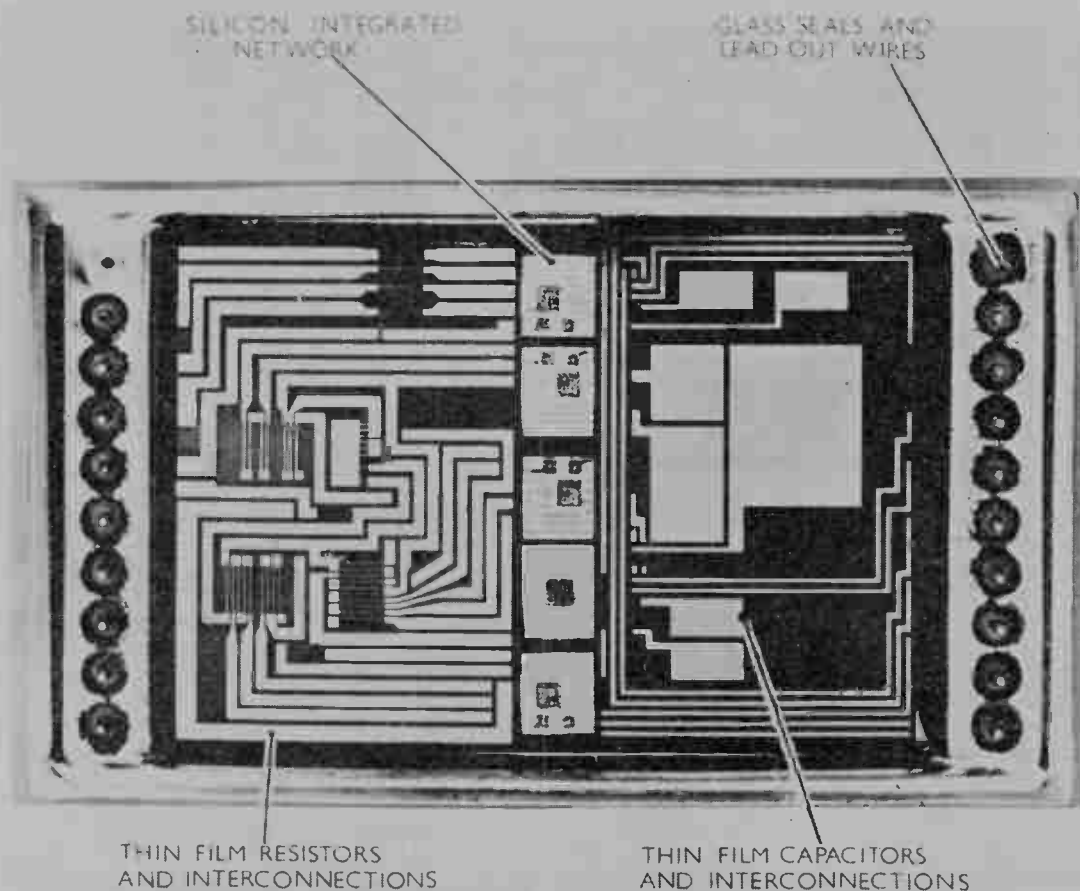
Resistors and capacitors for printed circuits. These have special terminals for high-speed vertical or horizontal printed circuit assembly and trouble-free automatic soldering.

FERRANTI LTD.
Hollinwood, Lancashire.

Electronics Department

ALLÉE 42
STAND 83

The emphasis will be on semiconductor devices and parametric amplifiers. A selection from the large range of transistors and diodes produced by the Company will be shown and also miniaturized solid state circuits. Emphasis will also be given to work being carried out in conjunction with the Aircraft Equipment Department at Bracknell, Berkshire, on Multilin. This is a new solid state electronic sub-system concept which combines the linear elements available in the well-known Ferranti Microlin range and thin film circuits.



A typical Ferranti Multilin circuit. Actual size approximately 56 mm by 32 mm by 5 mm.

Ferranti parametric amplifiers are of the non-degenerate, negative resistance types, with a constant gain-band width product. The type VCA/LIO operates at a frequency of 570 Mc/s which is the transmission frequency of the British Broadcasting Corporation's 625 line television programme, and this amplifier has been primarily developed for purposes associated with this transmission. Four basic types of parametric amplifiers are available operating through the frequency range of 390 Mc/s to 4000 Mc/s.

Also on view will be a new type of light source based on radiative recombination at a *pn* junction, and known as a crystal lamp. The device is in effect a forward biased gallium phosphide diode suitably doped to provide electro-luminescent radiation of 700 angstroms (red). The average brightness is 10-40 ft lamberts, and the lamp is visible under an illumination of 20 foot candles. The size is typically 0.03 in × 0.04 in.

Tubes Department

ALLÉE 39
STAND 75

On this stand will be exhibited examples of the company's range of high resolution cathode-ray tubes and mounting units. The mounting units have been designed to hold the tubes rigidly and accurately in the correct plane so that optimum performance can be achieved. There are six basic types of unit, made of non-magnetic duralumin, stainless steel and brass, which are available in various sizes and lengths to accommodate the particular tube being used.

Components Department

ALLÉE 14
STAND 117

Logical circuit elements: three new ranges of logical circuit elements will be shown, the 400, 500 and 700 series. These offer rectangular shapes, higher switching speeds and lower costs without the sacrifice of quality or reliability.

Ferrite devices and microwave filters: exhibits of ferrite devices will include the series 100 SCD three-port coaxial circulators which cover the frequencies 2500 Mc/s to 6000 Mc/s in wide-band versions. A four-port circulator is also now available which covers any 1000 Mc/s band between 8500 Mc/s to 10 000 Mc/s.

Vacuum relays: these relays are for use in high voltage applications where they form an attractive alternative to conventional methods of switching high-voltage direct current, and in some cases low-voltage direct currents. The range includes relays capable of switching voltages up to 60 kV and currents of up to 50 A (continuous).

Optical shaft encoder: the new size 23 optical shaft encoder has been developed to indicate the angular position of a shaft in binary code.

TR cells and limiters: the most recent development is a new S-band cell, type JF.20, which has a radioactive filling and therefore does not need an external primer supply.

Potentiometers and test equipment: precision wire-wound potentiometers and carbon film potentiometers will be on display with a new potentiometer linearity test machine.

A.C. precision motors and external rotor motors: a range of precision 400 c/s motors manufactured to NATO and International frame sizes is available and some of these motors will be on display. The 400 c/s a.c. external rotor motors are a recently introduced range which were designed initially as gyroscopic spin motors but have found application in many other fields.

Transformers will be on view illustrating the various ranges manufactured. These vary from miniature resin cast units, suitable for insertion in printed circuit boards, to power distribution types for use in aircraft where the winding temperature is 250°C.



Garrard Model 2000 automatic turntables.

GARRARD ENGINEERING LIMITED ELECTRO-ACOUSTIC SECTION
Swindon, Wiltshire

A further addition to Garrard's range of automatic turntables, the Model 2000, will be shown. The new unit can be mounted conveniently into sound reproducing systems where space is limited but where high quality performance is nevertheless necessary.

Stiffening webs in the die-cast aluminium pick-up arm provide a non-resonant structure. The pick-up is integral with the arm and incorporates a stylus pressure adjustment to provide correct tracking conditions for a wide range of cartridges.

A large diameter turntable is fitted with a tailored rubber mat. For automatic playing, eight records of the same speed, but of any mixture of sizes, can be accommodated.

Each of the four nominal speeds of 16 $\frac{2}{3}$, 33 $\frac{1}{3}$, 45 and 78 rev/min can be obtained by means of a simple control; selection of manual or automatic operation is equally easy.

Model 2000 is suitable for use on 100-130 V or 200-250 V a.c. 50 or 60 c/s operation depending on the motor supplied. The unit is finished in dark metallic grey and aluminium.

HALLAM, SLEIGH & CHESTON LTD.
Widney Works, Bagot Street, Birmingham.

ALLÉE 26
STAND 167

The successful Widney Dorlec constructional system uses strong, light alloy members and corners quickly bolted together to form technical furniture to suit numerous applications. Making its debut this year is the '20/30 Series', which both simplifies and unifies the existing system. To cater for all requirements, from the very small to the very large, the Widney Dorlec 20/30 System embraces four different main frame members plus a comprehensive range of corresponding corners. In all cases, construction is simple, using a saw and a spanner.

A wide range of telescopic slides is also to be demonstrated. The Slimslide, a nylon-coated slide only $\frac{1}{8}$ in thick, leaves the designer with extra chassis space, and at the other end of the scale, slides are available to carry over 1000 lb (500 kg) with adequate safety. The complete range enables the manufacturer of any unit to use telescopic slides, so encouraging regular maintenance of his equipment.

THE INSTITUTION OF ELECTRONIC AND RADIO ENGINEERS
8-9 Bedford Square, London, W.C.1.

ALLÉE 20
STAND 132

The Radio and Electronic Engineer and other Institution publications will be displayed.

LONDON ELECTRICAL MANUFACTURING CO. LTD.
Bridges Place, Parsons Green Lane,
London, S.W.6.

ALLÉE 36
 STAND 128

The exhibit will display the well-known range of Lemco products, which include:

Silvered mica capacitors, in protected, insulated, and moulded types.

Silvered ceramic capacitors, tubular and disc, together with the specialized lead-through types for u.h.f. requirements.

A range of polystyrene foil capacitors, including the new type '7E' which is available in a wide range of capacitances in very small physical dimensions.

A range of polyester foil insulated tubular capacitors will be shown. These components are rapidly replacing the conventional paper capacitors as they show considerable technical and economic advantages.

The range of aluminium electrolytic tubular capacitors has been reduced to enable the Company to concentrate more fully on the more specialized miniature types for transistor circuit requirements. Considerable technical improvements have recently been made on this range of capacitors.

THE M-O VALVE CO. LTD.
Brook Green Works, London, W.6.

ALLÉE 36
 STAND 117

The exhibit features the world's largest travelling wave tube, specially designed for satellite communication ground stations. This tube, type TWC827, is a water-cooled C-band travelling wave amplifier giving a minimum operating power output of 8 kW at a frequency of 6300 Mc/s with 60 Mc/s bandwidth and wide tuning range. The tube uses a coupled-cavity slow wave structure of a type which gives high gain per unit length, good power handling capability and freedom from unwanted oscillations.

Another new device being shown for the first time is the RC1 dry reed capsule switch, which has an average life expectancy of 10^8 operations under low level signal conditions when operated in a solenoid. At full ratings the life expectancy is 10^7 operations. The contact is a single pole, normally open, with a resistive load of less than 100 milliohms and an operating time of less than 2 milliseconds, including bounce. With resistive load, maximum switched voltage is 50 V, and maximum switched current 100 mA. Several applications of the reed capsule will be demonstrated.

A complete new range of microwave components will be introduced at the show. This will include ferrite isolators, hybrid mixers, diode attenuators, diode switches, waveguide to coaxial transitions, and an X-band solid state signal source.

The Company's well-known range of double gun instrument cathode-ray tubes will be on show together with a small rectangular screen cathode-ray tube, type 700E, giving a display of 45 mm × 24 mm. This tube is designed to operate at high brightness and is particularly suited to the display of digital information under high ambient lighting conditions. Although high currents may be drawn from the cathode, little of this current flows to the focus electrode or the deflector plates, and this enables a large number of tubes to be conveniently operated by common focus and deflection supplies. The information is displayed by intensity modulation of the electron beam.

Rugged magnetron developments are represented by the MAG15, an X-band magnetron with a peak output of 7 kW and a warm-up time of less than 10 seconds. This device is capable of withstanding a swept vibration of from 20 c/s to 10 000 c/s with *g* levels commencing at 3 *g* and rising to 50 *g*.

Under these conditions, the output frequency will not change by more than ± 3 Mc/s. It is also capable of withstanding 40 *g* shocks of 10 millisecond duration.

New gas-filled valves include the E2816, a metal-bodied, deuterium-filled, grid controlled rectifier with an anode voltage of 40 kV, and the E2830, a deuterium-filled pulse modulator thyatron with a peak anode voltage of 20 kV, forward and reverse, and a mean anode current of 60 mA.

THE McMURDO INSTRUMENT CO. LTD.
Rodney Road, Portsmouth, Hampshire.

ALLÉE 32
 STAND 166

The Company will be displaying examples from their comprehensive range of plugs and sockets, valveholders, voltage selector panels, crystal holders and ancillary items.

MALLORY BATTERIES LTD.
Crawley, Sussex.

ALLÉE 28
 STAND 141

Important feature on the Mallory stand is the introduction of a new, improved version of their 1.5 V manganese alkaline dry cell system. Mallory have developed this proved-performance system further by modifying the anode and electrolyte construction to give greater internal contact—resulting in lower internal impedance, higher flash currents and better stability on high current drains. This makes the cells—produced in a range of five standard sizes—ideal for a wider range of heavy duty applications.

MARCONI INSTRUMENTS LTD.
St. Albans, Hertfordshire.

ALLÉE 46
 STAND 135

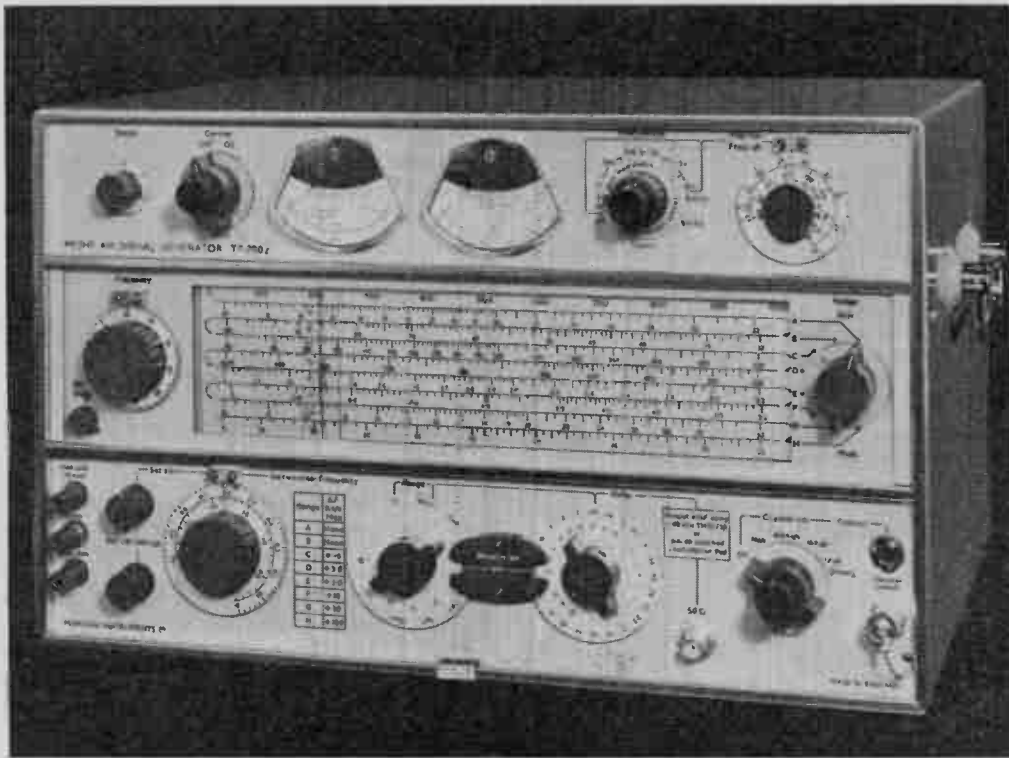
Of major interest is the Counter TF 2401. This design has the novel feature that all input channels are in the form of plug-in units. By this means a wide range of facilities can be achieved using a common basic instrument. The counter, which has an eight decade in-line readout, employs solid state circuitry throughout and makes extensive use of both diode and transistor logic. The Range Unit TM 7557 and Counter-Timer Function Unit TM 7558 allow a maximum count rate in excess of 50 Mc/s and time measurements as short as 0.1 μ s. A plug-in converter extends the range to 500 Mc/s, whilst other units permit the operation of the equipment as an integrating digital voltmeter or digital phase meter.

A new range of accessory instruments has been designed to extend the use of the transistorized Marconi counters in the fields of recording and control. By means of a flexible mechanical design, common to all these instruments, and plug-in printed circuit boards, further new instrument types can easily be added to the range, and special customer modifications can also be accommodated. The instruments may be used with other digital equipments, e.g. digital voltmeters, whose output is in the correct form, namely 1–2–4–8 BCD. The range comprises:

TF 2402 Digital-to-Analogue Converter: This instrument produces a voltage or current analogue of any three consecutive digits or the last two of the counter reading, for driving pen recorders.

TF 2403 Digital Code Converter: The various versions convert the 1–2–4–8 BCD used in Marconi counters to alternative codes. Two output codes are produced as standard, namely a 10-line pulsed code suitable for Kienzle type D11E printer and 1–2–2–4 BCD.

TF 2404 Out-of-Limits Indicator: The TF 2404 monitors counter readings. The indication takes the form of a visual signal, plus either a relay contact closure or an electrical pulse.



Marconi Instruments solid state MF/HF AM Signal Generator, Type TF 2002.

TF 2405 Analogue-of-Difference Unit: The output from this instrument is an analogue of the difference, positive or negative, between counter readings and a manually set datum. Wide ranges of output are available up to ± 2.5 V or ± 2.5 mA.

TF 2406 Counter Time Base Distribution Unit amplifies the time-base from a master counter and distributes it at 75Ω impedance to as many as eight slave counters.

TF 2002 M.F./H.F. A.M. Signal Generator: This new fully-transistorized signal generator gives a high quality a.m. output in the carrier range 10 kc/s to 72 Mc/s. It has exceptionally high discrimination tuning with low drift, low leakage and spurious modulation.

Other equipments on show include a new fully transistorized White Noise Test Set, Type OA 2090, designed for testing cable and radio multi-channel links with capacities up to 2700 channels; and the M.F. Transmission Measuring Set TF 2333, which covers the frequency range 50 c/s to 560 kc/s.

THE MARCONI CO. LTD.
Specialised Components Division,
Radford Crescent, Billericay, Essex.

ALLÉE 14
STAND 167

New items to be shown will include the following:

Frequency Standard Type F3160: This is a transistor oscillator of high stability, which gives three outputs, namely $2\frac{1}{2}$ Mc/s, 1 Mc/s and 100 kc/s. The circuit is based on $2\frac{1}{2}$ Mc/s A.T.-cut crystal, which is housed in a double thermostatically controlled oven. A battery power supply is included to maintain temperature in case of power failure.

A three-port Stripline Circulator (Type F 1031) is available as three separate items covering the ranges of 500 Mc/s to 800 Mc/s, 750 Mc/s to 1000 Mc/s, and 950 Mc/s to 1500 Mc/s. These are intended to replace the original circulator which covered the range 500 Mc/s to 1500 Mc/s, but was often wider than necessary for some requirements. The items in the new range are smaller and cheaper and have been designed to the same specification as the original model used.

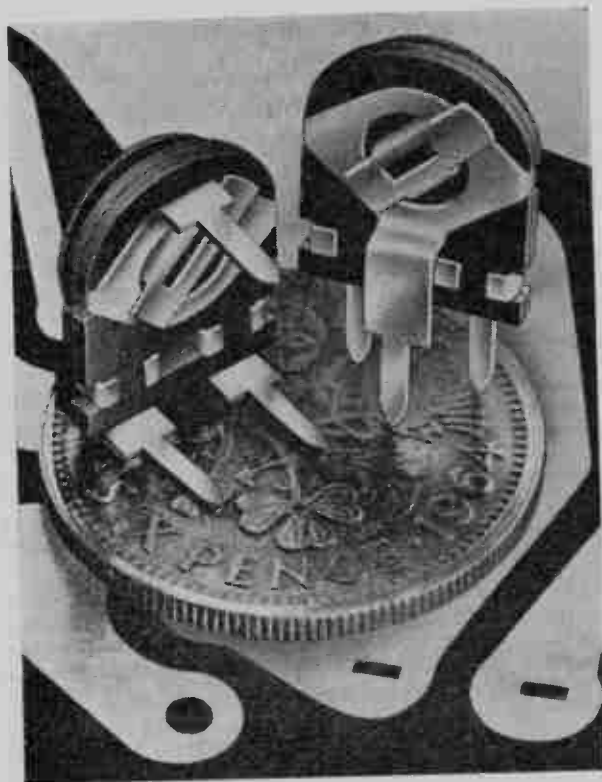
Other items to be shown will include a transistorized high-speed switch, intended as a replacement for the Carpenter polarized relay; four-port stripline circulator; low temperature circulator; and a range of crystal oscillators employing change-of-state ovens and covering, with a few gaps, the range 1 kc/s to 120 Mc/s.

MORGANITE RESISTORS LTD.
Bede Trading Estate, Jarrow, Co. Durham.

ALLÉE 22
STAND 155

The Company is showing the new additions to its range of 'Filmet' high stability metal film resistors. The special feature of these new resistors is a coating of epoxy resin which, in addition to providing full insulation, also gives complete protection in conditions of extreme humidity. The new type is so far available in two sizes, LFM02 and LFM03, with ratings of 0.25 W and 0.5 W respectively. Also on display will be the hot moulded version of the 'Filmet', types FM02 and FM03, intended for use in the most critical circuitry where only a resistor of the highest precision is acceptable.

The full range of Morganite carbon-composition and ceramic-bonded linear and non-linear resistors is being exhibited,



Morganite Resistors' Miniature preset resistor Type 62.

together with carbon potentiometers for every application in the radio and electronics industries. Recently developed and being exhibited for the first time, is a new miniature preset resistor, the type 62, which measures only 12×9 mm overall when mounted. This component is rated at 0.2 W at 40°C and is made in a range of values from 100 Ω to 1 M Ω .

Of interest to manufacturers of microwave equipment are the 'TERMILODE' high power terminations which are made in three styles, dissipating up to 1.5 kW in the WG 16 (WR 90) size. Other loads are available in sizes from WG 22 (WR 28) to WG 10 (WR 284).

MULLARD LTD. ALLÉE 42
Mullard House, Torrington Place, London, W.C.1. STAND 136

Mullard will be showing examples from their wide range of semiconductors, valves and other components for industrial and entertainment applications.

MULTICORE SOLDERS LTD. ELECTRO-ACOUSTIC SECTION
Maylands Avenue,
Hemel Hempstead,
Hertfordshire.

A representative selection of cored solders and accessories will be shown including Ersin Multicore Solder, with five cores of non-corrosive Ersin Flux, and Savbit Alloy, containing a small percentage of copper which, with the normal tin/lead constituents, is claimed to prolong the life of soldering iron bits by ten times.

Accessories shown will include a new version of the Bib Wire Stripper, having a pre-setting device for eight standard wire gauges, shown for the first time at an exhibition.

The Multicore Solderability Test Machine will be demonstrated daily on the stand. This machine was developed by the Electronic Engineering Association in collaboration with the International Electrotechnical Commission, with a view to establishing it as a standard for testing the solderability of round wires.

ROBAND ELECTRONICS LTD. ALLÉE 62
Charlwood Works, Lowfield Heath Road, STAND 83
Charlwood, Horley, Surrey.

Two precision oscilloscopes will be prominent items.

The Roband RO50 is a precision high speed d.c. to 32 Mc/s oscilloscope with signal delay and tunnel diode triggering for single and multiple trace operation. Versatility is increased

The Roband Oscilloscope Type R050.



through the use of the Roband 5 series plug-in units. All d.c. rails, including a special d.c. rail for amplifier valve heaters, are stabilized. High brightness displays at any sweep speeds are ensured with a 13 kV stabilized e.h.t. and can be easily observed even in high ambient lighting conditions.

The oscilloscope Type RO55 is designed for d.c. to 16 Mc/s operation and employs tunnel diode triggering for single and multiple trace operation. E.h.t. supply is 3.5 kV stabilized.

SEAELECTRO LTD.
Hersham Trading Estate,
Walton-on-Thames, Surrey.

ALLÉE 32
STAND 137

Besides many additions to the established ranges several entirely new products will be shown for the first time. Product groups in the exhibit include the following:

The Seaelectboard Cordless Programming and Switching System which has received a very wide acceptance by the electronics industry, is being constantly extended. Typical examples of Seaelectboard applications will be featured together with a dynamic display.

Static Punched Card Reader. A prototype model will be shown and demonstrated. This device is a logical extension of the Seaelectboard system, it accepts standard 80 × 12 punched card features instead re-programming with low volume program storage.

Conhex Sub-Miniature Coaxial Connectors. Matching impedances of 75 ohms and 50 ohms are basic, each being available in screw-on, snap-on and slide-on mating forms, and to accommodate a variety of flexible and semi-rigid cables. The main feature of the Conhex exhibit will be types conforming to Pattern 17 of British Defence specification DEF 5322A.

Seaelectro P.T.F.E. Press-fit Terminals. The extremely wide range of press-fit terminals which achieves high reliability and performance under the most severe environmental conditions has been extended to include two-piece types which have received type approval to British Defence specification DEF 5334B. These styles together with new test sockets and probes, will be exhibited for the first time. A continuous demonstration will illustrate the ease of installation and high retention.

Cloverleaf Receptacles. These unique feedthrough terminals, which enable dip or flow soldering with metal panels or plates, are now available in two sizes, which accommodate a wide range of wire gauges.

Seaelectro Press-Fit Transistor and Micro-Logic Sockets. A new beryllium-copper socket, with a small end area has enabled a closer spacing on pitch circles of 0.2 in (TO-5) and 0.1 in (TO-18) to be achieved, and sockets to accept all pin or wire configurations on these two bases will be on show. The features of this range of sockets are one piece p.t.f.e. bodies and single-hole, press-fit mounting.

Actan Rotary Programming Switches. These recently introduced drum-type programming switches can store up to 60 programs on a drum of less than 2 in diameter. Actuation can be manual or motorized and the program may be changed in the field with the switch installed.

Semi-Rigid Coaxial Cable and Tubing. Semi-rigid coaxial cables with an outer jacket of seamless drawn copper or aluminium have many advantages over cables having braided jackets, e.g. better shielding and a greater freedom from vibration noise.

Several styles of cable will be shown together with examples of Pointer and Bourdon tubing.

S. SMITH & SONS (ENGLAND) LTD.
Aviation Division, Kelvin House,
Wembley Park Drive, Wembley, Middlesex.

ALLÉE 28
STAND 167

The new items to be shown at this exhibition include a miniature rate-gyroscope self-testing display, a synchro fault detector, and the new Elfin module system.

Basically the smallest racking system module used for aircraft equipment up to now has been the $\frac{1}{4}$ dwarf ATR, but this has proved to be too large for the latest constructional techniques. The Elfin module system is a quarter of the height of the full height $\frac{1}{4}$ ATR, and it has been specifically designed for micro-miniature equipment.

In addition, series of digital components will be shown, which will include optical pulse generators, an optical digitizer, and stepping motors. A selection of aircraft instruments will also be shown and will include a radio altimeter, ground-speed and drift indicator, a radio magnetic indicator, DME indicator, and hover indicator.

S. SMITH & SONS (ENGLAND) LTD.
Spark Plug and Ceramics Division,
St. Peter's Road, Rugby, Warwickshire.

ALLÉE 62
STAND 134

This year the Company's exhibition of alumina ceramic components will stress the use of high strength ceramic/metal assemblies for use as silicon rectifier encapsulations. The ideal properties of the material for use in thermionic valves and as a substrate will also be displayed.

ULTRA ELECTRONICS (COMPONENTS) LTD.
Industrial Estate, Long Drive,
Greenford, Middlesex.

ALLÉE 28
STAND 163

This Company (formerly known as Continental Connectors) will be showing a comprehensive range of plugs and sockets, miniature, sub-miniature and micro-miniature, and printed wiring and connector test points.

The most recently developed item is a design of printed wiring wire-wrapped connectors which employs bellows connection contacts.

VACTRIC CONTROL EQUIPMENT LTD.
(and Associate Companies)
Garth Road, Morden, Surrey.

ALLÉE 04
STAND 156

Highlight of Vactric's display will be a working demonstration of the new brushless d.c. motor in international frame size 11, and the recently introduced range of synchros and resolvers in international frame size 08 will also be on view. In addition, examples of standard precision servo components will be displayed, including a.c. and d.c. servo motors, servo gearheads, a.c. motor tachogenerators, rotary sampling switches and breadboard components.

On the same stand, Rotron-Vactric Europe, the Company recently formed in collaboration with Rotron Manufacturing Co. Inc. of New York, will be showing examples of their extensive range of precision air-moving devices for commercial and electronic cooling applications, including fans of the propeller, vane-axial and tube-axial types and blowers of the squirrel cage centrifugal, radial wheel and multi-stage types.

A. P. Besson & Partner Ltd., specialists in miniature electronic and electro-mechanical components, will be exhibiting their range of miniature transformers, acoustic units, micro-phones, and earphone inserts and specialized miniature coil windings.